



RESEARCH TRIANGLE INSTITUTE

AFCL-67-0069

RESEARCH DIRECTED TOWARD THE STUDY OF SEISMICITY
IN THE SOUTHEASTERN UNITED STATES

AD 648458

John W. Minear

Research Triangle Institute
P. O. Box 12194
Research Triangle Park, North Carolina 27709

Contract No. AF 19(628)-3892

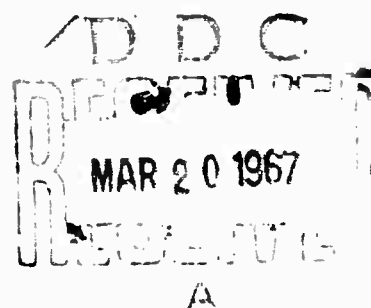
Project No. 8652

Task No. 865207

FINAL REPORT

January 2, 1964 thru December 15, 1966

January 1967



Work sponsored by Advanced Research Projects Agency, Project VELA-UNIFORM
ARPA Order No. 792, Project Code No. 8100 Task 2

Prepared for

AIR FORCE CAMBRIDGE RESEARCH LABORATORIES
OFFICE OF AEROSPACE RESEARCH
UNITED STATES AIR FORCE
BEDFORD, MASSACHUSETTS

ARCHIVE COPY

RESEARCH TRIANGLE PARK, NORTH CAROLINA 27709

F

DISCLAIMER NOTICE

THIS DOCUMENT IS THE BEST
QUALITY AVAILABLE.

COPY FURNISHED CONTAINED
A SIGNIFICANT NUMBER OF
PAGES WHICH DO NOT
REPRODUCE LEGIBLY.

AFCRL-67-0069

RESEARCH DIRECTED TOWARD THE STUDY OF SEISMICITY
IN THE SOUTHEASTERN UNITED STATES

John W. Minear

Research Triangle Institute
P. O. Box 12194
Research Triangle Park, North Carolina 27709

Contract No. AF 19(628)-3892

Project No. 8652

Task No. 865207

FINAL REPORT

January 2, 1964 thru December 15, 1966

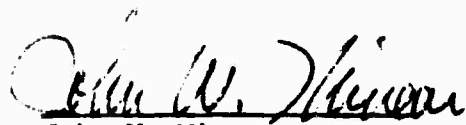
January 1967

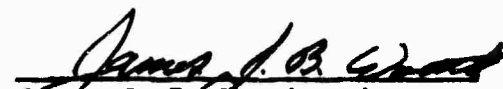
Work sponsored by Advanced Research Projects Agency, Project VELA-UNIFORM
ARPA Order No. 292, Project Code No. 8100 Task 2

Prepared for

AIR FORCE CAMBRIDGE RESEARCH LABORATORIES
OFFICE OF AEROSPACE RESEARCH
UNITED STATES AIR FORCE
BEDFORD, MASSACHUSETTS

Approved by:


John W. Minear
Project Director


James J. B. Worth, Director
Geophysics Laboratory

Distribution of this document is unlimited.

ABSTRACT

This is the final report covering research directed toward the study of the seismicity of the Southeastern United States. Travel-times determined from local earthquake and refraction data are presented which indicate a crustal structure of $h_1 = 33.0$ km ($\alpha = 5.88$ km/sec), $h_2 = 10.8$ km ($\alpha = 6.58$ km/sec), and an upper mantle velocity of 8.10 km/sec. Fundamental and first higher order Rayleigh group-velocity data determined by digital bandpass filtering are presented for the Southern Appalachian region. The Dunkin modification of the Thomson-Haskell matrix method is used to compute theoretical Rayleigh dispersion curves for comparison with the observed curves. A slight velocity reversal in the upper crust centered at about 15 km, a general increase of crustal velocities and densities with depth below this zone, and an upper mantle low velocity zone beginning at a depth of 70 km are indicated beneath the Southern Appalachians. The Appalachian foreland has crustal structure similar to the Gutenberg-Birch II continental model with a total thickness of 40 km.

A $\sin x/x$ analysis of the Bouguer gravity data yields a total crustal thickness of about 50 km beneath the Southern Appalachians.

P-residuals computed at Chapel Hill, North Carolina and McMinnville, Tennessee show a systematic deviation of as much as ± 3 sec.

TABLE OF CONTENTS

1.0	INTRODUCTION	1
2.0	TRAVEL-TIME CURVES FOR THE SOUTHEASTERN UNITED STATES	4
3.0	CRUSTAL THICKNESS FROM GRAVITY DATA	8
4.0	DETERMINATION OF RAYLEIGH GROUP VELOCITY	12
5.0	THEORETICAL RAYLEIGH DISPERSION CURVES	18
5.1	Thomson-Haskell Matrix Method	18
5.2	Numerical Difficulties in the Thomson-Haskell Method	20
5.3	Dunkin Modification of the Haskell Method	25
5.4	Computational Procedure	26
5.5	Variation of Phase Velocity with Layer Parameters	35
6.0	CRUSTAL AND UPPER MANTLE STRUCTURE IN THE SOUTHEASTERN UNITED STATES	40
7.0	CONCLUSIONS	59
	ACKNOWLEDGMENTS	
	REFERENCES	
APPENDIX I:	Evaluation of the Secular Equation in Computing Rayleigh Dispersion	
APPENDIX II:	Modal Shape Computations	
APPENDIX III:	Fortran Listings of Computer Programs FLATRAY, STRESS, INTEGRAL, TRAVEL, VARGRAV, and PRESID	
APPENDIX IV.	Curves of Particle Displacements and Partial Derivatives of Phase Velocity with respect to Layer Parameters	

1.0 INTRODUCTION

This final report covers the work done on contract AF 19(628)-3892, "Research Directed Toward the Study of the Seismicity of the Southeastern United States". The report is mainly concerned with the work done over the past year; the determination of crustal and upper mantle structure in the Southeastern United States. The First Annual Technical Report [Minear, 1965] covers the development, installation, and calibration of the short-period displacement seismograph at the University of North Carolina and the RTI field refraction system. The Second Annual Technical Report [Minear, 1966] includes the location of local epicenters, the results of the field refraction studies, the results of the computation of P-residuals, the calculations of magnitude, focal depth, and energy release for several local earthquakes, and preliminary crustal structure estimates from gravity data.

Research accomplishments during the performance of the contract are briefly summarized below.

- 1) During the first year of work a short-period displacement seismograph system was designed, constructed, and placed on routine operation at the University of North Carolina seismograph vault at Chapel Hill, North Carolina. Although the system performed well [Minear, 1965], the background noise level at the UNC station was too high to permit recording of local earthquakes located mainly in the Southern Appalachians. At present, a remote vault is currently under construction by the University to provide an up-to-date seismic facility.

- 2) Refraction work was carried out using local quarry blasts as energy sources.

3) Local travel-time curves were developed using several of the major local earthquakes which were well recorded by portable and permanent stations in the region.

4) P-residuals were computed for several hundred epicenters recorded at the Cumberland Plateau Seismological Observatory and Chapel Hill, North Carolina. A systematic deviation of the residuals similar to that noted by other investigators was found. This deviation cannot be explained by crustal velocity variations and must indicate a real error in the Jeffreys-Bullen travel-times.

5) Estimation of focal depth, magnitude, and energy release from previous intensity studies of four Southeastern earthquakes were made.

6) Total thickness of the Southern Appalachian crust was determined using Bouguer gravity anomalies and the $\sin x/x$ method of computing the mass anomaly producing a given gravity anomaly.

7) Crustal and upper mantle structure was determined using fundamental and first higher Rayleigh mode group velocity dispersion.

8) Computer programs were written for bandpass filtering, computation of P-residuals, least squares epicenter location, computation of theoretical travel-times from a given velocity structure, computation of theoretical Rayleigh dispersion curves and modal shape, computation of the variation of phase velocity with layer parameter variations, and the computation of the mass anomaly from a given gravity anomaly profile.

At the start of the project, it was anticipated to do considerable work on phase and amplitude spectra of both seismic signals and background noise. Also, it was hoped that more work could have been done on general seismicity, distribution of epicenters, focal depth, and energy release. Failure to

acquire a digital system and the fact that much work had been done on background noise did not make the study of spectra appear worthwhile. The general seismicity study was frustrated by the poor recording station distribution in the region. Therefore, crustal and upper mantle structural studies utilizing refraction, gravity, and surface wave dispersion were concentrated on.

This report specifically covers the local travel-time curves for the Southern Appalachian region (Sec. 2), the determination of crustal thickness from gravity data (Sec. 3), the computation of theoretical dispersion curves (Sec. 4), the determination of Rayleigh group velocities (Sec. 5), and the crustal and upper mantle structure in the Southeastern United States (Sec. 6).

Numerical computational methods, tables, charts, and computer program listings are presented in the Appendices.

2.0 TRAVEL-TIME CURVES FOR THE SOUTHEASTERN UNITED STATES

Travel-time curves were determined by using data from three local earthquakes which were well recorded by Worldwide Standard Seismograph Stations and portable Vela stations operating in the Southeastern United States [Minear, 1966]. Fig. 4 shows the location of the epicenters and recording stations. Travel-time curves drawn from the local earthquake data are shown in Fig. 1. Refraction data obtained from quarry blasts and during the East Coast Onshore Offshore Seismic Experiment and theoretical travel-times computed for a typical linear mountain from the Herglotz-Wiechert equations are also plotted in Fig. 1.

Travel-time curves corresponding to arrivals from the first crustal layer and from the crust mantle boundary are drawn from first arrivals and are estimated accurate to within $\pm .1$ km/sec. Second arrivals were used to define curves corresponding to two major crustal layers. No major third layer in the crust is indicated by the refraction and earthquake data. However, first arrivals from the refraction profiles and second arrivals from 250 to 550 km, indicate that the crustal velocity may increase rather continuously from about 10 km to around 45 km. The local travel-time data yields a crustal model of $h_1 = 33.0$ km ($\alpha = 5.88$ km/sec), $h_2 = 10.8$ km ($\alpha = 6.58$ km/sec), and an upper mantle velocity of 8.10 km/sec. As can be seen from Fig. 4, the epicenters and recording stations are generally located to the west of the core of the Appalachians. Crustal structure determined from the travel-time data thus corresponds to the crust beneath the Appalachian foreland.

Velocity structures of the crust and upper mantle for the Appalachian foreland, the Northern Alps (N), Central Alps (C), and Northern Alpine foreland (F) [Knopoff, et al, 1966], and a linear mountain belt are shown in Fig. 2. Crustal velocities for the Appalachian foreland generally agree

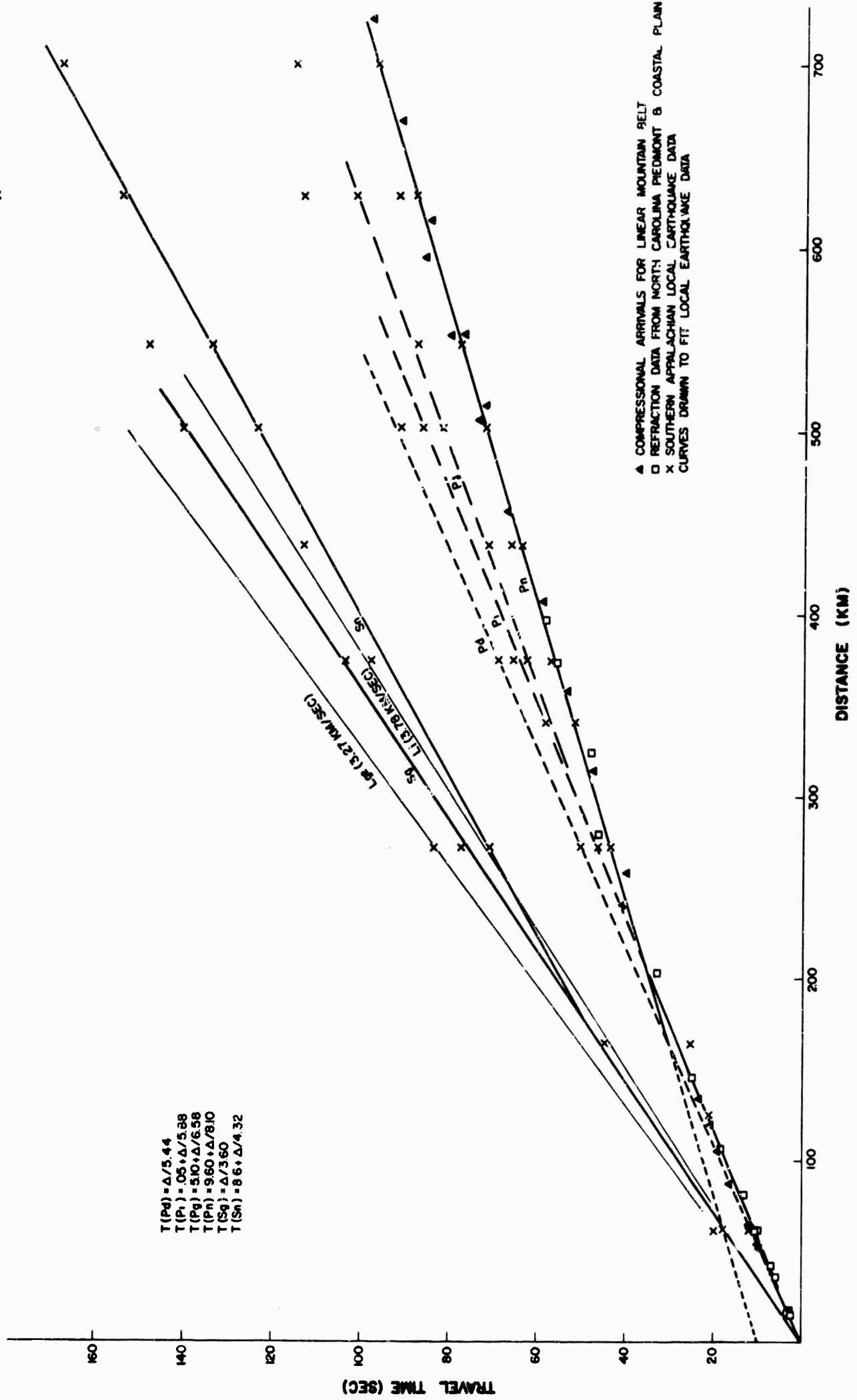
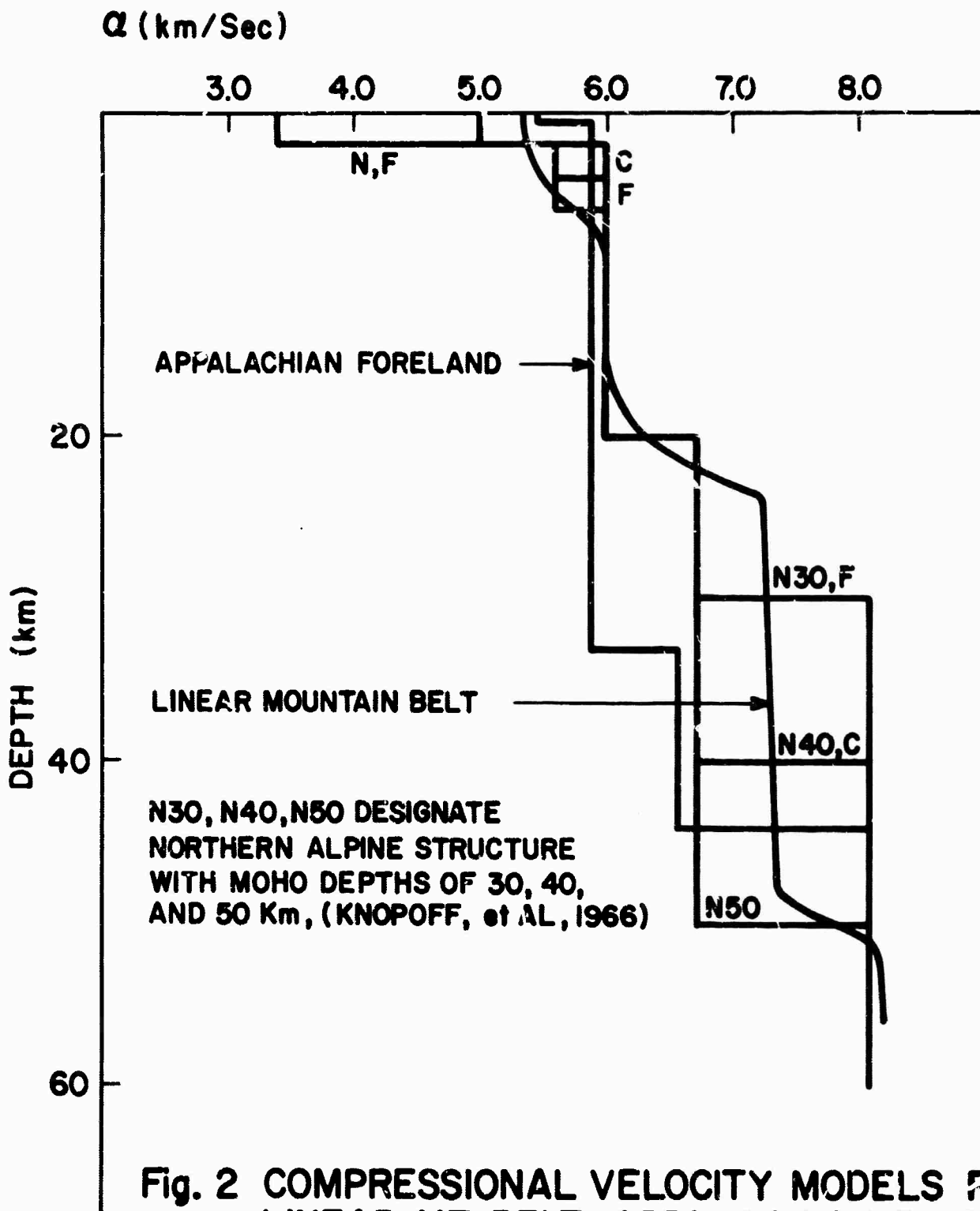


Fig. 1



**Fig. 2 COMPRESSSIONAL VELOCITY MODELS FOR
LINEAR MT. BELT, APPALACHIAN FORELAND,
AND ALPINE STRUCTURE (KNOPOFF, et AL, 1966)**

with those for the Northern Alps at depths greater than about 2 km. The disagreement for depths less than 2 km can probably be accounted for by the sedimentary cover present in the Northern Alps. The 5.85 km/sec layer in the Appalachian foreland, extending to a depth of 33 km, is thicker than any of the Alpine structures. However, as mentioned, the Appalachian foreland velocities may increase rather continuously from about 10 to 40 km. Upper mantle depth in the Appalachian foreland is greater than beneath the foreland to the north of the Alps by 14 km and greater than beneath the central Alps by 4 km.

A preliminary summary of seismic refraction work in the vicinity of the Cumberland Plateau Seismological Observatory [Bozcherdt et al, 1966] indicates a crustal model of $h_1 = 12$ km ($v_1 = 6.1$ km/sec); $h_2 = 28$ km ($v_2 = 6.7$ km/sec) and an upper mantle velocity of $8.0 \pm$ km/sec.

3.0 CRUSTAL THICKNESS FROM GRAVITY DATA

Total crustal thickness was computed from Bouguer gravity values along a Northwest-Southeast profile extending from about 460 km off the North Carolina coast (33°N, 73°W) to the Kentucky-Illinois border (38°N, 88°W). The $\sin x/x$ method of Tomoda and Aki [1955] was used to compute the depth to a mass anomaly producing the observed gravity anomalies. Bouguer gravity values were taken from the American Geophysical Union Bouguer Gravity Anomaly Map of the United States. Fig. 3 shows the gravity profile values, the total crustal thickness computed from these anomalies, and regional subsurface geology. The subsurface geological information was obtained from McGuire and Howell [1963] in Kentucky, Hersey, et al [1959] for the North Carolina continental margin, and from the geologic map of North Carolina. Crustal structure to the crust-mantle boundary at location H', and to 2 km at 12-13 is based on refraction profiles of Hersey, et al. The subsurface geology in North Carolina is intended only to indicate possible near surface relations between geology and Bouguer gravity anomalies.

In the $\sin x/x$ method, crustal thickness is computed from

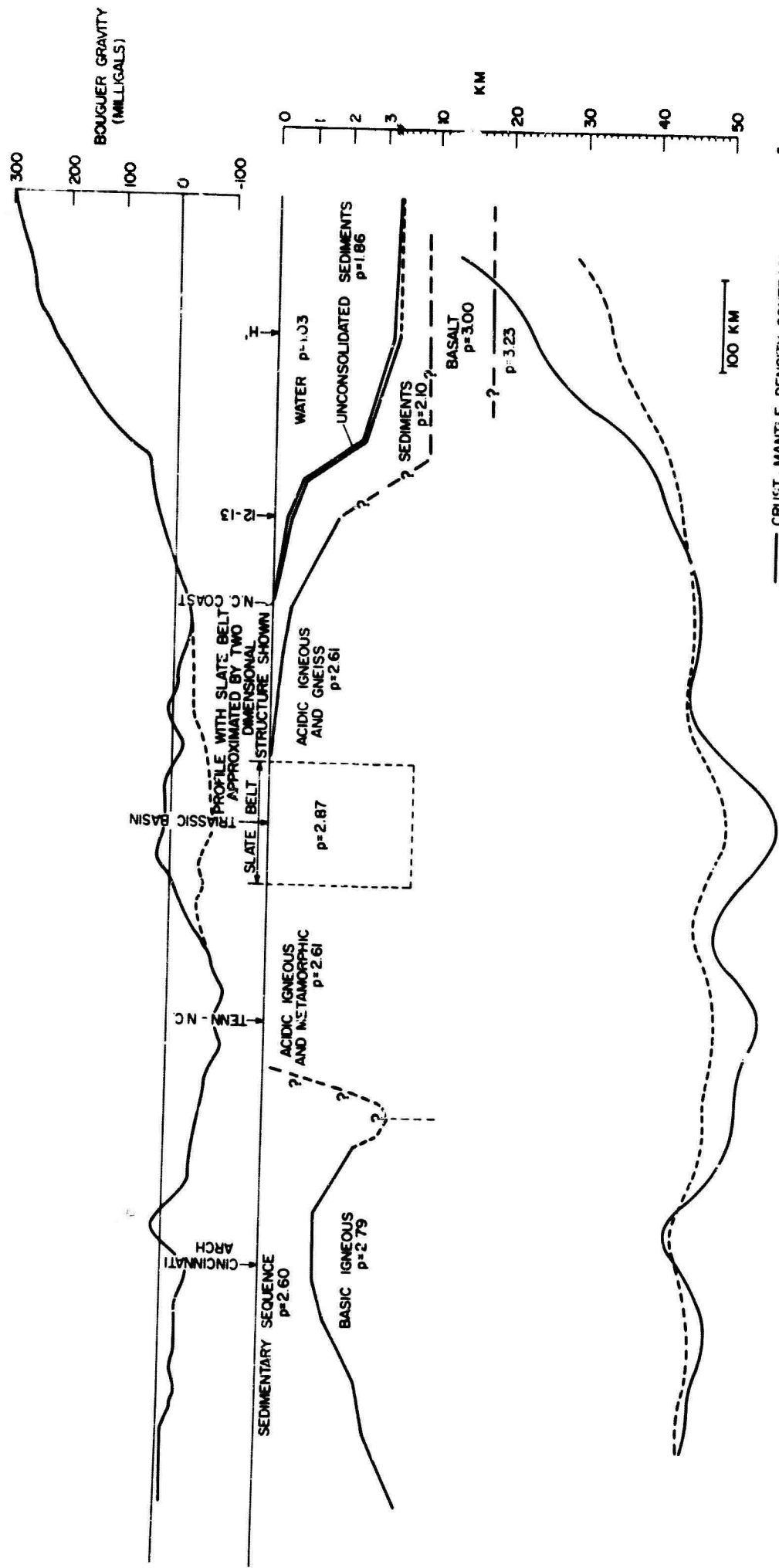
$$d(nx) = d - d'(nx) \quad 3.0-1$$

where d is an assumed thickness and $d'(nx)$ is a correction to this thickness given by

$$d'(nx) = \frac{M(nx)}{\Delta\rho} \quad 3.0-2$$

$M(nx)$ is the convolution of the observed gravity anomalies $\Delta g(q\Delta x)$ with a symmetric function ϕ_n which is a function of assumed crustal thickness and station spacing. Thus,

$$M(nx) = \frac{1}{2\pi^2 k^2} \sum_{q=-m}^{q=m} \Delta g(q\Delta x) \phi_{n-q} \quad 3.0-3$$



CRUSTAL THICKNESS FROM BOUGUER GRAVITY ANOMALIES

Fig. 3

Oscillations in the gravity values $\Delta q(q\Delta x)$ due to near surface density irregularities can result in $\Delta q(q\Delta x)$ going positive and negative, such as in the region over the slate belt in Fig. 3. Thus, $M(nx)$ may oscillate between positive and negative values which in turn yields positive and negative oscillations of $d'(nx)$. The ultimate effect is that in the regions of local near surface perturbations, the total crustal thickness, $d(nx)$, may oscillate widely about the assumed thickness, d , as can be seen from 3.0-1. Introduction of a density contrast $\Delta\rho$ which varies with depth will not eliminate these oscillations. One must either choose the station spacing wide enough so that the convolution of the anomalies with the function ϕ_n effectively filters out the local perturbations or smooth the total depth function $d(nx)$.

From Fig. 3, it can be seen that the Carolina Slate Belt is associated with a gravity high which effectively introduces a positive perturbation on the regionally decreasing gravity. If the crustal thickness is computed without removing this perturbation, the thickness oscillates about the assumed thickness beneath the belt. As shown in Fig. 3, the local gravity high over the slate belt can be largely accounted for if the belt is approximated by a two-dimensional block with lateral extent equal to the slate belt, an 8 km depth and a density contrast of $.26 \text{ gm/cm}^{-3}$.

Crustal thickness was computed from 3.0-1 using 3.0-2 and 3.0-3 with an assumed crustal thickness of 45 km and a station spacing of 60 km. The thickness values were then smoothed with a three point moving average filter (.25, .50, .25) resulting in the smoothed crustal thickness curves shown in Fig. 3. Two curves are plotted, corresponding to crustal-upper mantle density contrasts of $.3$ and $.6 \text{ gm/cm}^{-3}$. Since the ocean's crust is denser than the continental crust, the $\Delta\rho = .3$ curve approximates the crustal thickness

better under the continental margin. The agreement with the thickness as determined by refraction work [Hersey, et.al., 1959] at point H' is good. Both curves indicate a crustal thickness of at least 50 km under the Southern Appalachians. Perturbations in the crustal thickness are caused by the Cincinnati Arch and the Carolina Slate Belt. The thinning of the crust necessary to produce the Bouguer anomaly over the Cincinnati arch and the slate belt is about 9 km for the $\Delta\rho = .6$ curve and about 4.5 km for the $\Delta\rho = .3$ curve. Due to the magnitude of the crustal thickness changes, it appears that the sources of the local highs over the Cincinnati Arch and the Carolina Slate Belt are relatively near surface.

The crust thus thickens from about 83 km at the North Carolina coast to about 51 km beneath the core of the Appalachians and then thins to about 43 km at the Kentucky-Illinois border.

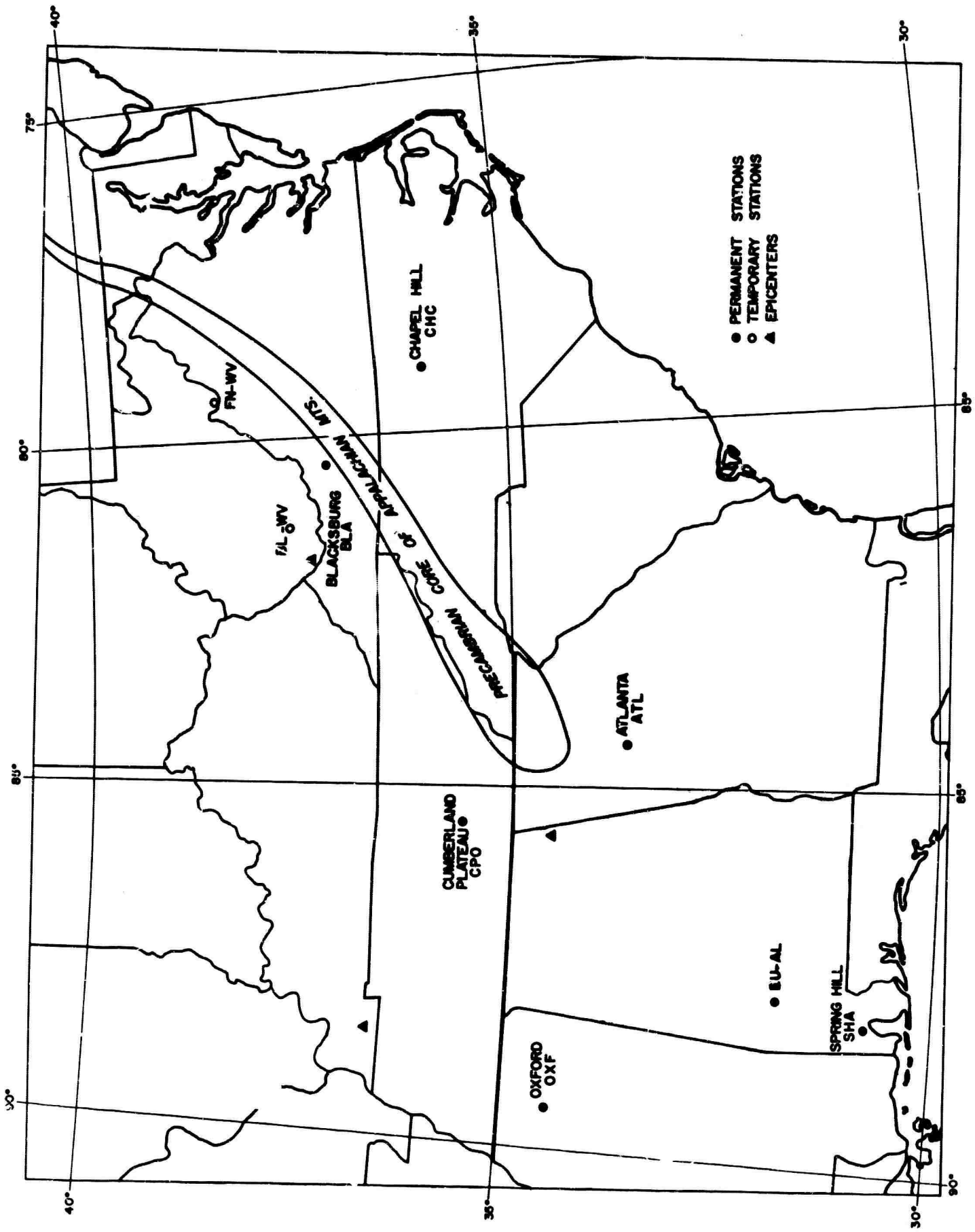
4.0 DETERMINATION OF RAYLEIGH GROUP VELOCITY

The locations of permanent recording stations in the Southeastern United States lie principally along the Appalachian trend (See Fig. 4). Permanent worldwide standard stations capable of recording long-period seismic signals are located at Spring Hill, Alabama (SHA); Atlanta, Georgia (ATL); McMinnville, Tennessee (CPO) ; Blacksburg, Virginia (BLA); and Oxford, Mississippi (OXF). Portable long-period units have been operated by the Geotechnical Corporation under project Vela, but these stations are also located along the Appalachians. Because of the widely spaced stations, it was impossible to calculate phase velocities directly using triangular arrays of stations. Therefore, epicenters were selected to give travel paths parallel or perpendicular to the Appalachian trend. It was hoped that variations in crustal and upper mantle structure between stations located along the Appalachians could be detected by observing the variation of group velocity of a wave train traveling the station sequence SHA -ATL -BLA parallel to the Appalachian trend or by comparing group velocities at BLA and ATL from waves arriving perpendicular to the Appalachian with those of a normal continental structure.

On the basis of epicentral location, signal amplitude, and availability of records, two epicenters were selected for study. Table II gives the information pertinent to these epicenters.

Table II

Epicenter Location (USGS)	Date	Time (USGS)	Magnitude (USGS)	Focal Depth (km) (USGS)	Distance (km) to station
Jalisco, Mex. 17.8N, 105.9W	11 Oct., 1963	10:17:07.6	5.0	33	BLA - 3286.3 OXF - 2467.3 SHA - 2291.0 ATL - 2757.6
S. Alaska 62.7N, 152.0W	29 June, 1964	07:21:32.8	5.6	33	BLA - 5488.0 OXF - 5276.3 SHA - 5110.0 ATL - 5633.9



LOCATION MAP OF PERMANENT AND TEMPORARY SEISMOGRAPH STATIONS
 USED IN TRAVEL-TIME AND RAYLEIGH WAVE DISPERSION STUDIES

Fig. 4

Records from the standard stations were hand digitized at two second intervals using a plastic grid overlay. This digital data was stored on magnetic tape for processing. Since the azimuths of the epicenters measured from the recording stations did not coincide with either of the horizontal component seismograph orientations, Rayleigh wave motion was contaminated by Love wave motion. In order to separate the Rayleigh and Love wave motions, radial and transverse seismograms were generated from the North-South and East-West components at each station. The relations used in the transformations were

$$\begin{aligned} \text{radial component} &= r = \overline{OE} \cos\theta + \overline{ON} \sin\theta, \text{ and} \\ \text{transverse component} &= t = \overline{OE} \sin\theta - \overline{ON} \cos\theta. \end{aligned}$$

where

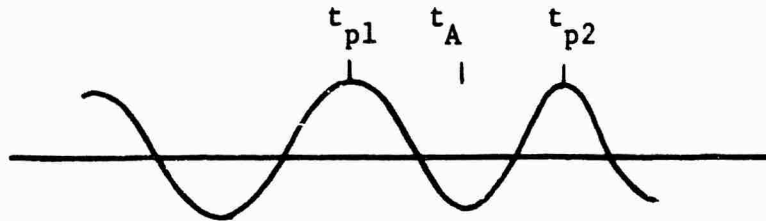
- θ = azimuth of epicenter from station measured counterclockwise from east,
- \overline{OE} = east-west component amplitude, positive toward east,
- \overline{ON} = north-south component amplitude, positive toward north
- $r > 0$ => radial motion toward epicenter, and
- $t > 0$ => transverse motion to right of propagation direction.

Sections of Rayleigh wave motion were then determined from visual inspection of plots of the radial and transverse components. Determination of the particle motion of small amplitude high frequency motion in the presence of large amplitude low frequency motion is difficult. Ideally, the radial and transverse components should be band-pass filtered to separate the frequencies and particle motion then determined for specified frequency intervals. However, due to the computer time involved, this was not feasible for this study. Since only the first higher Rayleigh mode was present on the recordings, the particle motion for the frequencies involved could be fairly well obtained from the unfiltered radial and transverse components.

Vertical component records were convolved with 101 point, digital, band-pass filters described by Minear [1966]. Pass bands of 60-100, 25-62, 16-30, 10-17, and 7-13 sec were used successively. The filtered data was plotted by using a Calcomp plotter. Period was obtained by reading the peak-to-peak period from the Calcomp plots. Arrival time for the period was taken as the time defined by

$$t_A = t_{p1} + \frac{t_{p2} - t_{p1}}{2}$$

with the quantities defined in the following figure.



Group velocity was then obtained by dividing the epicentral distance by the arrival time.

Group velocity vs. period data for the Southern Appalachians is presented in Table III and Figs. 8-11.

TABLE 111. RAYLEIGH WAVE GROUP VELOCITIES FOR THE SOUTHERN APPALACHIANS

EPICENTER-S. ALASKA
STATION-ATLANTA, GA.

Fundamental Rayleigh		First Higher Rayleigh	
Period(sec)	Group Velocity (km/sec)	Period(sec)	Group Velocity (km/sec)
59.66	3.72	8.64	3.52
52.75	3.72	7.85	3.56
41.13	3.53	7.85	3.55
36.99	3.62	7.85	3.51
32.81	3.42	7.07	3.49
30.62	3.38	7.07	3.47
26.69	3.29	7.07	3.49
27.00	3.24	6.28	3.46
27.00	3.19	6.28	3.45
24.02	3.14	6.91	3.50
19.31	3.05	6.12	3.54
18.68	3.02	6.12	3.47
18.84	2.96	5.65	3.52
18.21	2.99	5.34	3.43
18.06	2.86	4.55	3.53
18.06	2.31		
17.90	2.91		
16.80	2.94		
16.17	2.88		
15.70	2.81		
15.17	3.04		
14.13	2.98		
13.25	3.02		
13.03	3.07		
12.09	3.13		
12.09	3.00		
10.99	3.11		
9.99	3.09		
9.26	3.01		
7.54	3.01		
7.54	3.00		
7.22	2.99		
6.59	2.98		

EPICENTER-S. ALASKA
STATION-OXFORD, MISS.

Fundamental Rayleigh		Fundamental Rayleigh	
Period(sec)	Group Velocity (km/sec)	Period(sec)	Group Velocity (km/sec)
67.04	3.84	12.40	3.01
54.79	3.67	12.40	2.96
40.04	3.57	11.78	3.07
34.54	3.49	11.62	3.05
31.40	3.41	10.52	2.98
29.05	3.35	9.89	2.97
26.85	3.14	9.89	2.92
24.81	3.29	9.89	2.70
24.65	3.24	9.73	2.95
23.71	3.09	9.73	2.88
23.08	3.05	8.32	2.93
21.51	2.97	8.16	2.86
20.25	3.01	8.01	2.89
19.94	2.94		
19.94	2.93		
18.37	2.91		
18.06	2.85		
17.74	2.90		
17.43	2.88		
16.64	2.73		
16.17	2.83		
16.17	2.76		
16.01	2.78		
15.86	2.80		
14.97	2.88		
14.86	2.86		
14.70	2.83		
13.56	2.81		
13.19	3.03		
12.87	2.98		

EPICENTER-JALISCO, MEX.
STATION-ATLANTA, GA.

Fundamental Rayleigh		First Higher Rayleigh	
Period(sec)	Group Velocity (km/sec)	Period(sec)	Group Velocity (km/sec)
55.89	3.76	10.05	3.25
44.90	3.52	9.89	3.29
38.78	3.34	9.89	3.22
33.76	3.20	8.79	3.16
27.48	3.20	8.32	2.98
22.45	3.11	8.01	3.13
19.94	3.03	8.01	3.05
17.11	2.97	8.01	3.00
16.80	2.92	7.85	3.08
12.40	2.89	7.07	3.18
12.09	2.70	6.28	3.10
11.93	2.66	5.81	3.03
11.78	2.85		
11.78	2.82		
11.62	2.78		
10.99	2.69		
10.99	2.66		
10.36	2.75		
10.21	2.75		
10.05	2.72		
10.00	2.69		
9.89	2.73		
8.99	2.62		
8.80	2.60		
8.70	2.64		
8.19	2.60		
8.16	2.58		
8.16	2.56		
7.69	2.64		
6.44	2.51		

EPICENTER-JALISCO, MEX.
STATION-BLACKSBURG, VA.

Fundamental Rayleigh		First Higher Rayleigh	
Period(sec)	Group Velocity (km/sec)	Period(sec)	Group Velocity (km/sec)
65.16	4.11	18.37	3.76
62.02	3.81	16.17	3.84
50.08	3.55	16.01	3.98
39.41	3.38	14.13	3.32
32.34	3.36	13.97	3.23
31.87	3.26	13.82	3.91
29.67	3.07	13.66	3.59
26.38	2.99	13.35	3.70
25.90	2.92	13.35	3.54
25.40	2.87	13.03	3.49
19.80	2.77	12.25	3.64
19.50	2.79	12.09	3.66
18.10	2.69	11.93	3.45
14.29	2.77	11.93	3.27
13.50	2.74	11.78	3.19
12.56	2.70	11.66	3.40
12.09	2.63	10.68	3.13
11.93	2.65	10.05	3.16
11.78	2.60	9.73	3.09
9.89	2.58	9.26	3.10
8.01	2.56	8.16	3.05
6.12	2.55	8.01	3.07
		7.85	3.01
		5.97	3.03

TABLE 111 (CONT'D)

EPICENTER-S. ALASKA
STATION-BLACKSBURG, VA.

Fundamental Rayleigh		First Higher Rayleigh	
Period(sec)	Group Velocity(km/sec)	Period(sec)	Group Velocity(km/sec)
66.88	4.06	33.13	4.27
62.64	3.88	32.97	4.16
58.88	3.72	31.09	4.43
49.14	3.73	30.93	4.32
39.41	3.62	30.46	4.54
39.41	3.53	28.73	4.09
31.40	3.45	20.72	4.23
27.00	3.20	20.10	4.35
25.43	3.15	17.11	4.18
25.28	3.10	15.54	4.29
21.82	3.06	15.23	3.94
19.94	3.03	14.44	3.98
19.94	2.97	13.50	4.12
18.68	2.89	13.03	4.20
18.06	3.00	13.03	4.16
18.06	2.94	13.03	4.02
17.58	2.87	12.72	3.90
17.58	2.84	12.72	3.80
16.17	2.89	12.40	3.86
15.86	2.92	12.25	3.83
15.39	2.87	11.93	3.76
13.97	2.84	11.46	3.73
11.62	3.08	11.78	3.70
11.62	3.04	9.89	3.49
11.30	3.06	8.01	3.52
10.21	3.10	7.85	3.46
9.42	3.02	7.69	3.60
9.26	3.00	6.12	3.58
8.32	2.98	6.12	3.54
8.16	2.92	6.12	3.51
8.01	2.93	6.12	3.47
7.85	3.06	5.87	3.55
7.85	2.94	5.65	3.57
7.22	3.00		
7.22	2.99		
7.22	2.97		
6.91	3.07		
6.91	3.04		
6.75	3.05		
6.75	3.03		
6.28	2.96		
6.28	2.90		
6.12	3.02		
5.65	2.91		

5.0 THEORETICAL RAYLEIGH DISPERSION CURVES

The basic Thomson-Haskell matrix method was used to compute phase and group velocity vs. period curves for layered earth models. A computer program was written to compute Rayleigh wave dispersion curves and mode shape using the modified formulation of the Thomson-Haskell method presented by Dunkin [1965]. A program was also written to compute mode shape using the Thomson-Haskell method. A discussion and comparison of the computation methods used is given in this section. Appendix I and II contain detailed descriptions of the actual mechanics of computation and computer programming. Fortran listings of the programs are given in Appendix III.

5.1 Thomson-Haskell Matrix Method

As is well known, the Thomson-Haskell matrix method consists of evaluating the roots of a determinant formed by the repeated multiplication of 4 x 4 layer matrices which are functions of the layer parameters of density, thickness, compressional velocity, shear velocity, as well as phase velocity and period.

Using Haskell's notation, the displacement-stress matrices at the top and bottom of the m^{th} layer are given by

$$\begin{bmatrix} \frac{\dot{u}_m}{c} \\ \frac{\dot{w}_m}{c} \\ \sigma_m \\ \tau_m \end{bmatrix} = a_m \begin{bmatrix} \frac{\dot{u}_{m-1}}{c} \\ \frac{\dot{w}_{m-1}}{c} \\ \frac{\sigma_{m-1}}{c} \\ \frac{\tau_{m-1}}{c} \end{bmatrix} \quad (5.1-1)$$

where $a_m = D_m F_m^{-1}$ is the m^{th} layer matrix. By repeated application of (5.1-1), Haskell shows that, assuming no stresses at the free surface ($\delta = \tau_0 = 0$) and no sources at infinity,

$$\begin{bmatrix} \Delta_n' \\ \Delta_n' \\ \omega_n' \\ \omega_n' \end{bmatrix} = J \begin{bmatrix} \dot{u}_0 \\ c | \dot{u}_0 \\ c | \dot{w}_0 \\ 0 \\ 0 \end{bmatrix} \quad (5.1-2)$$

where $J = F_n^{-1} a_{n-1} \dots a_1$ is the matrix product of the 4 x 4 layer matrices a_m , eliminating Δ_n' and ω_n' between the four equations yields

$$\frac{\dot{u}_0}{\dot{w}_0} = \frac{J_{22} - J_{12}}{J_{11} - J_{21}} = \frac{J_{42} - J_{32}}{J_{31} - J_{41}} \quad (5.1-3)$$

Since the J_{ij} , are functions of phase velocity and wave number, (5.1-3) is an implicit relation between c and k and thus the phase velocity dispersion function. The layer matrix elements of a_m are either trigonometric or hyperbolic functions depending on whether the phase velocity is greater than or less than the layer compressional and/or shear velocities. The multiplication of real and imaginary components of matrices on a computer which does not have complex number sub-routines would in general add considerable complexity to the problem. However, as is shown in Appendix I, the form of the layer matrices leads to a simple solution by which the multiplication of the matrices with real and imaginary elements can be accomplished by the multiplication of certain elements by ± 1 .

5.2 Numerical Difficulties in the Thomson-Haskell Method

In practice, numerical computational difficulties are encountered in the repeated matrix multiplication required to evaluate the roots of (5.1-3). These difficulties are encountered as the product of kH , where k is the wave number, and H is the total thickness of the layered earth model, becomes large. Dorman, Ewing, and Oliver [1960] have used an upper limit of about 30 for kH . When the value of kH reaches about 30, the number of layers can be reduced and the computation continued with a reduced thickness. Little error is introduced by this technique. However, for higher modes and hence, higher frequencies, the product kH may be relatively large even for layered earth models of small total thickness, H .

Dunkin [1965] has shown the numerical difficulties are caused by the computation of large exponentials and a resulting loss of significant figures. Dunkin's development is briefly repeated below in order to show the effect of loss of significance due to the addition of large and small quantities on the Haskell matrix. The argument is applied directly to the Haskell dispersion equation (5.1-3) rather than to the secular equation used by Dunkin.

Let the scalar and vector potential functions for an elastic body have the form

$$\begin{aligned}
 \phi_n &= \exp ik(ct-x) [A_n \exp(ikz \sqrt{c^2/\alpha^2-1}) + B_n \exp(-ikz \sqrt{c^2/\alpha^2-1})] \\
 &= \exp ik(ct-x) [\phi_n^+ + \phi_n^-] \\
 \psi_n &= \exp ik(ct-x) [C_n \exp(ikz \sqrt{c^2/\beta^2-1}) + D_n \exp(-ikz \sqrt{c^2/\beta^2-1})] \\
 &= \exp ik(ct-x) [\psi_n^+ - \psi_n^-]
 \end{aligned}
 \tag{5.2-1}$$

Using (5.2-1) and the equation

$$\bar{S}(u,v,w) = \nabla \cdot \phi + \nabla \times \psi(\psi_1, \psi_2, \psi_3) \quad (5.2-2)$$

the displacement-stress vector, S_n , can be expressed as

$$S_n(z) = T_n \phi_n(z) \quad (5.2-3)$$

where

$$\phi_n(z) = \begin{bmatrix} \phi_n^+ \\ \psi_n^+ \\ \phi_n^- \\ \psi_n^- \end{bmatrix}$$

and T_n is a 4 x 4 matrix function of c , k , and the layer parameters.

Taking the origin at the z_{n-1} interface (5.2-1) gives

$$\phi_{n-1} = A_n + B_n = \phi_n^+(z_{n-1}) + \phi_n^-(z_{n-1})$$

$$\psi_{n-1} = C_n + D_n = \psi_n^+(z_{n-1}) + \psi_n^-(z_{n-1})$$

At the z_n interface

$$\phi_n = A_n \exp(ik_n r_{\alpha n}) + B_n \exp(-ik_n r_{\alpha n}) = \phi_n^+(z_n) + \phi_n^-(z_n)$$

$$\psi_n = C_n \exp(ik_n r_{\beta n}) + D_n \exp(-ik_n r_{\beta n}) = \psi_n^+(z_n) + \psi_n^-(z_n)$$

The relation between $\phi_n(z_n)$ at the z_n interface and $\phi_n(z_{n-1})$ at the z_{n-1} interface is then

$$\phi_n(z_n) = E_n \phi_n(z_{n-1}) \quad (5.2-4)$$

where

$$E_n = \begin{bmatrix} \exp(ik_n r_{\alpha n}) & 0 & 0 & 0 \\ 0 & \exp(ik_n r_{\beta n}) & 0 & 0 \\ 0 & 0 & \exp(-ik_n r_{\alpha n}) & 0 \\ 0 & 0 & 0 & \exp(-ik_n r_{\beta n}) \end{bmatrix} \quad (5.2-5)$$

At the $n-1$ interface

$$S_n(z_{n-1}) = T_n \phi_n(z_{n-1})$$

or

$$\phi_n(z_{n-1}) = T_n^{-1} S_n(z_{n-1}) \quad (5.2-6)$$

Now, by the boundary conditions of the continuity of stress and displacement

$$S_n(z_n) = S_{n+1}(z_n) = T_n \phi_n(z_n) \quad (5.2-7)$$

Substituting (5.2-4) for $\phi_n(z_n)$ and (5.2-6) for $\phi_n(z_{n-1})$ in (5.2-7) gives

$$S_{n+1}(z_n) = T_n E_n T_n^{-1} S_n(z_{n-1}) . \quad (5.2-8)$$

This equation is equivalent to Haskell's equation

$$S_{n+1}(z_n) = a_n S_n(z_{n-1}) , \quad (5.2-9)$$

with $a_n = T_n E_n T_n^{-1}$.

By (5.2-8) the displacement-stress vector is converted into Φ_n , continued through the layer z_n by E_n , and converted back into $S_n(z_n)$ at the interface $n+1$ which is equal to $S_{n+1}(z_n)$. The Haskell layer matrix carries the displacement-stress vector from the n^{th} interface, through the layer, and across the $n+1$ interface in one operation. Eq. (5.2-8) brings into evidence the effect of the "continuing" matrix E_n .

Consider the matrix linking the displacement-stress vectors at the free surface and the last layer of an assumed layered sequence.

$$S_{n-1} = G_{n-1} \cdots G_1 S_0 = P S_0 , \quad (5.2-10)$$

where

$$G_n = T_n E_n T_n^{-1}$$

In the Haskell formulation, the matrix from which the dispersion relation is obtained is given by $J = F_n^{-1} P$ and in the Dunkin formulation this matrix is $T_n^{-1} P$. However, considerations of the numerical evaluation of the P matrix will yield results valid to both developments since the T_n^{-1} or F_n^{-1} do not contain exponential powers.

Let P be written as

$$P = A T_m E_m T_m^{-1} B \quad (5.2-11)$$

where

$$A = G_{n-1} \cdots G_{m+1}$$

$$B = G_{m-1} \cdots G_1$$

Using the definitions of T_m and E_m , it can be shown that the components of P are of the form

$$P_{ij} = B_{ij} \exp i k d_m r_{\alpha m} + C_{ij} \exp i k d_m r_{\beta m} + D_{ij} \exp i k d_m r_{\alpha m} + E_{ij} \exp i k d_m r_{\beta m} \quad (5.2-12)$$

For the Haskell development, F_n^{-1} is of the form

$$F_n^{-1} = \begin{bmatrix} F_{11} & 0 & F_{23} & 0 \\ 0 & F_{22} & 0 & F_{24} \\ F_{31} & 0 & F_{33} & 0 \\ 0 & F_{42} & 0 & F_{44} \end{bmatrix}$$

which gives for the two components J_{12} and J_{22}

$$J_{12} = F_{11} P_{12} + F_{13} P_{32}, \text{ and} \quad (5.2-13)$$

$$J_{22} = F_{22} P_{22} + F_{24} P_{42}$$

Now suppose that for the m^{th} layer $r_{\alpha m}$ and $r_{\beta m}$ are negative imaginary ($c < \alpha$) so that $\exp i k_m r_{\alpha m}$ and $\exp i k_m r_{\beta m}$ may be large depending on the value of k . If the exponential term is large enough, the effect of the smaller terms in P_{ij} will be neglected in computing the P_{ij} , because of loss of significance. In the evaluation of the roots of (5.1-3) the difference ($J_{12} - J_{22}$) must be taken. Although the P_{ij} are large, their differences may be small. Therefore, terms which were lost because of loss of significance in computing the P_{ij} would be important in the difference of J_{12} and J_{22} . Mode shape is computed from repeated applications of (5.1-1) using the starting values of \dot{u}_0 and \dot{w}_0 from (5.1-3). Therefore, the same problem with loss of significance is inherent in the Haskell method of computing modal shape.

5.3 Dunkin Modification of the Haskell Method

Dunkin derives the secular or period equation in the form

$$\text{Det } R_{11} = 0 \quad (5.3-1)$$

Where

$$R = \begin{bmatrix} R_{11} & R_{12} \\ R_{21} & R_{22} \end{bmatrix} = T_p^{-1} G_{p-1} \dots G_1 \quad (5.3-2)$$

He shows that $\text{Det } R_{11}$ can be expanded as a product of the second order subdeterminants of T_p^{-1} and G_p yielding

$$\text{Det } R_{11} = t^{p-1} \begin{vmatrix} 12 \\ ab \end{vmatrix} g^{p-1} \begin{vmatrix} ah \\ cd \end{vmatrix} \dots g^1 \begin{vmatrix} ef \\ 12 \end{vmatrix} , \quad (5.3-3)$$

where $g^p \begin{vmatrix} ij \\ kl \end{vmatrix}$ is the second order subdeterminant of G_p involving rows i and j and columns k and l . Dunkin has shown that by using algebraic expressions for the subdeterminants of the G_p , numerical difficulties with loss of significance can be avoided since the products of like exponentials normally occurring in the secular function are excluded at the start. Products of unlike exponentials for a given layer effectively increase the magnitude of $\text{Det } R_{11}$. To prevent machine overflow, the secular function can be divided by the two largest exponents when these exponents become real and the exponential expression becomes hyperbolic. This results in no loss of significance.

Explicit expressions for the g_{kl}^{ij} and the g_{ij} are given in Appendix II for real frequencies and wave numbers. These are slightly different from the definitions of Dunkin, since he assumes complex frequencies.

Mode shapes are computed using the following relation of Dunkin discussed in Appendix II ,

$$R_n^m(z;a) = r_{11}^{-1} \begin{vmatrix} p \\ 1r \end{vmatrix} g_{rs}^{p-1} \dots g_{vb}^n (z_n - z) g^n (z - z_{n-1}) \begin{vmatrix} ab \\ cd \end{vmatrix} \dots g^1 \begin{vmatrix} ef \\ 21 \end{vmatrix} \quad (5.3-4)$$

5.4 Computational Procedure

The Dunkin method was programmed in Fortran II for the Bunker-Ramo 340 computer. Equation (5.3-1) was used for the determination of Rayleigh wave dispersion curves. Equation (5.3-4) was used to compute the mode shape once the roots of (5.3-1) were obtained. A double precision program was written in Fortran II for the IBM 360-75 using the Haskell method for computing mode shape. Equation (5.1-1) was used for this computation. Figs. 5 and 6 are flow charts of the computer program FLATRAY used in the computation of Rayleigh dispersion and modal shape. A computer listing of the program is given in Appendix III.

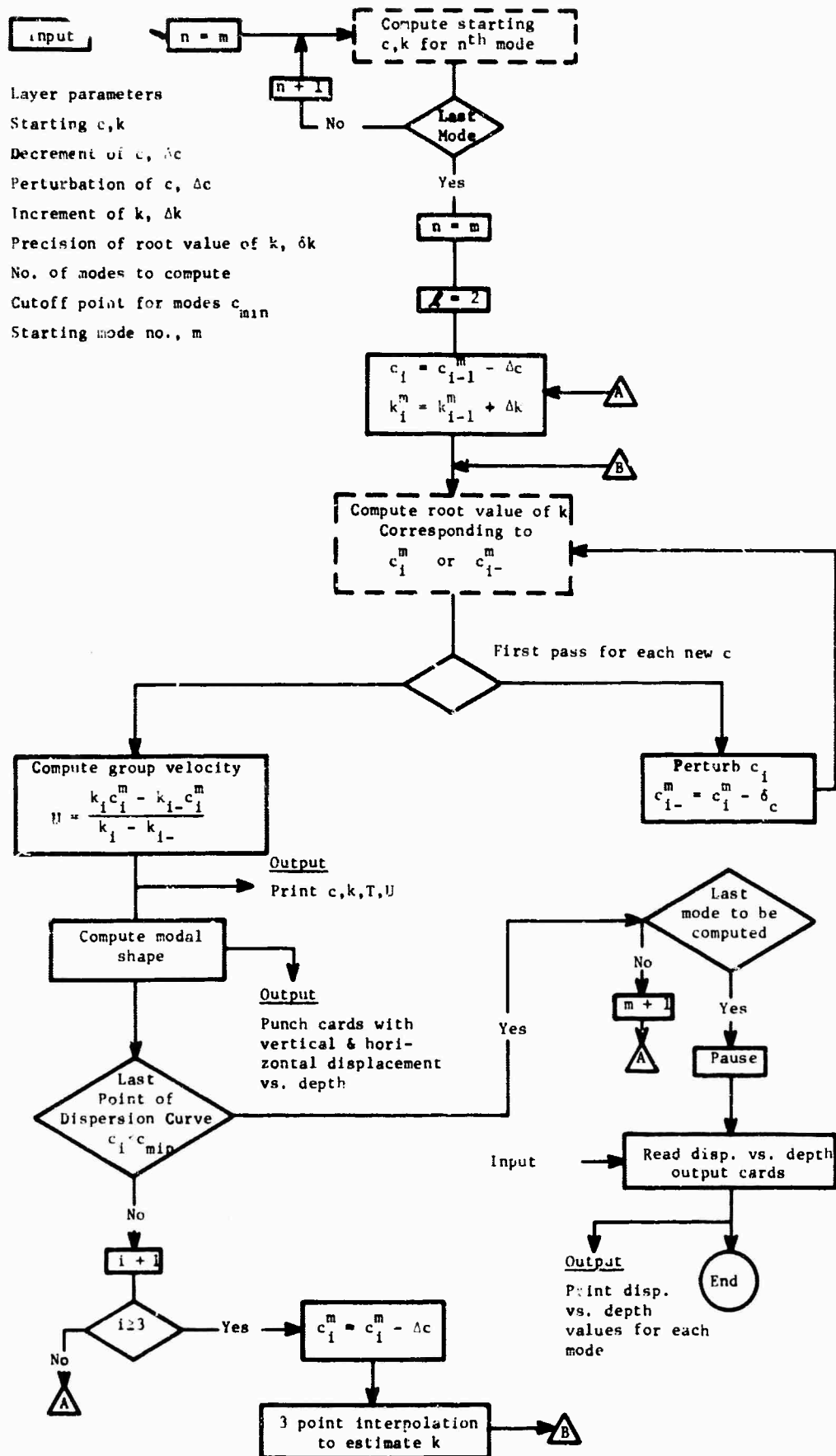


Fig. 5. Flow chart of FLATRAY

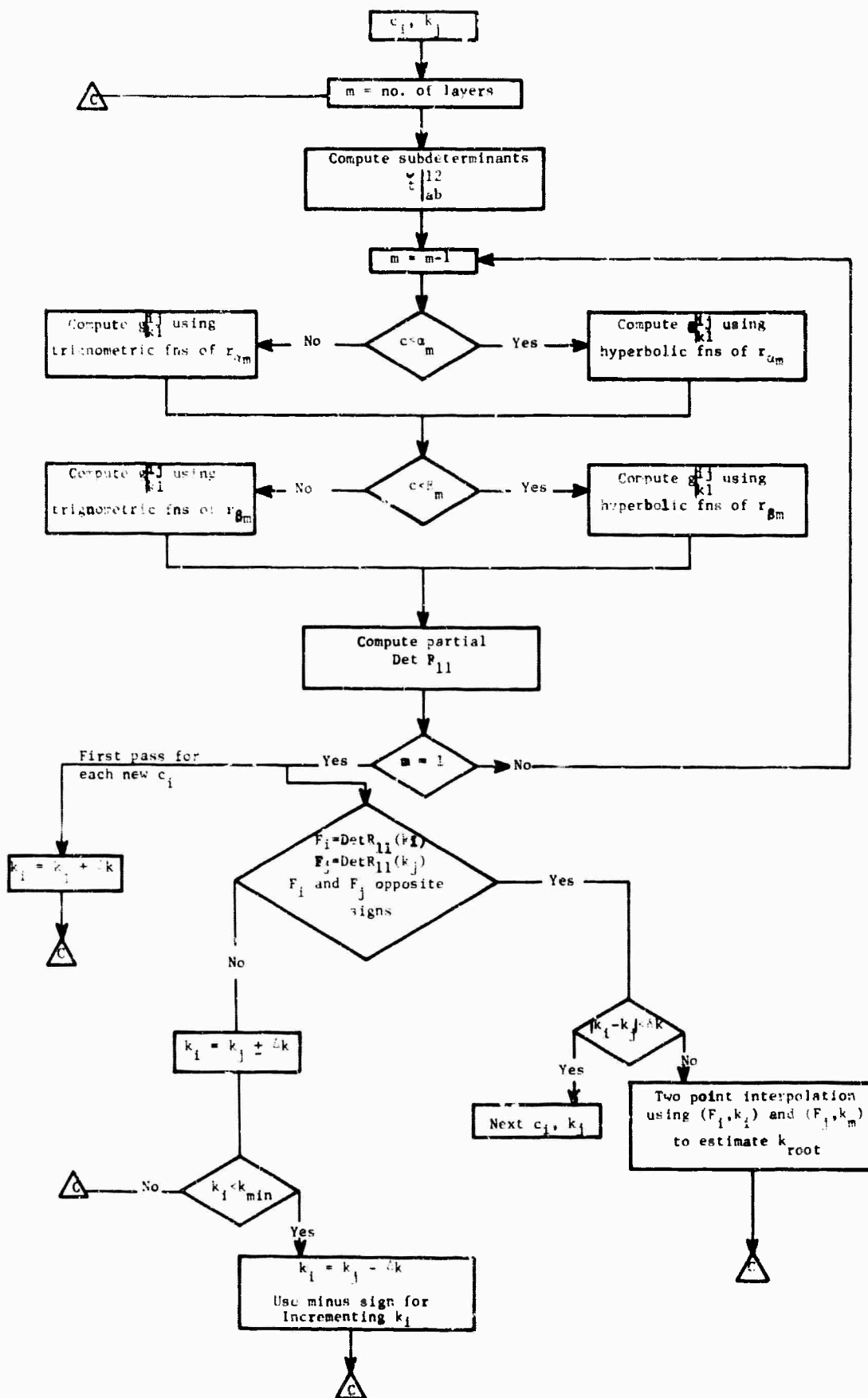


Fig. 6. Flow chart for determining roots of secular function, $\text{Det } R_{11}$ (Dashed boxes of Fig. 5)

Root Finding Scheme

The technique used for finding the roots of (5.3-1) consists of two steps. In order to determine roots for different modes, a given phase velocity, c_0 , and starting wave number, k_{i0} , are specified. k_{i0} is then incremented using the constant c_0 value until a root is bracketed. A two point interpolation scheme is then used until the difference between two values of k which successively bracket the root is less than an input value. If more than one mode is to be investigated, k is incremented from its value at the last root found using the same value of c_0 until the next root is found. Thus, the roots along a constant c curve are found which correspond to different modes. In order to define a particular mode, computation begins at c_0 and the k_{i0} corresponding to the desired mode. c is decremented and k incremented by values specified as input parameters. k is varied at the new $c - \Delta c$ until the root is bracketed. Two point interpolation is then used until k is obtained with the desired accuracy. The process of decrementing c and incrementing k is continued until three points on a given modal dispersion curve are found. A three point Gregory-Newton interpolation scheme is then used to estimate the next root on the curve. The process of interpolation and bracketing continues until a dispersion curve is defined to some minimum specified value of c .

Group velocity values are computed by perturbing c a small amount from a value at which a corresponding k has been found. k is found for the perturbed c and a two point difference scheme used to evaluate group velocity, U , according to

$$U = \frac{d\omega}{dk} = \frac{\frac{2\pi}{T_2} - \frac{2\pi}{T_1}}{k_2 - k_1}$$

From Table VI it can be seen that the group velocity curves computed by the Dunkin method for many layered models agree with those computed for models with reduced thickness to within a few tenths of a per cent. However, the section must be taken thick enough to include the entire depth to which appreciable particle motion extends. This is illustrated by the first higher mode for the Gutenberg-Birch II model. The period value at 5.00 km/sec is 50.0301 sec for the 400 km section, and 46.4060 sec for the 1000 km section. However, reference to the displacement vs. depth curves in Appendix IV shows that the 400 km section does not include the total depth to which vertical particle motion extends at this period.

Although thick sequences can be used to compute shorter period group velocity curves, it is considerably more economical in computer time to use thinner sequences of fewer layers. Displacement depth curves, such as those in Appendix IV, can be used to indicate the necessary total thickness to be used at given periods.

Modal Shape

After a point (c,k) was found on a given dispersion curve, the mode shape for the given (c,k) was computed using (5.3-4). Horizontal and vertical displacements vs. depth values were then punched out on cards to be used in computing the variation of phase velocity due to variation in layer parameters from INTEGRAL. Modal shape was computed using both the Dunkin and Haskell methods. A double precision program was used in computing modal shape by the Haskell Method. Table IV shows the comparative results for the two methods. Values for horizontal and vertical particle amplitudes agree very well ($<.03\%$) for the first four layers in each case considered in Table IV. After this, the differences between the two methods increase rapidly. The rapid increase of particle amplitude with depth in

TABLE IV. Fundamental Rayleigh mode vertical and horizontal Particle amplitudes computed by Dunkin and Haskell Methods for the Gutenberg-Birch II model. Displacement normalized to the vertical displacement at the surface

Period = 25.440
 Phase Velocity = 3.8000
 7 Layer model

Section Thickness = 140 km

HASKELL METHOD		DUNKIN METHOD	
Vertical	Horizontal	Vertical	Horizontal
1.000000	.6950871	1.000000	-.6950871
.886979	.0084581	.886972	.0084451
.518503	.0569591	.518524	.0568251
.303885	.1063181	.304132	.0400851
.164817	.0761211	.062881	.0126391
.078571	.0509691	.014165	.0034631
.018264	.0484311	.002693	.0009951

Period = 25.1380
 Phase Velocity 3.8000
 17 Layer model

Section Thickness = 400 km

1.000000	-.6950441	1.000000	-.6950441
.886837	.0086111	.886883	.0085831
.518193	.0569161	.518278	.0569481
.303773	.1056621	.303749	.0401191
.165958	.0734501	.062646	.0126671
.084840	.0412981	.013984	.0034971
.043072	.0154241	.002541	.0010301
.034665	-.0212121	-.000083	.0004061
.087474	-.1191061	-.000034	.0002461
.324986	-.4357481	-.000713	.0001991
1.117859	-1.4845031	-.000685	.0001791
4.078959	-4.9270861	-.000643	.0001651
13.757256	-16.1905901	-.000595	.0001531
45.749210	-53.0181841	-.000553	.0001431
150.983339	-173.2435981	-.000512	.0001331

TABLE IV (Cont'd)

Period = 25.1380 (Cont'd)
 Phase Velocity=3.8000
 17 Layer model

Section Thickness = 400 km

HASKELL METHOD		DUNKIN. METHOD	
Vertical	Horizontal	Vertical	Horizontal
8.176407	-567.580725i	-.000474	.000123i
10070.040164	-11362.129728i	-.001556	.000026i

Period = 106.4400
 Phase Velocity=4.2000
 35 Layer model

Section Thickness = 2898 km

1.000000	-.838062i	1.000000	-.838062i
1.047271	-.599088i	1.047270	-.599012i
1.054375	-.406096i	1.054340	-.405972i
1.048108	-.190905i	1.048030	-.182671i
1.010899	-.052715i	.968018	-.048623i
.954535	.043822i	.883244	.039389i
.886795	.109889i	.793526	.095305i
.812528	.152015i	.703175	.127442i
.735438	.175957i	.615440	.142587i
.658577	.186915i	.532770	.146331i
.583974	.187969i	.456412	.142087i
.513373	.182590i	.387350	.133150i
.447853	.173001i	.325880	.121633i
.387824	.160789i	.271911	.108862i
.333572	.147617i	.225107	.096133i
.284944	.134126i	.184894	.083957i
.184929	.099159i	.115100	.048651i
.174067	.072333i	.055227	.027497i
.024591	.043435i	.008158	.006575i
-.005338	.039627i	-.001498	.004761i
-.034168	.043999i	-.004566	.004231i
-.117644	.086439i	-.011717	.003220i
-.299466	.195575i	-.010744	.002691i

TABLE IV (Cont'd)

Period = 106.4400 (Cont'd)
 Phase Velocity=4.2000
 35 Layer model

Section Thickness = 2898 km

HASKELL METHOD		DUNKIN METHOD	
Vertical	Horizontal	Vertical	Horizontal
-.734195	.438798i	-.009416	.002297i
-1.730194	.869893i	-.008134	.001934i
-7.174500	-1.427081i	-.023747	.000546i
67.316536	-162.893231i	-.006543	.000141i
2727.220784	-3866.697396i	-.001763	.000036i
58523.227239	-72877.252431i	-.000463	.000009i
.108 x 10 ⁷	-.127 x 10 ⁷ i	-.000119	.000002i
.188 x 10 ⁸	-.214 x 10 ⁸ i	-.000030	.000000i
.319 x 10 ⁹	-.355 x 10 ⁹ i	-.000007	.000000i
.525 x 10 ¹⁰	-.576 x 10 ¹⁰ i	-.000002	.000000i
.855 x 10 ¹¹	-.928 x 10 ¹¹ i	-.000000	.000000i
.329 x 10 ¹²	-.352 x 10 ¹² i	-.000000	.000000i

the Haskell Method results from the repeated multiplication of 4 x 4 layer matrices and gradual loss of significance in the matrix multiplication. Since the Haskell Method starts at the top layer and works down, and the Dunkin Method starts at the bottom layer and works up, the agreement of the two methods in the near surface layers indicates that the Dunkin Method is yielding correct displacement values over the entire layered sequence. In some cases when relative high frequency points on a dispersion curve were being computed with a many layered model, displacements computed by the Dunkin Method showed some slight perturbations with depth rather than a smooth decrease. Displacement values also tended to change signs as they decreased to very small quantities with depth. This is seen in the vertical displacements for the 35 layer case in Table IV. Horizontal displacement curves generally have one more lobe than the corresponding vertical displacement curves.

Modal shapes for the Gutenberg-Birch model are shown graphically in Appendix IV.

Earth Flattening Approximation

The earth flattening approximation introduced by Alterman, Jarosch, and Pekeris [1961] was used to modify the layer velocities. As has been shown by Kovach & Anderson [1964], the effect of sphericity is not negligible even for higher modes. The linear increase in velocity introduced in the earth flattening approximation is specified by the parameter

$$\xi = \left(\frac{r_m}{a} \right)^2$$

The value of r_m for a layer was taken as the radius to the center of the layer; a is the mean radius of the earth, 6371 km. Layer velocities approximately corrected for sphericity are then given by

$$\alpha'_m = \alpha_m \xi^{-1/2}$$

$$\beta'_m = \beta_m \xi^{-1/2}$$

5.5 Variation of Phase Velocity with Layer Parameters

The energy integrals for elastic wave propagation [Meissner, 1926; Jeffreys, 1934] have been used by several authors, notably Anderson [1964] and Takeuchi and Dorman [1964] to derive explicit relations between the variation of phase velocity and the variation of layer parameters. Necessary data for the evaluation of the partial derivatives of phase velocity with respect to layer parameters are horizontal and vertical particle amplitude vs. depth values.

For Rayleigh waves, the potential and kinetic energy averaged over a cycle are

$$4T = \int \rho \omega^2 (u^2 + w^2) dz$$

$$4V = \int [\lambda(u-w')^2 + \mu(2k^2u^2 + 2w'^2) + k^2w^2 + u'^2 + 2ku'w] dz$$

where

u = horizontal displacement

w = vertical displacement

u' = $\frac{\partial u}{\partial z}$, and the integration extends over the entire depth.

Using the fact that the kinetic and potential energy averaged over a period are equal we obtain

$$\omega^2 I_1 = k^2(I_2 + I_5) + k(I_3 + I_6) + (I_4 + I_7), \quad (5.5-1)$$

where

$$\begin{aligned} I_1 &= \int \rho (u^2 + w^2) dz & I_2 &= \int \lambda u^2 dz \\ I_3 &= \int 2\lambda u w' dz & I_4 &= \int \lambda w'^2 dz \\ I_5 &= \int \mu (2u^2 + w^2) dz & I_6 &= -\int 2\mu u' w dz \\ I_7 &= \int \mu (2w'^2 + u^2) dz \end{aligned} \quad (5.5-2)$$

For a layered sequence of n layers, one can define

$$I_{1m} = \int_{z_m}^{z_{m+1}} \rho (u^2 + w^2) dz \quad (5.5-3)$$

and similarly for the other integrals. Thus,

$$I_i = \sum_{m=1}^n I_{im} \quad (5.5-4)$$

A perturbation of a layer parameter in the m^{th} layer will cause a perturbation in the integral, I_i , for the entire layered sequence of

$$\delta I_i = \delta I_{im} \quad (5.5-5)$$

Differentiating (5.5-1) with respect to the layer parameters, the partial derivatives of c with respect to the layer parameters are obtained. Thus,

$$\left(\frac{\partial c}{\partial \mu_m}\right)_{\rho, \lambda, d, \omega} = (ck^2 \frac{\partial I_{5m}}{\partial \mu} + ck \frac{\partial I_{6m}}{\partial \mu} + c \frac{\partial I_{7m}}{\partial \mu}) / D \quad (5.5-6)$$

where

$$D = k[2k(I_2 + I_5) + I_3 + I_6]$$

with the integration of the integrals in D extending over the entire layered sequence.

$$\left(\frac{\partial c}{\partial \rho_m}\right)_{\lambda, \mu, d, \omega} = -c\omega^2 \frac{\partial I_{1m}}{\partial \rho} / D \quad (5.5-7)$$

$$\left(\frac{\partial c}{\partial \lambda_m}\right)_{\mu, \rho, d, \omega} = (ck^2 \frac{\partial I_{2m}}{\partial \lambda} + ck \frac{\partial I_{3m}}{\partial \lambda} + c \frac{\partial I_{4m}}{\partial \lambda}) / D \quad (5.5-8)$$

$$\left(\frac{\partial c}{\partial \beta_m}\right)_{\rho, \alpha, d, \omega} = 2\rho\beta \left[\left(\frac{\partial c}{\partial \mu_m}\right)_{\rho, \lambda, d, \omega} - 2 \left(\frac{\partial c}{\partial \lambda_m}\right)_{\mu, \rho, d, \omega} \right] \quad (5.5-9)$$

Assuming ρ, α, β as independent and ρ, λ, μ as dependent

$$\left(\frac{\partial c}{\partial \rho_m}\right)_{\alpha, \beta, d, \omega} = \left(\frac{\partial c}{\partial \rho_m}\right)_{\lambda, \mu} + \left(\frac{\partial c}{\partial \lambda_m}\right)_{\rho, \mu} \left(\frac{\partial \lambda}{\partial \rho_m}\right)_{\alpha, \beta} + \left(\frac{\partial c}{\partial \mu_m}\right)_{\rho, \lambda} \left(\frac{\partial \mu}{\partial \rho_m}\right)_{\alpha, \beta} .$$

Substituting

$$\left(\frac{\partial \lambda}{\partial \rho_m}\right)_{\alpha, \beta} = \alpha_m^2 - 2\beta_m^2 \quad \text{and}$$

$$\left(\frac{\partial \mu}{\partial \rho_m}\right)_{\alpha, \beta} = \beta_m^2 ,$$

gives

$$\left(\frac{\partial c}{\partial \rho_m}\right)_{\alpha, \beta, d, \omega} = -c\omega^2 \frac{\partial I_{1m}}{\partial \rho} / D + \left(\frac{\partial c}{\partial \lambda_m}\right)_{\mu, \rho, \omega, d} (\alpha_m^2 - 2\beta_m^2) + \beta_m^2 \left(\frac{\partial c}{\partial \mu_m}\right)_{\rho, \lambda, d, \omega} \quad (5.5-10)$$

$$\left(\frac{\partial c}{\partial \alpha_m}\right)_{\rho, \beta, d, \omega} = 2\rho_m \alpha_m \left(\frac{\partial c}{\partial \lambda_m}\right)_{\rho, \mu, d, \omega} \quad (5.5-11)$$

$$\left(\frac{\partial c}{\partial d}\right)_{\mu, \lambda, \rho, \omega} = [-c\omega^2 \frac{\partial I_1}{\partial d} + ck^2 \left(\frac{\partial I_2}{\partial d} + \frac{\partial I_5}{\partial d}\right) + ck \left(\frac{\partial I_3}{\partial d} + \frac{\partial I_6}{\partial d}\right) + c \left(\frac{\partial I_4}{\partial d} + \frac{\partial I_7}{\partial d}\right)] / D$$

The group velocity can be expressed in terms of the integrals I_i by

$$U = \frac{2(I_2 + I_5)k + (I_3 + I_6)}{1} \quad (5.5-12)$$

Equations (5.5-6), (5.5-8), (5.5-9), (5.5-10), (5.5-11), (5.5-12), and (5.5-13) with the definitions of (5.5-2) were programmed for the IBM 360-75 computer. The integrals of (5.5-2) were evaluated numerically using polynomial approximations to the particle displacements obtained from the modal shape calculations. A sliding fitting procedure was used in determining the polynomials. In this procedure, a polynomial is fitted to say n points at the depths $z_i, z_{i+1}, \dots, z_{i+n}$; and the integrals and their derivatives evaluated over the interval $z_{i+n} - z_i$. The polynomial fit is then shifted to drop one layer and pick up one layer, i.e., to the points at depths

z_{i+1} , z_{i+2} , ... z_{i+1+n} . By using polynomial approximations, the integrals of the derivatives are simply the integrals of the derivatives of the polynomials. Third degree polynomials were found to give adequate fits to the displacement data.

A Fortran listing of the program, INTEGRAL, for computing the partial derivatives of phase velocity , c , with respect to layer parameters is given in Appendix III. Results of computation of the partial derivatives for the Gutenberg-Birch 11 continental model are given in Appendix IV.

6.0 CRUSTAL AND UPPER MANTLE STRUCTURE IN THE SOUTHEASTERN UNITED STATES

Gravity, local travel-time, and Rayleigh wave dispersion data were used to determine crustal and upper mantle structure for the Southeastern United States. Results of the Rayleigh dispersion study and a comparison with the gravity and travel-time results are given in this section.

Observed dispersion curves could be constructed only for periods less than about 50 seconds. Therefore, crustal structure was concentrated on and the upper mantle structure below 70 km was assumed to be that of the Gutenberg-Birch II continental model. The Gutenberg-Birch II crustal structure was used as the basic model for estimating the Southern Appalachian structure. Variations of phase velocity with layer parameters computed for the Gutenberg-Birch II model (See Appendix IV) were used to vary this basic model to yield dispersion curves fitting the observed data. Velocity and density structure of the models considered are given in Table V and Fig. 7. Values of the "earth flattening" velocities for the Gutenberg-Birch II are also given to indicate the effective increase of velocity with depth.

Fundamental and first higher Rayleigh mode group velocity vs. period data observed in the Southern Appalachians (Table III) are shown in Figs. 8-11. Rayleigh wave dispersion curves computed as described in Section 5.0 are given in Table VI and Figs. 8-11 for the models Gutenberg-Birch II, 310, 314, 315, and 320 defined in Table V.

Group velocity curves for waves traveling approximately perpendicular (perpendicular waves) to the Appalachians are quite similar (Figs. 8-11). They all have a local minimum of about 2.85 km/sec at a period of 17 sec, and a local maximum of about 3.10 km/sec at around 12 sec. For periods shorter than about 10 seconds the curves flatten out at about 3.0 km/sec. First higher Rayleigh mode curves indicate a broad minimum of 3.5 km/sec

TABLE V. Layer Parameters for Crustal and Upper Mantle Models

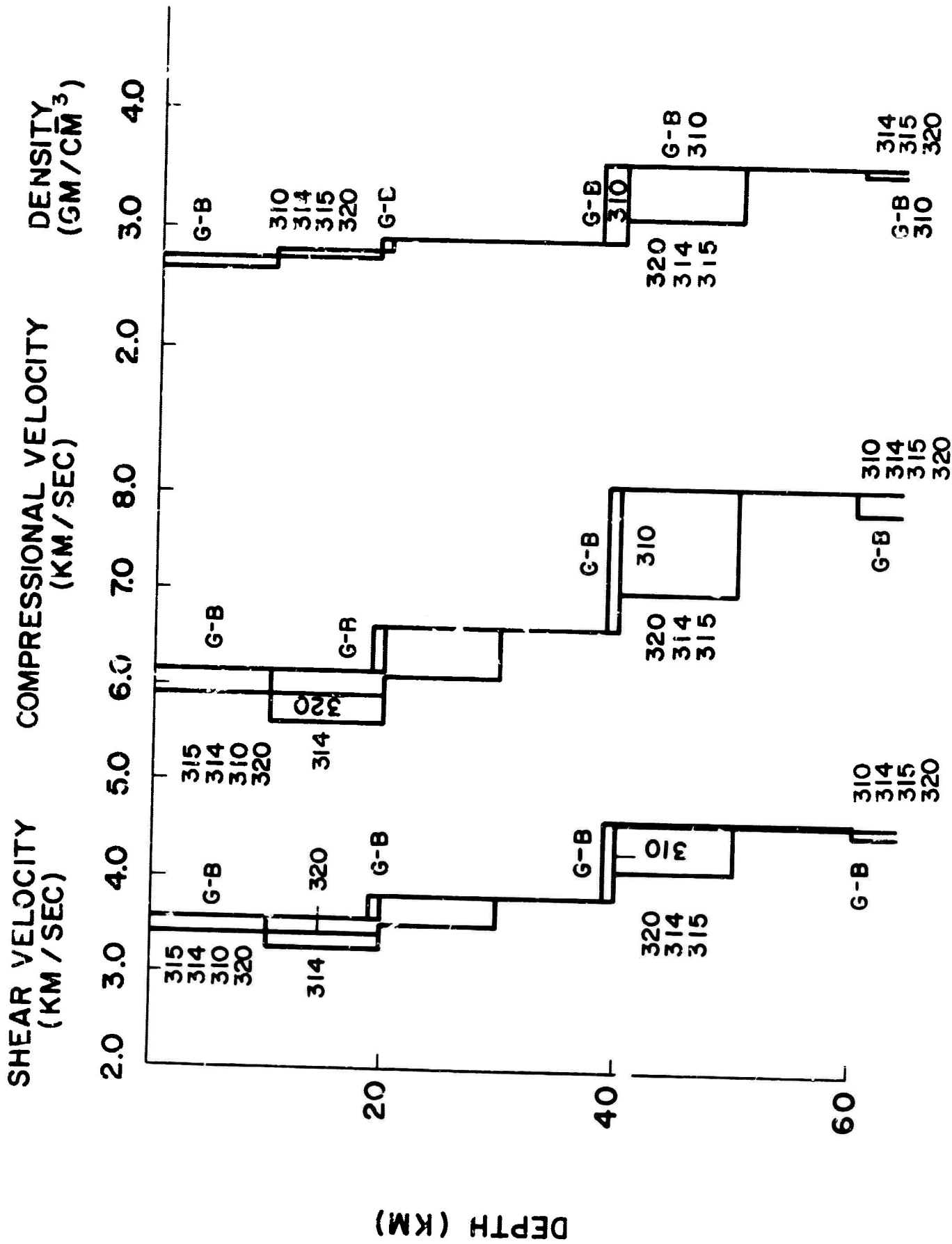
GUTENBERG-BIRCH II

FLAT EARTH				EARTH FLATTENING			
α	β	ρ	d	α	β	ρ	d
6.1400	3.5500	2.7500	19.00	6.1486	3.5550	2.7500	19.00
6.5800	3.8000	2.9000	19.00	6.6090	3.8167	2.9000	19.00
8.0800	4.6000	3.5700	22.00	8.1422	4.6354	3.5700	22.00
7.8700	4.5100	3.5100	20.00	7.9574	4.5601	3.5100	20.00
7.8000	4.4500	3.4900	20.00	7.9115	4.5136	3.4900	20.00
7.8300	4.4200	3.5000	20.00	7.9670	4.4974	3.5000	20.00
7.8900	4.4000	3.5100	20.00	8.0541	4.4915	3.5100	20.00
7.9400	4.3900	3.5300	20.00	8.1314	4.4958	3.5300	20.00
8.0000	4.4000	3.5500	20.00	8.2192	4.5206	3.5500	20.00
8.0600	4.4200	3.5600	20.00	8.3074	4.5557	3.5600	20.00
8.1200	4.4500	3.5800	20.00	8.3961	4.6013	3.5800	20.00
8.2000	4.4800	3.6100	20.00	8.5067	4.6476	3.6100	20.00
8.2700	4.5200	3.6300	20.00	8.6074	4.7044	3.6300	20.00
8.3500	4.5700	3.6500	20.00	8.7191	4.7720	3.6500	20.00
8.4300	4.6100	3.6800	20.00	8.8313	4.8294	3.6800	20.00
8.5100	4.6600	3.7000	50.00	8.9670	4.9102	3.7000	50.00
8.7500	4.8100	3.7700	50.00	9.2969	5.1106	3.7700	50.00
9.0000	4.9500	3.8500	100.00	9.6840	5.3262	3.8500	100.00
9.4900	5.2200	4.0000	50.00	10.3422	5.6888	4.0000	50.00
9.7400	5.3600	4.0700	50.00	10.7062	5.8917	4.0700	50.00
9.9900	5.5000	4.1500	100.00	11.1249	6.1248	4.1500	100.00
10.5000	5.7700	4.3000	100.00	11.9007	6.5397	4.3000	100.00
10.9000	6.0400	4.4200	100.00	12.5775	6.9696	4.4200	100.00
11.3000	6.3000	4.5400	100.00	13.2798	7.4038	4.5400	100.00
11.4000	6.3500	4.5700	200.00	13.7780	7.6746	4.5700	200.00
11.8000	6.5000	4.6900	200.00	14.8243	8.1660	4.6900	200.00
12.0500	6.6000	4.7700	200.00	15.7602	8.6321	4.7700	200.00
12.3000	6.7500	4.8500	200.00	16.7759	9.2063	4.8500	200.00
12.5500	6.8500	4.9200	200.00	17.8824	9.7606	4.9200	200.00
12.8000	6.9500	5.0000	200.00	19.0925	10.3666	5.0000	200.00
13.0000	7.0000	5.0600	200.00	20.3437	10.9543	5.0600	200.00
13.2000	7.1000	5.1200	200.00	21.7245	11.6852	5.1200	200.00
13.4500	7.2000	5.1900	200.00	23.3411	12.4949	5.1900	200.00
13.7000	7.2500	5.2700	98.00	24.7819	13.1145	5.2700	98.00
13.6500	7.2000	5.2500	∞	25.0395	13.2077	5.2500	∞

TABLE V. (Cont'd)

MODEL 310				MODEL 314			
α	β	ν	d	α	β	ρ	d
5.8800	3.3800	2.6700	10.00	5.8800	3.3800	2.6700	10.00
6.1400	3.5500	2.7600	10.00	5.6000	3.2400	2.7600	10.00
6.5800	3.8000	2.9000	10.00	6.1000	3.5000	2.9000	10.00
6.5800	3.8000	2.9000	10.00	6.6000	3.8000	2.9000	10.00
8.0800	4.6000	3.5700	20.00	7.0000	4.1000	3.1000	10.00
				8.0800	4.6000	3.5700	20.00
Same as Gutenberg-Birch II to 400 km				Same as Gutenberg-Birch II to 810 km			

MODEL 315				MODEL 320			
α	β	ρ	d	α	β	ρ	d
5.8800	3.3800	2.6700	10.00	5.8800	3.3800	2.6700	10.00
6.1400	3.5500	2.7600	10.00	5.8800	3.3800	2.7500	10.00
6.5800	3.8000	2.9000	10.00	6.1000	3.5000	2.9000	10.00
6.5800	3.8000	2.9000	10.00	6.6000	3.8000	2.9000	10.00
7.0000	4.1000	3.1000	10.00	7.0000	4.1000	3.1000	10.00
8.0800	4.6000	3.5700	20.00	8.0800	4.6000	3.5700	20.00
Same as Gutenberg-Birch II to 810 km				Same as Gutenberg-Birch II to 810 km			



CRIJSTM AND UPPER MANTLE MODELS

Fig. 7

TABLE VI. Rayleigh wave dispersion curves for Gutenberg-Birch II models,
and models 310, 314, and 315

GUTENBERG-BIRCH II

FUNDAMENTAL RAYLEIGH MODE

Section Thickness 2898.00

c	k	T	U	T
4.5000	.00850	164.2671		
4.4000	.00961	148.5391	3.6990	143.8940
4.3000	.01131	129.1709	3.7695	123.5369
4.1999	.01405	106.4402	3.8361	99.2251
4.0999	.01984	77.2556	3.9112	65.9224
3.9999	.03815	41.1794	3.7346	37.1515
3.8999	.05419	29.7316	3.4039	28.3452
3.7999	.06624	24.9623	3.1759	24.0856
3.6999	.07815	21.7314	3.0493	21.0107
3.5998	.09202	18.9673	2.9510	18.3398
3.4998	.10996	16.3264	3.0336	15.5185
3.3998	.14161	13.0509	3.1084	11.9219

Section Thickness 400.00

4.0000	.03801	41.3293		
3.9000	.05594	29.8693	3.4253	28.4013
3.8000	.06578	25.1380	3.2096	24.1929
3.7000	.07808	21.7493	3.0305	21.0535
3.5999	.09207	18.9572	2.9639	18.3140
3.4999	.11010	16.3054	3.0331	15.4998
3.3999	.14220	12.9958	3.1018	11.9019

Section Thickness 140.00

4.0000	.03730	42.1107		
3.9000	.05409	29.7861	3.4066	28.3880
3.8000	.06576	25.1423	3.1768	24.2579
3.7000	.07762	21.8791	3.0923	21.0892
3.5999	.09150	19.0747	2.9947	18.3862
3.4999	.11001	16.3184	3.0426	15.4971
3.3999	.14249	12.9695	3.0988	11.8907

FIRST HIGHER RAYLEIGH MODE

Section Thickness 2898.00

c	k	T	U	T
6.0000	.01020	102.6767		
5.9000	.01091	97.6155	4.5030	96.2532
5.8000	.01174	92.2541	4.4644	90.8938
5.6999	.01269	86.8711	4.4340	85.5044
5.5999	.01377	81.4673	4.4137	80.0789
5.4999	.01503	75.9839	4.3971	74.5686
5.3999	.01653	70.4033	4.3821	68.9585
5.2999	.01832	64.7021	4.3720	63.2178

TABLE VI. (Cont'd)

FIRST HIGHER RAYLEIGH MODE (Cont'd)

Section Thickness 2898.00 (Continued)				
c	k	T	U	T
5.1998	.02053	59.578	4.3631	57.3296
5.0998	.02331	52.5603	4.3539	51.2881
4.9999	.02690	46.7207	4.3448	45.1023
4.8999	.03172	40.4258	4.3363	38.7565
4.7999	.03854	33.9652	4.3316	32.2275
4.6998	.04900	27.2834	4.3340	25.4277
4.5998	.06780	20.1477	4.3586	17.9272
Section Thickness 1000.00				
5.4000	.01661	70.0684		
5.3000	.01837	64.5405	4.4587	62.8706
5.2000	.02062	58.5864	4.3608	57.0707
5.0999	.02345	52.5303	4.3509	50.9751
4.9999	.02708	46.4060	4.2904	44.9442
4.8999	.03199	40.0905	4.3225	38.4821
4.7999	.03879	33.7500	4.3062	32.1265
4.6998	.04933	27.1034	4.3338	25.2612
Section Thickness 400.00				
5.0000	.02512	50.0301		
4.9000	.03111	41.2115	4.4079	39.2169
4.8000	.03846	34.0337	4.3302	32.2991
4.6999	.04883	27.3780	4.3458	25.4449
4.5999	.06819	20.0320	4.3531	17.8824
4.4999	.11357	12.2945	4.1959	11.2612
4.4000	.15149	9.4265		
4.3000	.17634	8.2863	3.5422	8.0520
4.2000	.20128	7.4324	3.3111	7.2619
4.0999	.22937	6.6814	3.3545	6.4906
3.9999	.25763	5.8694	3.4094	5.6467
3.8999	.32599	4.9423	3.4869	4.6556
3.7999	.43139	3.8330	3.4694	3.5446
3.6999	.61350	2.7681	3.4616	2.4623
Section Thickness 140.00				
3.9000	.32410	4.9709	3.9114	8.4005
3.8000	.43142	3.8327	3.4763	3.5371
3.7000	.61704	2.7521	3.4545	2.4586

TABLE VI. (Cont'd)

SECOND HIGHER RAYLEIGH MODE

Section Thickness 400.00

c	k	T	U	T
4.9000	.05537	23.1581	4.2866	22.2932
4.8000	.06549	19.9891	4.2627	19.1184
4.6999	.08015	16.6789	4.2938	15.6739
4.5999	.10807	12.6396	4.3836	11.0562
4.5000	.25165	5.5484	3.9105	5.3337
4.3999	.29310	4.8721	4.4642	6.2623
4.2999	.32739	4.4632	3.2661	4.3787
4.1999	.36497	4.0990	3.1949	4.0190
4.0999	.40722	3.7634	3.4253	3.6417
3.9999	.47463	3.3096	3.4644	3.1683
3.8999	.59153	2.7237	3.5669	2.5201
3.7998	.84393	1.9593	3.4754	1.8086

Section Thickness 140.00

4.6000	.09402	14.5273		
4.5000	.25218	5.5369	3.8832	5.3339
4.3999	.29289	4.8756	3.5369	4.7581
4.2999	.32734	4.4640	3.3107	4.3744
4.1999	.36532	4.0951	3.3051	4.0019
4.0999	.40970	3.7406	3.3130	3.6409
3.9999	.47503	3.3069	3.4600	3.1671
3.8999	.58812	2.7395	3.5842	2.5214
3.7998	.84289	1.9617	3.4812	1.8076

TABLE VI. (Cont'd)

MODEL 314

FUNDAMENTAL RAYLEIGH MODE

Section Thickness 810 km

c	k	T	U	T
4.5000	.00800	174.4980	3.6546	152.3970
4.4000	.00910	156.9458	3.6739	133.7163
4.3000	.01054	138.6728	3.7362	111.4856
4.1999	.01273	117.4773	3.8025	84.3855
4.0999	.01661	92.2917		

Section Thickness 310

c	k	T	U	T
4.0000	.02547	61.6759	3.4695	39.4730
3.9000	.03856	41.7795	3.1635	33.1033
3.8000	.04824	34.2777	2.9694	29.2182
3.7000	.05646	30.0793	2.8125	26.2169
3.5999	.06486	26.9112	2.7168	23.4925
3.4999	.07445	24.1143	2.7635	20.7638
3.3999	.08602	21.4831	2.8034	17.8086
3.2999	.10206	18.6555	2.8919	13.9951
3.1999	.12901	15.2204		

FIRST HIGHER RAYLEIGH MODE

Section Thickness 310 km

c	k	T	U	T
5.0000	.02685	46.8048	4.4483	36.2523
4.9000	.02886	44.4386	4.3098	27.9880
4.8000	.03353	39.0360	4.2401	21.5914
4.6999	.04475	29.8741	4.1392	16.2429
4.5999	.05888	23.1967	3.8165	13.1554
4.4999	.08004	17.4449	3.5115	11.5744
4.3999	.10431	13.6899	3.3171	10.4853
4.2999	.12285	11.8943	3.2139	9.5683
4.1998	.13938	10.7339	3.1330	8.6651
4.0993	.15650	9.7925	3.1344	7.7859
3.9999	.17704	8.8727	3.1097	6.8751
3.8999	.20128	8.0045	3.1614	5.9217
3.7999	.23306	7.0948		
3.6999	.27476	6.1807		

TABLE VI. (Cont'd)

MODEL 315

FUNDAMENTAL RAYLEIGH MODE

Section Thickness 810 km

c	k	T	U	T
4.5000	.00820	170.2393		
4.4000	.00930	153.5283	3.6992	148.7251
4.3000	.01086	134.5723	3.7313	129.1714
4.1999	.01334	112.1333	3.8018	105.2905
4.0999	.01812	84.5767	3.8692	74.8110

Section Thickness 310 km

c	k	T	U	T
4.0000	.03053	51.4482		
3.9000	.04399	36.6250	3.4296	34.8049
3.8000	.05404	30.5995	3.2226	29.4172
3.7000	.06472	26.2377	3.0726	25.3270
3.5999	.07614	22.9218	3.0533	21.9835
3.4999	.09221	19.4693	3.0333	18.5069
3.3999	.11718	15.7708	3.0416	14.7044
3.2999	.16256	11.7130	3.0354	10.5790
3.1999	.25847	7.5969	3.0323	6.3232

FIRST HIGHER RAYLEIGH MODE

Section Thickness 310 km

c	k	T	U	T
5.0000	.02700	46.5387		
4.9000	.02898	44.2546		
4.8000	.03375	38.7906	4.4580	35.9338
4.6999	.04593	29.1047	4.3170	27.2273
4.5999	.06249	21.8596	4.3459	19.5919
4.4999	.09907	14.0942	4.1502	13.0875
4.3999	.12798	11.1578	3.7883	10.7461
4.2999	.14814	9.8638	3.4936	9.6058
4.1998	.16823	8.8928	3.4019	8.6584
4.0998	.19220	7.9737	3.4011	7.7268
3.9999	.22623	6.9435		
3.8999	.27637	5.8296	3.4963	5.4822
3.7999	.36302	4.5549	3.4527	4.2315
3.6999	.49743	3.4140	3.3824	3.1453
3.5998	.72066	2.4220	3.3589	2.1583
3.4998	1.18182	1.5191	3.3175	1.2885
3.3998	3.20689	.5763		

TABLE VI. (Cont'd)

MODEL 310

FUNDAMENTAL RAYLEIGH MODE

Section Thickness 400 km

c	k	T	U	T
4.0000	.02439	64.4070		
3.9000	.04255	37.8649	3.5912	34.7723
3.8000	.05805	28.4813	3.2801	27.2310
3.7000	.07023	24.1816	3.1144	23.2675
3.5999	.08334	20.9422	2.9759	20.2145
3.4999	.09981	17.9868	2.9384	17.2780
3.3999	.12365	14.9456	2.9835	14.1014
3.2999	.16535	11.5152	3.0190	10.4775

FIRST HIGHER RAYLEIGH MODE

Section Thickness 140 km

c	k	T	U	T
4.4000	.12476	11.4457		
4.3000	.16172	9.0352	3.6088	8.7490
4.2000	.18471	8.0990	3.3507	7.9020
4.0999	.21052	7.2797	3.2917	7.0921
3.9999	.24138	6.5077	3.4153	6.2579
3.8999	.29117	5.5333	3.4070	5.2734
3.7999	.36986	4.4707	3.4199	4.1854
3.6999	.49765	3.4125	3.3786	3.1475

MODEL 320

FUNDAMENTAL RAYLEIGH MODE

Section Thickness 310 km

c	k	T	U	T
4.0000	.02676	58.6913		
3.9000	.03996	40.3191	3.4514	38.1989
3.8000	.04957	33.3568	3.1758	32.1857
3.7000	.05820	29.1794	2.9781	28.3310
3.5999	.06716	25.9897	2.8662	25.2547
3.4999	.07764	23.1217	2.7526	22.4878
3.3999	.09056	20.4061	2.8481	19.5889
3.2999	.11217	16.9749	2.8978	16.0079
3.1999	.15391	12.7579	3.0158	10.8511

TABLE VI. (Cont'd)

FIRST HIGHER RAYLEIGH MODE

Section Thickness 310 km

c	k	T	U	T
5.0000	.02694	46.6523		
4.9000	.02888	44.4016		
4.8000	.03358	38.9835	4.4617	36.0753
4.6999	.04490	29.7720	4.2997	27.9473
4.5999	.05957	22.9299	4.2645	21.2086
4.5000	.08333	16.7565		
4.4000	.11006	12.9742	3.8455	12.4357
4.3000	.12959	11.2758	3.5636	10.9456
4.1999	.14771	10.1280	3.3148	9.8943
4.0999	.16573	9.2470	3.2854	9.0110
3.9999	.18724	8.3893	3.1800	8.1781
3.8999	.21377	7.5367	3.1997	7.3062
3.7999	.24984	6.6182	3.2181	6.3649
3.6999	.30270	5.6103	3.2358	5.3289

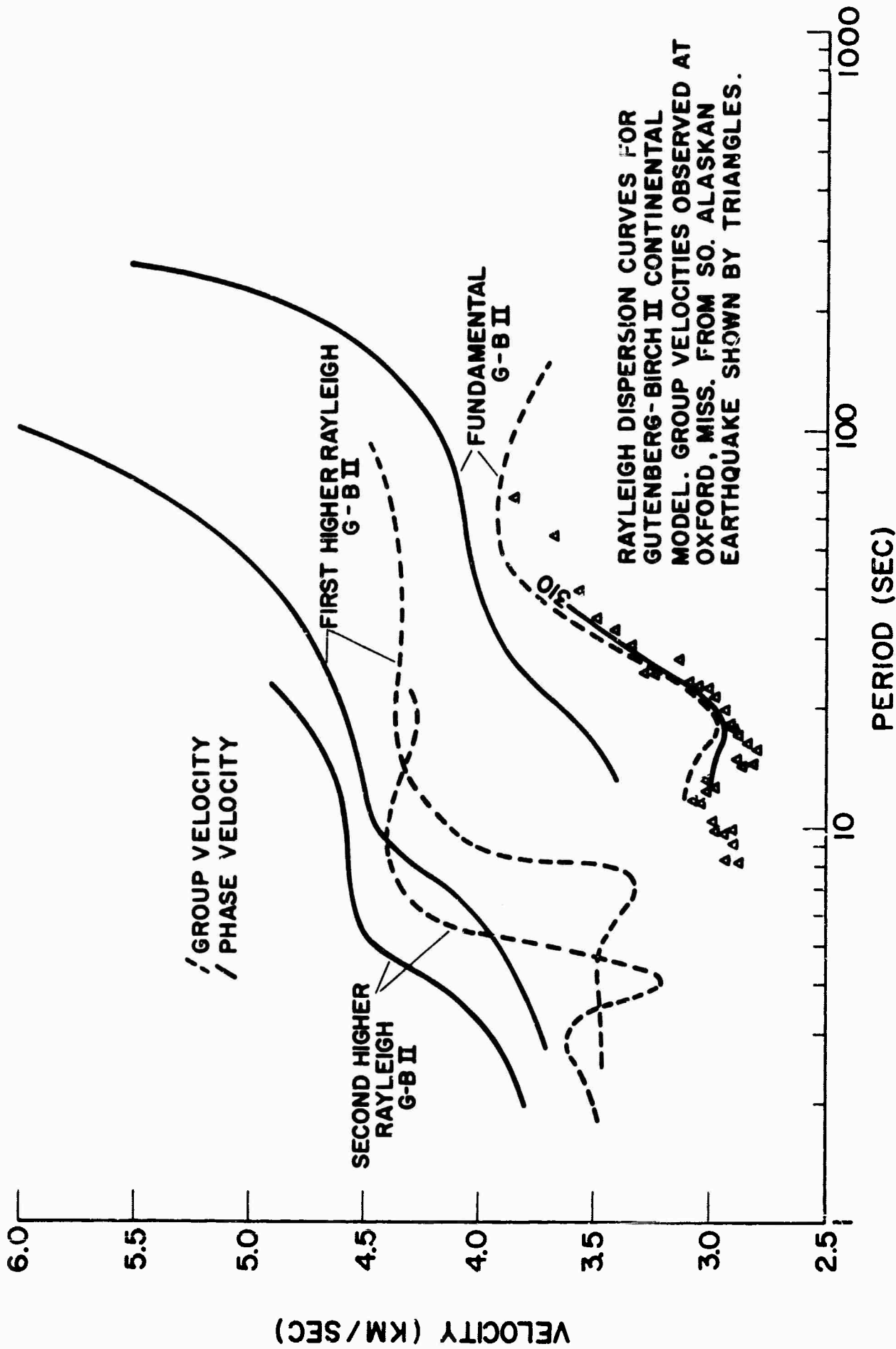


Fig. 8

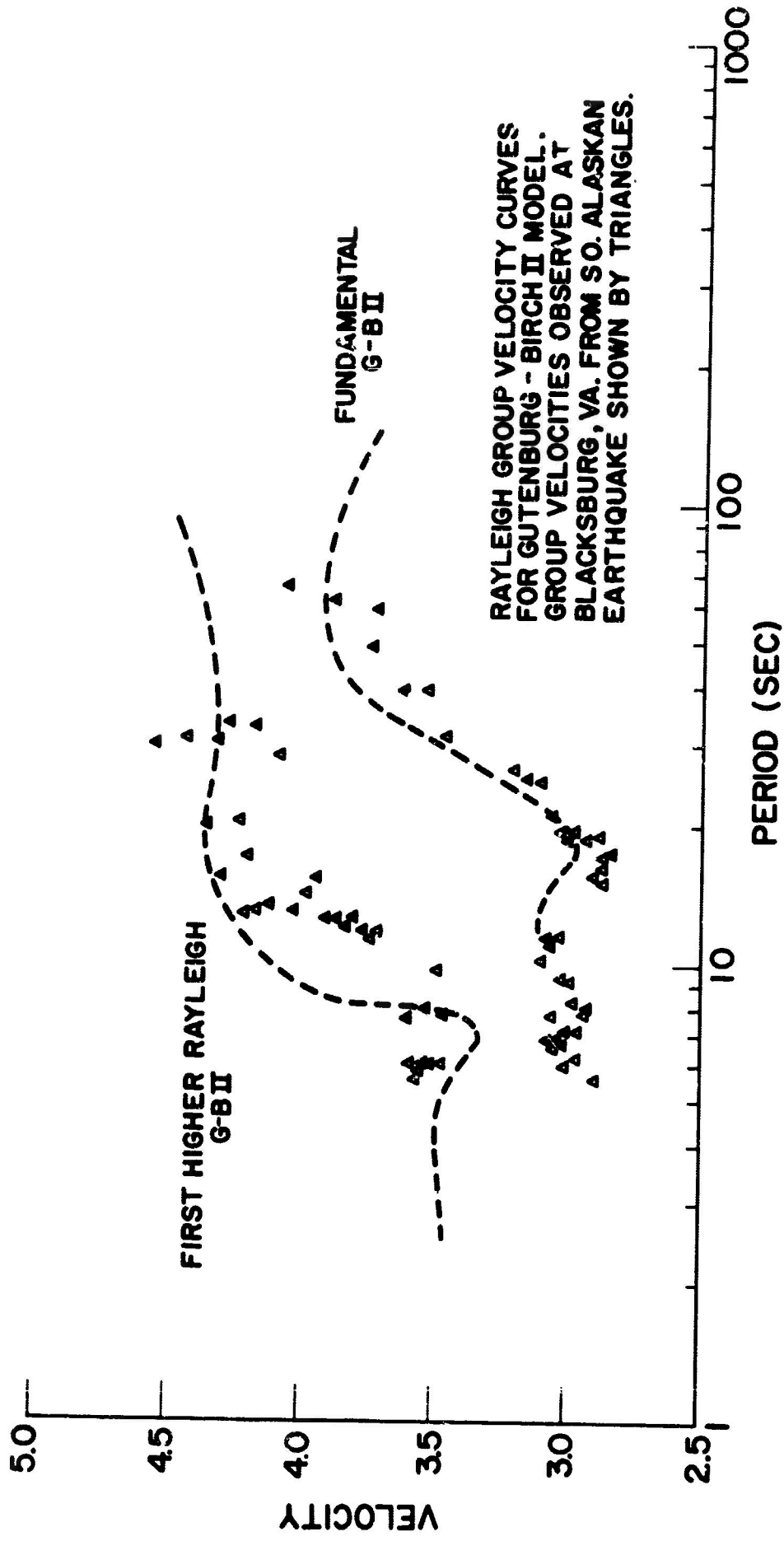


Fig. 9

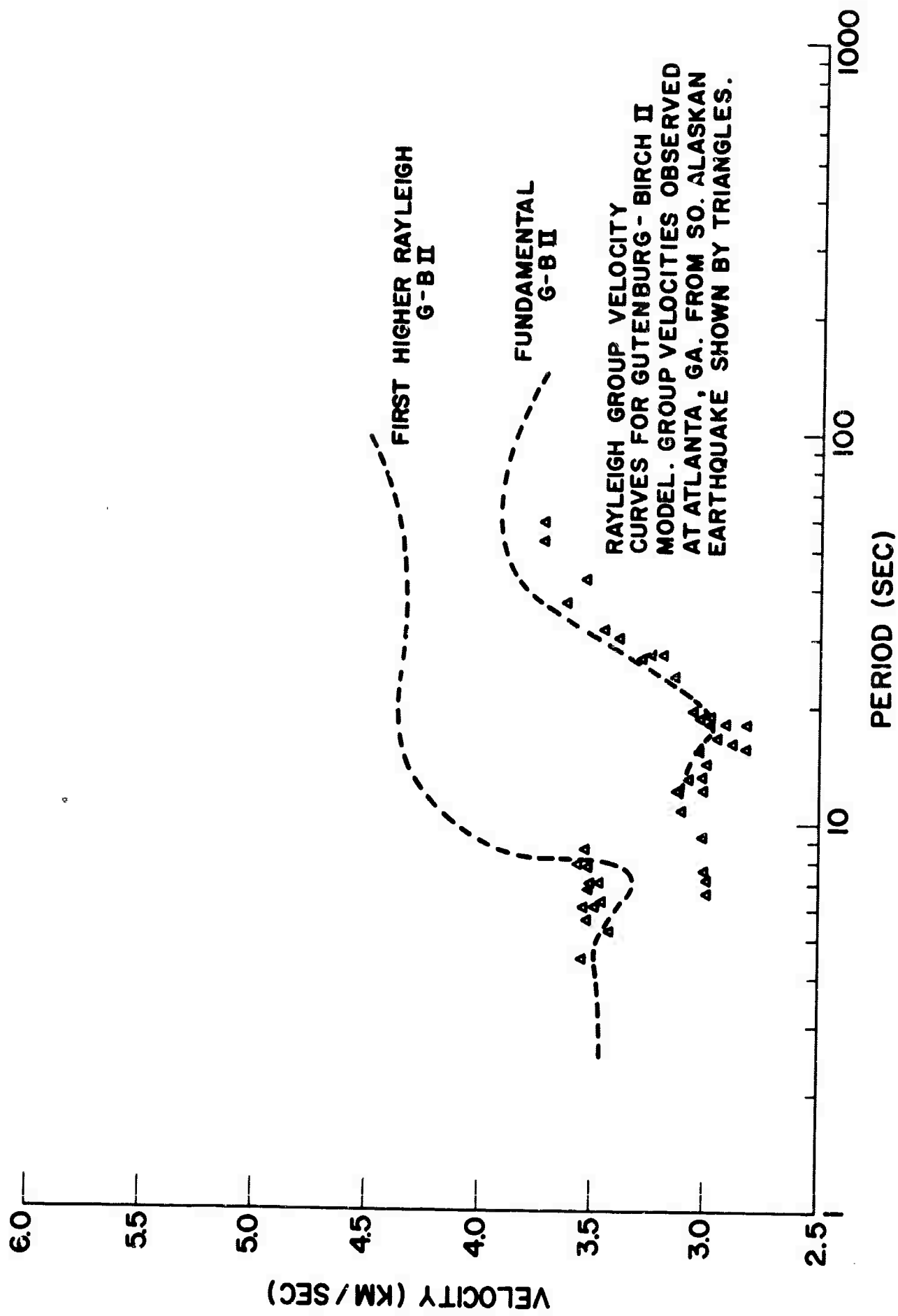


Fig. 10

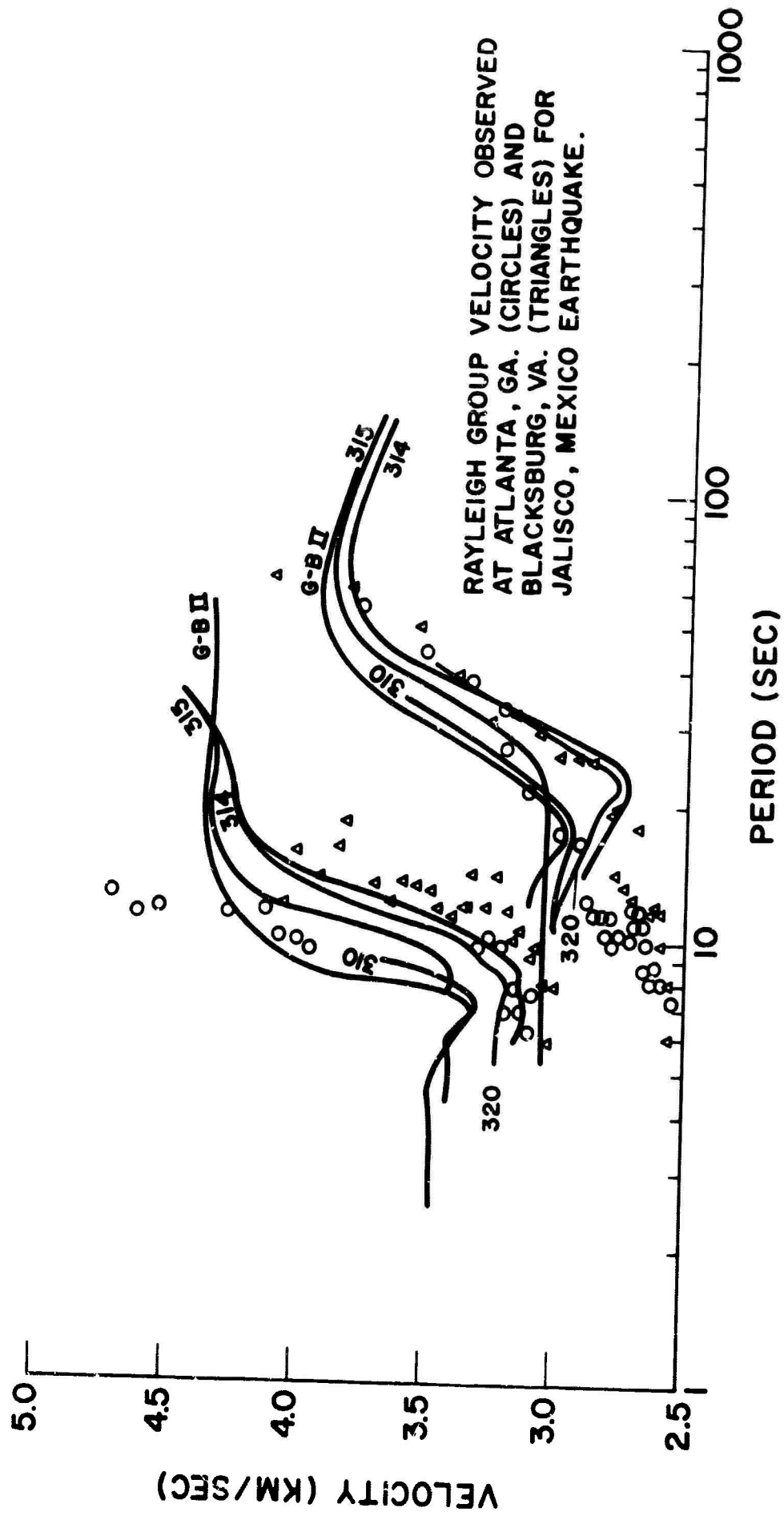


Fig. 11

from 6-10 sec. Group velocities recorded at Oxford indicate a slightly shorter period for the minimum and a gradual decrease in velocity for periods shorter than 12 sec. However, in general the curves are quite similar to those for Atlanta and Blacksburg. Waves arriving at Atlanta from Jalisco, Mexico, (parallel waves) have both fundamental and first higher Rayleigh mode group velocities considerably lower than do the perpendicular wave trains for periods less than about 20 sec. The rapidly "tailing-off" of group velocities below 15 sec is probably due to a thick sedimentary sequence (approximately 400 km of the travel path for these waves lie across the Gulf Coastal Plain).

The most significant difference is between the Blacksburg and Atlanta group velocities for parallel wave trains. A minimum of 2.75 km/sec occurs at a period of 22 sec and a maximum of 2.80 km/sec occurs at a period of 16 sec for the Blacksburg velocities. Group velocities at periods greater than 30 sec trend toward those for the perpendicular waves. First higher mode Rayleigh group velocities for Blacksburg are lower by about .1 km/sec than those for Atlanta.

Several models were constructed using the variation of phase velocity with layer parameter curves for the Gutenberg-Birch II model. Basic differences in the models are:

- 1) 314, 315, and 320 have a crustal thickness of 50 km, while 310 and G-B (Gutenberg-Birch II) have a crustal thickness of 40 km;
- 2) 314 has a low velocity zone centered at 15 km in the upper crust. Except for this low velocity zone, 320 is identical to 314;
- 3) G-B and 310 have a low velocity zone in the upper mantle beginning at 60 km while the low velocity begins at 70 km for 314, 315, and 320.
- 4) Velocities in the first 10 km of G-B are slightly higher than those in the other models.

For waves traveling perpendicular to the Appalachians, the group velocity data agree well with model 310 or G-B values for the fundamental Rayleigh mode at periods less than 30 sec. At longer periods, the values fall below those for 310 and approach those for 314 and 315. First higher Rayleigh mode values observed at Blacksburg lie between those for 314 and 315 for periods greater than 10 sec. Thus, it appears that waves arriving at Atlanta, Oxford, and Blacksburg from the Southern Alaska epicenter are just beginning to "feel" the Appalachian structure. The length of the "Appalachian path" is about 240 km in the Appalachian foreland in each case, assuming that the Appalachian structure extends beneath the Mississippi Embayment (Oxford station).

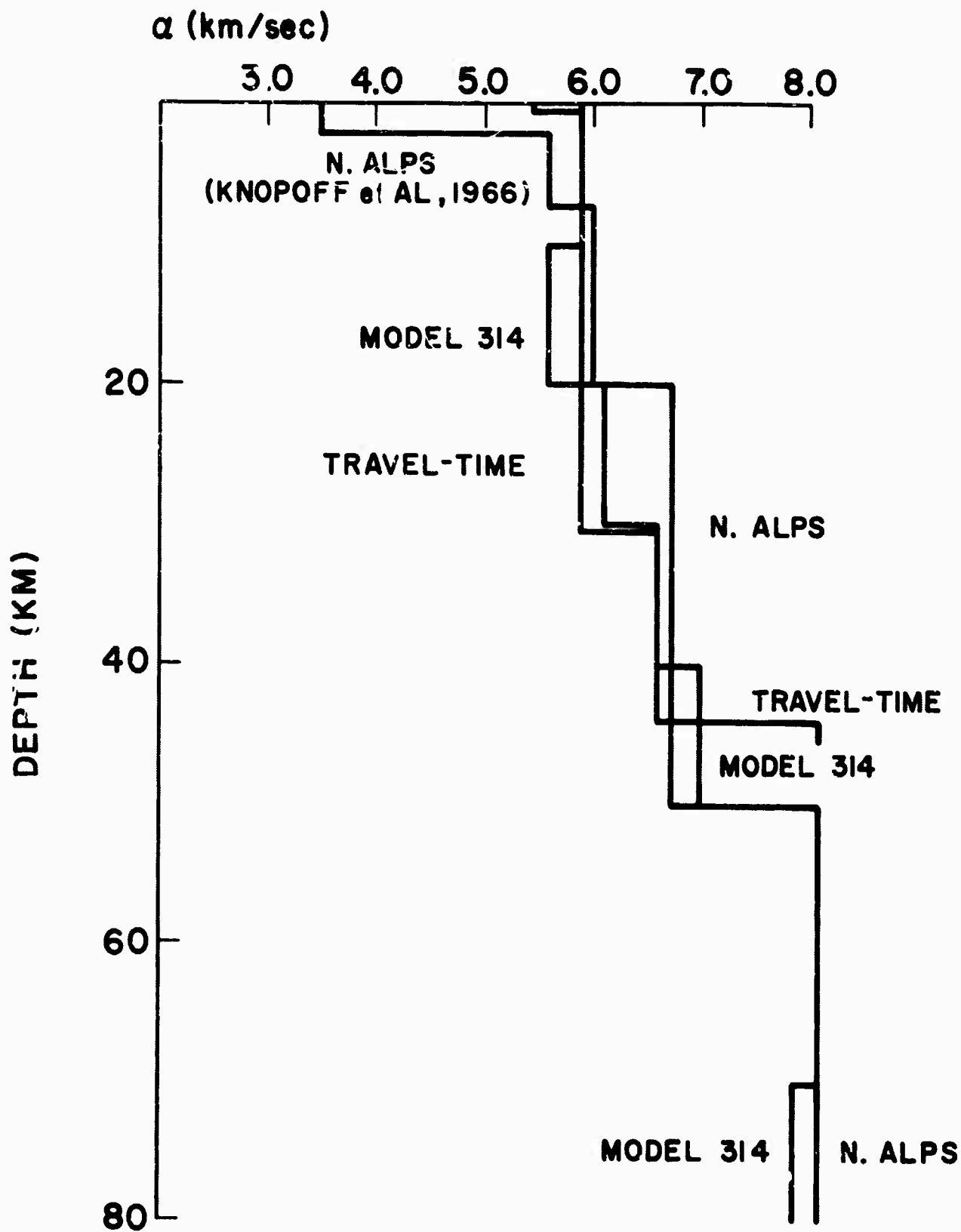
Waves arriving at Atlanta from Jalisco, Mexico yield group velocities considerably below those of G-B for periods less than 20 sec (See Fig. 11). Fundamental mode group velocities at Blacksburg show fair agreement with the theoretical curves for either models 314 or 320 being considerably below curves for G-B, 315, and 310 at all periods. On the basis of fundamental mode group velocities it is impossible to determine which of models 314 or 320 most closely approximate the crustal structure. However, first higher Rayleigh mode group velocities from model 314 give a considerably better fit to the observed data than do those from model 320 in the period range from 6 to 15 sec. In this period range, the group velocity curve for 314 lies between that for 320 and the observed group velocities. Thus, a slight velocity reversal in the crust is indicated by the first higher mode group velocities.

An alternative to the low velocity zone is to lower the velocities and/or densities in the first 10 km of the crust. However, refraction data give a compressional velocity of 5.88 km/sec for the upper crust which has

been used in models 314 and 320. The shear velocity value of 3.88 km/sec in models 314 and 320 corresponds to a Poisson ratio of .25.

Group velocities for periods greater than about 30 sec indicate a mantle low velocity zone beginning at about 70 km.

Compressional velocity crustal and upper mantle structure to the west of the Southern Appalachians determined from the travel times of local earthquakes and for the Southern Appalachian structure as determined from Rayleigh wave dispersion are shown in Fig. 12. Gravity and Rayleigh wave dispersion data indicate a total crustal thickness of about 50 km beneath the Southern Appalachians. Travel-time and dispersion data indicate an upper mantle velocity of 8.10 km/sec. Dispersion data indicate a slight low velocity zone in the upper crust and a general increase of velocity and density with depth below this zone. With the exception of the higher crustal velocity in the first 2 km, the Southern Appalachian structure approximated by model 314 is similar to the Northern Alpine structure with a 50 km crust reported by Knopoff et al [1966].



COMPRESSONAL VELOCITY STRUCTURE FOR THE SOUTHEASTERN UNITED STATES AND THE NORTHERN ALPS.

Fig. 12

7.0 CONCLUSIONS

The conclusions which have been drawn from this study are:

1) Focal depths of local earthquakes in the Southeastern United States are shallow ranging from about 7 to 18 km.

2) Systematic deviations in P-residuals observed at Chapel Hill, North Carolina, and McMinnville, Tennessee, have magnitudes from + 3 to -3 sec. The deviations indicate systematic errors in the Jeffreys-Bullen travel-times.

3) Travel-time curves constructed from local earthquakes and refraction data indicate a crustal structure for the Appalachian foreland of $h_1 = 33.0$ km ($\alpha = 5.88$ km/sec), $h_2 = 10.8$ km ($\alpha = 6.58$ km/sec), and an upper mantle velocity of 8.10 km/sec.

4) Rayleigh wave dispersion data indicate a crustal low velocity zone centered at about 15 km, an upper mantle low velocity zone beginning at 70 km, and a total crustal thickness of 50 km beneath the core of the Southern Appalachians.

5) Gravity data indicate a total crustal thickness beneath the Southern Appalachians of at least 50 km which is in agreement with the Rayleigh dispersion data. Gravity data indicate a crustal thickness of about 45 km in central Kentucky thickening eastward to about 50 km beneath the core of the Appalachian and thinning to 23 km beneath the North Carolina continental margin at about the 2400 fathom contour.

6) Higher Rayleigh modes can be observed using digital filtering techniques. Care must be taken to isolate Rayleigh type motion and to remove interference effects. This is particularly true for higher modes than the first.

7) It should be possible to use higher modes than the first to delineate fine detail in the crust.

ACKNOWLEDGEMENTS

I wish to particularly express my gratitude and thanks to the Superior Stone Company of Raleigh, North Carolina, and to the many local quarry managers who made possible the refraction program of this research.

REFERENCES

- Anderson, D. L. Universal dispersion tables, I, Love waves across oceans and continents on a spherical earth, Bull. Seismol. Soc. Am., 54, 681-726, 1964.
- Alterman, Z., H. Jarosch, and C. L. Pekeris, Propagation of Rayleigh waves in the earth, Geophys. J., 4, 219-241, 1961.
- Borcherdt, R. D., and John C. Roller. A preliminary summary of a seismic-refraction survey in the vicinity of the Cumberland Plateau Observatory, Tennessee, USGS Technical Letter, Crustal Studies-43, February, 1966.
- Dorman, James, Maurice Ewing, and Jack Oliver. Study of shear-velocity distribution in the upper mantle by mantle Rayleigh waves. Bull. Seismol. Soc. Am., 50, 87-115, 1960.
- Dunkin, John W. Computations of modal solutions in layered, elastic media at high frequencies, Bull. Seismol. Soc. Am., 55, 335-358, 1965.
- Gutenberg, B., and C. F. Richter. Earthquake magnitude, intensity, energy, and acceleration, Bull. Seismol. Soc. Am., 32, 163-191, 1942.
- Haskell, N. A. The dispersion of surface waves on multilayered media, Bull. Seismol. Soc. Am., 43, 17-34, 1953.
- Hersey, J. B., Elizabeth T. Bunce, R. F. Wyrick, and F. T. Dietz. Geophysical investigation of the continental margin between Cape Henry, Virginia, and Jacksonville, Florida, Bull. Geol. Soc. Am., 70, 437-466, 1959.
- Jeffreys, H. The surface waves of earthquakes, MNRAS, Geophys. Supp., 3, 253-261, 1934.
- Knopoff, L., S. Mueller, and W. L. Pilant. Structure of the crust and upper mantle in the Alps from the phase velocity of Rayleigh waves, Bull. Seismol. Soc. Am., 56, 1009-1044, 1966.
- Kovach, R. L., and D. L. Anderson. Higher mode surface waves and their bearing on the structure of the earth's mantle, Bull. Seis. Soc. Am., 54, 161-182, 1964.
- MacCarthy, G. R., and E. Z. Sinha. North Carolina earthquakes, 1957, J. Elisha Mitchell Soc., 117-274, November, 1957.
- MacCarthy, G. R., and J. D. Waskom. The Virginia-North Carolina Blue Ridge earthquake of October 28, 1963, J. Elisha Mitchell Soc., 82-84, December, 1964.
- McGuire, W. H., and Paul Howell. Oil and gas possibilities in the Cambrian and Lower Ordovician in Kentucky, Spindletop Research Center Report, 1963.
- Meissner, E. Elastische Oberflächen Querwellen Verhandl., Intern., Kongr. Tech. Mech., 2nd, Zurich, 3-11, 1926.

Minear, John W. Quarterly Report No. 9, Seismicity of the Southeastern United States, AFCRL Project CRL-46116, 1966.

_____. Research directed toward the study of seismicity in the Southeastern United States, Annual Technical Report #2, Air Force Cambridge Research Lab, Project CRL-46116, January, 1966.

_____. Semi-Annual Technical Report, Seismicity of the Southeastern United States, Project CRL-46116, January 1965.

Takeuchi, H., and J. Dorman. Partial derivatives of surface wave phase velocity with respect to physical parameter changes within the earth, J. Geophys. Research, 69, 3429-3441, 1964.

Tomoda, Y., and K. Aki. Use of the function $\sin x/x$ in gravity problems, Bull. Earthquake Res. Inst., Tokyo, 443-448.

APPENDIX I

EVALUATION OF THE SECULAR EQUATION IN COMPUTING RAYLEIGH DISPERSION

In the Dunkin Method, the Rayleigh dispersion equation is the secular equation

$$\text{Det } R_{11} = r \begin{vmatrix} 12 \\ 12 \end{vmatrix} = t \begin{vmatrix} 12 \\ ab \end{vmatrix} g^{p-1} \begin{vmatrix} ab \\ cd \end{vmatrix} \dots g^1 \begin{vmatrix} mn \\ 12 \end{vmatrix} \quad (I-1)$$

Writing out (I-1) explicitly yields

$$\begin{aligned} \text{Det } R_{11} = & \check{t} \begin{vmatrix} 12 \\ 12 \end{vmatrix} g^{p-1} \begin{vmatrix} 12 \\ cd \end{vmatrix} \dots \\ & + \check{t} \begin{vmatrix} 12 \\ 13 \end{vmatrix} g^{p-1} \begin{vmatrix} 13 \\ cd \end{vmatrix} \dots \\ & + \check{t} \begin{vmatrix} 12 \\ 14 \end{vmatrix} g^{p-1} \begin{vmatrix} 14 \\ cd \end{vmatrix} \dots \\ & + \check{t} \begin{vmatrix} 12 \\ 23 \end{vmatrix} g^{p-1} \begin{vmatrix} 23 \\ cd \end{vmatrix} \dots \\ & + \check{t} \begin{vmatrix} 12 \\ 24 \end{vmatrix} g^{p-1} \begin{vmatrix} 24 \\ cd \end{vmatrix} \dots \\ & + \check{t} \begin{vmatrix} 12 \\ 34 \end{vmatrix} g^{p-1} \begin{vmatrix} 34 \\ cd \end{vmatrix} \dots \end{aligned} \quad (I-2)$$

where the ... signifies multiplication of the form $g^{p-2} \begin{vmatrix} cd \\ ef \end{vmatrix} \dots g^1 \begin{vmatrix} mn \\ 12 \end{vmatrix}$.

Continuing the process

$$\text{Det } R_{11} = a_1 g^{p-1} \begin{vmatrix} 12 \\ 12 \end{vmatrix} g^{p-2} \begin{vmatrix} 12 \\ ef \end{vmatrix} \dots + a_1 g^{p-1} \begin{vmatrix} 12 \\ 13 \end{vmatrix} g^{p-2} \begin{vmatrix} 13 \\ ef \end{vmatrix} \dots +$$

+ 4 more similar terms with a_1 as a factor

+ 5 more expressions with $a_2, a_3, a_4, a_5,$ and a_6 replacing a_1

where

$$a_1 = \check{t} \begin{vmatrix} 12 \\ 12 \end{vmatrix}$$

$$a_2 = \check{t} \begin{vmatrix} 12 \\ 13 \end{vmatrix}, \text{ etc.}$$
(I-3)

Collecting terms with like coefficients $g^{p-1} \begin{vmatrix} 12 \\ ef \end{vmatrix}$, $g^{p-1} \begin{vmatrix} 13 \\ ef \end{vmatrix}$, etc., gives

$$\text{Det } R_{11} = A_1 g^{p-2} \begin{vmatrix} 12 \\ ef \end{vmatrix} \dots + A_2 g^{p-2} \begin{vmatrix} 13 \\ ef \end{vmatrix} \dots + A_3 g^{p-2} \begin{vmatrix} 14 \\ ef \end{vmatrix} \dots$$

$$+ A_4 g^{p-2} \begin{vmatrix} 23 \\ ef \end{vmatrix} \dots + A_5 g^{p-2} \begin{vmatrix} 24 \\ ef \end{vmatrix} \dots + A_6 g^{p-2} \begin{vmatrix} 34 \\ ef \end{vmatrix} \dots$$
(I-4)

where

$$A_1 = (a_1 b_{11} + a_2 b_{21} + a_3 b_{31} + a_4 b_{41} + a_5 b_{51} + a_6 b_{61}),$$

$$b_{11} = g^n \begin{vmatrix} 12 \\ 12 \end{vmatrix},$$

$$b_{21} = g \begin{vmatrix} 13 \\ 12 \end{vmatrix},$$

$$b_{31} = g \begin{vmatrix} 14 \\ 12 \end{vmatrix}, \text{ etc.}$$

(I-4) is of the form (I-2); the sum of six terms which are each products of the second order subdeterminants. The process of evaluating the second order subdeterminants of a given layer, multiplying by six previously determined coefficients, a_i , and summing to obtain six new coefficients, A_i , is repeated until the entire layered sequence has been traversed from bottom to top. This can be quickly and easily adapted to computer processing

as is indicated in the following considerations of the real and imaginary structure of $\check{t} \begin{smallmatrix} 12 \\ ab \end{smallmatrix}$ and $g^p \begin{smallmatrix} 12 \\ ab \end{smallmatrix}$ is of the form of a 6 x 1 row matrix

$$\begin{aligned} [R R I I R R] \quad I &= \text{pure imaginary quantity} \\ R &= \text{pure real quantity} \end{aligned} \tag{I-5}$$

The real and imaginary structure of the $g \begin{smallmatrix} ab \\ cd \end{smallmatrix}$ is of the form of a 6 x 6 matrix

$$g \begin{smallmatrix} ab \\ cd \end{smallmatrix} = \begin{bmatrix} R & R & I & I & R & R \\ R & R & I & I & R & R \\ -I & -I & R & R & -I & -I \\ -I & -I & R & R & -I & -I \\ R & R & I & I & R & R \\ R & R & I & I & R & R \end{bmatrix} \tag{I-6}$$

The ab indices have been taken as the row indices and the cd indices the column indices with 1=12, 2=13, 3=14, 4=23, 5=24, and 6=34; $g \begin{smallmatrix} 12 \\ 34 \end{smallmatrix} = g_{16}$, etc. Multiplication of $\check{t} \begin{smallmatrix} 12 \\ ab \end{smallmatrix}$ by the $g^{p-1} \begin{smallmatrix} ab \\ ef \end{smallmatrix}$ in (I-2) yields a matrix of the form

$$\begin{bmatrix} R & R & I & I & R & R \\ R & R & I & I & R & R \\ R & R & I & I & R & R \\ R & R & I & I & R & R \\ R & R & I & I & R & R \\ R & R & I & I & R & R \end{bmatrix} \tag{I-7}$$

Elements of this matrix correspond to the terms $a_1 b_{11}$, $a_2 b_{21}$, etc. in (I-4). Thus, the six new coefficients A_1 are simply the sum of the elements in a column of (I-7). The six new coefficients can then be considered as just another 6 x 1 row matrix of the form of (I-5), minus ones have been inserted in (I-6) to account for the multiplication of two like-signed imaginary quantities.

APPENDIX II

MODAL SHAPE COMPUTATIONS

In the Dunkin Method, mode shape is computed from the relation

$$R_n^m(z;a) = r_{11}^{-1} \check{t}_{1r}^p g_{rs}^{p-1} \dots g_{vb}^n (z_n - z) g^{n(z-z_{n-1})} \Big|_{cd}^{ab} \dots g^1 \Big|_{21}^{ef} \quad (II-1)$$

where a denotes the component of displacement. $R_n^m(z;a)$ is the a^{th} component of the displacement-stress vector, at the depth z , normalized to the vertical displacement at the free surface. Note that r_{11}^{-1} is simply a constant multiplier for all of the displacement-stress components. Thus, it may be dropped and the $R_n^m(z;a)$ at different depths divided by the vertical displacement at the surface to normalize the displacements. The equation actually used for the determination of mode shape was

$$R_n^m(z;a) = \check{t}_{1r}^p g_{rs}^{p-1} \dots g_{vb}^n (z_n - z) g^{n(z-z_{n-1})} \Big|_{cd}^{ab} \dots g^1 \Big|_{21}^{ef} \quad (II-2)$$

Writing (II-2) explicitly

$$\begin{aligned} R_n^m(z;a) &= \check{t}_{11}^1 g_{1s}^{p-1} g_{st}^{p-2} \dots \\ &+ \check{t}_{12}^p g_{2s}^{p-1} g_{st}^{p-2} \dots \\ &+ \check{t}_{13}^p g_{3s}^{p-1} g_{st}^{p-2} \dots \\ &+ \check{t}_{14}^p g_{4s}^{p-1} g_{st}^{p-2} \dots \end{aligned} \quad (II-3)$$

When the dots denote the product of g_{ij}^n post multiplying g_{st}^{p-2} .

$$R_n^m(z;a) = a_1 g_{11}^{p-1} g_{1t}^{p-2} \dots + a_1 g_{12}^{p-1} g_{2t}^{p-2} \dots + a_1 g_{13}^{p-1} g_{3t}^{p-2} \dots + a_1 g_{14}^{p-1} g_{4t}^{p-2} \dots$$

$$\begin{array}{c} \text{Sum over } r \\ \downarrow \\ a_2 g_{21}^{p-1} g_{1t}^{p-2} \dots + a_2 g_{22}^{p-1} g_{2t}^{p-2} \dots + \dots \\ \downarrow \\ a_4 g_{41}^{p-1} g_{1t}^{p-2} \dots + \dots \end{array} \quad (\text{II-4})$$

where

$$a_1 = \check{t}_{11}^p, \quad a_2 = \check{t}_{12}^p, \quad a_3 = \check{t}_{13}^p, \quad \text{and} \quad a_4 = \check{t}_{14}^p.$$

$R_n^m(z;a)$ has been expanded into 16 terms of the form $a_i g_{ij}^{p-1} g_{jt}^{p-2} \dots$

Now the g^{p-1} which have explicit subscripts can be included in the constant factor a_i . Collecting terms with common factors of g_{ij}^{p-2} yields

$$\begin{aligned} R_n^m(z;a) &= (a'_1 + a'_2 + a'_3 + a'_4) g_{1t}^{p-2} \dots + (a'_1 + a'_2 + a'_3 + a'_4) g_{2t}^{p-2} \dots \\ &+ \dots + (a'_1 + a'_2 + a'_3 + a'_4) g_{4t}^{p-2} \dots \end{aligned} \quad (\text{II-5})$$

$$a'_i = a_i g_{ik}^{p-1}, \text{ etc.}$$

which is of the form of (II-3).

Continuing this process yields

$$\begin{aligned} R_n^m(z;a) &= a_1 g^n(z-z_{n-1}) \begin{vmatrix} a1 & \dots & g^1 \\ cd & \dots & 12 \end{vmatrix} ef \\ &+ a_2 g^n(z-z_{n-1}) \begin{vmatrix} a2 & \dots & g^1 \\ cd & \dots & 12 \end{vmatrix} ef \\ &+ a_3 g^n(z-z_{n-1}) \begin{vmatrix} a3 & \dots & g^1 \\ cd & \dots & 12 \end{vmatrix} ef \\ &+ a_4 g^n(z-z_{n-1}) \begin{vmatrix} a4 & \dots & g^1 \\ cd & \dots & 12 \end{vmatrix} ef \end{aligned} \quad (\text{II-6})$$

The horizontal component, u , of displacement corresponds to $a=1$ and the vertical component, w , to $a=2$, so that

$$u = a_2 g^n \begin{vmatrix} 12 \\ cd \end{vmatrix} \dots + a_3 g^n \begin{vmatrix} 13 \\ cd \end{vmatrix} \dots + a_4 g^n \begin{vmatrix} 14 \\ cd \end{vmatrix} \dots \text{ and} \quad (\text{II-7})$$

$$w = a_1 g^n \begin{vmatrix} 21 \\ cd \end{vmatrix} \dots + a_3 g^n \begin{vmatrix} 23 \\ cd \end{vmatrix} \dots + a_4 g^n \begin{vmatrix} 24 \\ cd \end{vmatrix} \dots \quad (\text{II-8})$$

Note that $z^n \begin{vmatrix} ij \\ kl \end{vmatrix} = 0$, if $i=j$ or $k=l$.

Writing (II-7) explicitly

$$\begin{aligned} u = & a_2 g^n \begin{vmatrix} 12 \\ 12 \end{vmatrix} g^{n-1} \begin{vmatrix} 1 \\ ef \end{vmatrix} \dots + a_2 g^n \begin{vmatrix} 12 \\ 13 \end{vmatrix} g^{n-1} \begin{vmatrix} 13 \\ ef \end{vmatrix} \dots + a_2 g^n \begin{vmatrix} 12 \\ 14 \end{vmatrix} g^{n-1} \begin{vmatrix} 14 \\ ef \end{vmatrix} \dots \\ & + a_2 g^n \begin{vmatrix} 12 \\ 23 \end{vmatrix} g^{n-1} \begin{vmatrix} 23 \\ ef \end{vmatrix} \dots + a_2 g^n \begin{vmatrix} 12 \\ 24 \end{vmatrix} g^{n-1} \begin{vmatrix} 24 \\ ef \end{vmatrix} \dots + a_2 g^n \begin{vmatrix} 12 \\ 34 \end{vmatrix} g^{n-1} \begin{vmatrix} 34 \\ ef \end{vmatrix} \dots \\ & + a_3 g^n \begin{vmatrix} 13 \\ 12 \end{vmatrix} g^{n-1} \begin{vmatrix} 12 \\ ef \end{vmatrix} \dots + 5 \text{ more terms in } a_3 \\ & + a_4 g^n \begin{vmatrix} 14 \\ 12 \end{vmatrix} g^{n-1} \begin{vmatrix} 12 \\ ef \end{vmatrix} \dots + 5 \text{ more terms in } a_4 \end{aligned} \quad (\text{II-9})$$

u is expressed in terms of the sum of 18 terms of the form $a_m g^n \begin{vmatrix} ij \\ kl \end{vmatrix} g^{n-1} \begin{vmatrix} kl \\ ef \end{vmatrix} \dots$.
Collecting terms with common $g^{n-1} \begin{vmatrix} kl \\ ef \end{vmatrix}$ gives u as the sum of six terms of the form $a_m g^{n-1} \begin{vmatrix} ij \\ ef \end{vmatrix} \dots$

$$\begin{aligned} u = & a'_1 g^{n-1} \begin{vmatrix} 12 \\ ef \end{vmatrix} \dots + a'_2 g^{n-1} \begin{vmatrix} 13 \\ ef \end{vmatrix} \dots + a'_3 g^{n-1} \begin{vmatrix} 14 \\ ef \end{vmatrix} \dots + \\ & a'_4 g^{n-1} \begin{vmatrix} 23 \\ ef \end{vmatrix} \dots + a'_5 g^{n-1} \begin{vmatrix} 24 \\ ef \end{vmatrix} \dots + a'_6 g^{n-1} \begin{vmatrix} 34 \\ ef \end{vmatrix} \dots, \end{aligned} \quad (\text{II-10})$$

where

$$a_1' = a_2 g_{12}^n + a_3 g_{12}^{i3} + a_4 g_{12}^{i4}, \text{ etc.}$$

The process of evaluating the displacements u and w now proceeds exactly as for the evaluation of $\text{Det } R_{11}$ described in Appendix I.

Let us consider the real and imaginary forms of the factors appearing in (II-4), (II-6), and (II-10). From the definition of T_p^{-1} given by Dunkin, t_{1r} is of the form

$$t_{1r} = [I R R I], \quad I = \text{pure imaginary quantity} \quad (\text{II-11})$$

$$R = \text{pure real quantity}$$

The layer matrices G_n are of the form

$$G_n = \begin{bmatrix} R & I & I & R \\ I & R & R & I \\ I & R & R & I \\ R & I & I & R \end{bmatrix} \quad (\text{II-12})$$

$$\text{Thus } \check{t}_{1r} g_{rs}^{p-1} = [I R R I] \quad (\text{II-13})$$

Each successive multiplication by a layer matrix G_n yields a row matrix of the form $[I R R I]$ until the first multiplication by a second order subdeterminant is encountered. In order to account for the multiplication of two imaginaries in the evaluation of column 2 and 3 in (II-13) minus ones are inserted in (II-12) to give

$$G_n = \begin{bmatrix} R & -I & -I & R \\ I & R & R & I \\ I & R & R & I \\ R & -I & -I & R \end{bmatrix} \quad (\text{II-14})$$

By (II-9) and the definitions of $g^n \begin{matrix} ij \\ kl \end{matrix}$, the form of the matrix by which a_2 , a_3 , and a_4 of (II-7) are multiplied is

$$\begin{bmatrix} R & R & I & I & R & R \\ R & R & I & I & R & R \\ I & I & R & R & I & I \end{bmatrix} \quad (\text{II-15})$$

and for a_1 , a_3 , a_4 in the case of the vertical component

$$\begin{bmatrix} R & R & I & I & R & R \\ I & I & R & R & I & I \\ R & R & I & I & R & R \end{bmatrix} \quad (\text{II-16})$$

For the u component

$$[R \ R \ I] \cdot \begin{bmatrix} R & R & I & I & R & R \\ R & R & I & I & R & R \\ -I & -I & R & R & -I & -I \end{bmatrix} = [R \ R \ I \ I \ R \ R] \quad (\text{II-17})$$

and for the w component

$$[I \ R \ I] \cdot \begin{bmatrix} R & R & -I & -I & R & R \\ I & I & R & R & I & I \\ R & R & -I & -I & R & R \end{bmatrix} = [I \ I \ R \ R \ I \ I] \quad (\text{II-18})$$

Minus ones have been inserted to account for multiplication of two imaginaries.

To continue the process to the surface, the form of the matrices composed of the second order subdeterminant elements is

$$\begin{bmatrix}
 R & R & I & I & R & R \\
 R & R & I & I & R & R \\
 -I & -I & R & R & -I & -I \\
 -I & -I & R & R & -I & -I \\
 R & R & I & I & R & R \\
 R & R & I & I & R & R
 \end{bmatrix}
 \tag{II-19}$$

for the u component and

$$\begin{bmatrix}
 R & R & -I & -I & R & R \\
 R & R & -I & -I & R & R \\
 I & I & R & R & I & I \\
 I & I & R & R & I & I \\
 R & R & -I & -I & R & R \\
 R & R & -I & -I & R & R
 \end{bmatrix}
 \tag{II-20}$$

and for the w component. Minus ones have been inserted in the appropriate elements to account for the multiplication of two pure imaginary quantities. Since the lower subscripts in (II-1) for the surface layer matrix are 21, the layer matrix of the surface layer is a 6 x 1 column matrix. The final multiplications are then of the forms:

u component

$$[R \ R \ I \ I \ R \ R] \cdot \begin{bmatrix} R \\ R \\ -I \\ -I \\ R \\ R \end{bmatrix} = [R \ R \ R \ R \ R \ R]$$

w component

$$[I I R R I I] \cdot \begin{bmatrix} R \\ R \\ I \\ I \\ R \\ R \end{bmatrix} = [I I I I I I]$$

EXPLICIT FORMS OF LAYER MATRIX COMPONENTS g_{ij}

$$g_{11} = g_{44} = \frac{2\beta^2}{c^2} \cosh P - \frac{p\beta^2}{k^2 c^2} \cosh Q$$

$$g_{12} = g_{34} = \frac{i\beta^2 p}{r_\alpha c^2 k^2} \sinh P + \frac{2ir_\beta \beta^2}{c^2} \sinh Q$$

$$g_{13} = g_{24} = \frac{i\beta^2}{\mu k c^2} \cosh P - \frac{i\beta^2}{k_\mu c^2} \cosh Q$$

$$g_{14} = \frac{\beta^2}{kr_\alpha c^2 \mu} \sinh P + \frac{p\beta^2 r_\beta}{\mu k c^2} \sinh Q$$

$$g_{21} = g_{43} = -\frac{2ir_\alpha \beta^2}{c^2} \sinh P - \frac{ip\beta^2}{k^2 r_\beta c^2} \sinh Q$$

$$g_{22} = g_{33} = -\frac{p\beta^2}{k^2 c^2} \cosh P + \frac{2\beta^2}{c^2} \cosh Q$$

$$g_{23} = \frac{r_\alpha \beta^2}{\mu k c^2} \sinh P + \frac{\beta^2}{\mu r_\beta c^2 k} \sinh Q$$

$$g_{31} = g_{42} = \frac{2i\mu\beta^2 p}{kc^2} \cosh P - \frac{2ip\mu\beta^2}{kc^2} \cosh Q$$

$$g_{32} = -\frac{\mu p^2 \beta^2}{k^3 c^2 r_\alpha} \sinh P - \frac{4\mu k r_\beta \beta^2}{c^2} \sinh Q$$

$$g_{41} = -\frac{4\mu k r_\alpha \beta^2}{c^2} \sinh P - \frac{\mu p^2 \beta^2}{r_\beta c^2 k^3} \sinh Q$$

SUMMARY OF EXPLICIT FORMS OF SECOND ORDER SUBDETERMINANTS $g \begin{vmatrix} i & j \\ k & l \end{vmatrix}$

$$g \begin{vmatrix} 1 & 2 \\ 1 & 2 \end{vmatrix} = g \begin{vmatrix} 3 & 4 \\ 3 & 4 \end{vmatrix} = -2\gamma(\gamma - 1) + (2\gamma^2 - \gamma + 1)\overline{CP} \overline{CQ} - \left[\frac{(\gamma-1)^2}{r_\alpha r_\beta} + \gamma^2 r_\alpha r_\beta \right] \overline{SQ} \overline{SP}$$

$$g \begin{vmatrix} 1 & 2 \\ 1 & 3 \end{vmatrix} = g \begin{vmatrix} 2 & 4 \\ 3 & 4 \end{vmatrix} = + (\rho \lambda^2 k)^{-1} \left[\frac{\overline{SQ} \overline{CP}}{r_\beta} + r_\alpha \overline{SP} \overline{CQ} \right]$$

$$g \begin{vmatrix} 1 & 2 \\ 1 & 4 \end{vmatrix} = g \begin{vmatrix} 1 & 2 \\ 2 & 3 \end{vmatrix} = g \begin{vmatrix} 1 & 4 \\ 3 & 4 \end{vmatrix} = g \begin{vmatrix} 2 & 3 \\ 3 & 4 \end{vmatrix} = i(\rho \lambda^2 k)^{-1} \left\{ (2\gamma-1)(1-\overline{CP} \overline{CQ}) + \left[\frac{(\gamma-1)}{r_\alpha r_\beta} + \gamma r_\alpha r_\beta \right] \overline{SP} \overline{SQ} \right\}$$

$$g \begin{vmatrix} 1 & 2 \\ 2 & 4 \end{vmatrix} = g \begin{vmatrix} 1 & 3 \\ 3 & 4 \end{vmatrix} = - (\rho \lambda^2 k)^{-1} \left[r_\beta \overline{CP} \overline{SQ} + \frac{1}{r_\alpha} \overline{SP} \overline{CQ} \right]$$

$$g \begin{vmatrix} 1 & 2 \\ 3 & 4 \end{vmatrix} = - (\rho \lambda^2 k)^{-2} \left[2(1-\overline{CP} \overline{CQ}) + \left(\frac{1}{r_\alpha r_\beta} + r_\alpha r_\beta \right) \overline{SQ} \overline{SP} \right]$$

$$g \begin{vmatrix} 1 & 3 \\ 1 & 2 \end{vmatrix} = g \begin{vmatrix} 3 & 4 \\ 2 & 4 \end{vmatrix} = - (\rho \lambda^2 k) \left[\gamma^2 r_\beta \overline{CP} \overline{SQ} + \frac{(\gamma-1)^2}{r_\alpha} \overline{SP} \overline{CQ} \right]$$

$$g \begin{vmatrix} 1 & 3 \\ 1 & 3 \end{vmatrix} = g \begin{vmatrix} 2 & 4 \\ 2 & 4 \end{vmatrix} = \overline{CQ} \overline{CP}$$

$$g \begin{vmatrix} 1 & 3 \\ 1 & 4 \end{vmatrix} = g \begin{vmatrix} 1 & 3 \\ 2 & 3 \end{vmatrix} = g \begin{vmatrix} 1 & 4 \\ 2 & 4 \end{vmatrix} = g \begin{vmatrix} 2 & 3 \\ 2 & 4 \end{vmatrix} = i(\gamma r_\beta \overline{CP} \overline{SQ} + \frac{(\gamma-1)}{r_\alpha} \overline{SP} \overline{CQ})$$

$$g \begin{vmatrix} 1 & 3 \\ 2 & 4 \end{vmatrix} = + \frac{r_\beta}{r_\alpha} \overline{SQ} \overline{SP}$$

$$g \begin{vmatrix} 14 \\ 12 \end{vmatrix} = g \begin{vmatrix} 23 \\ 12 \end{vmatrix} = g \begin{vmatrix} 34 \\ 14 \end{vmatrix} = g \begin{vmatrix} 34 \\ 23 \end{vmatrix} = i(\rho k \lambda^2) \left\{ \gamma(\gamma-1) (2\gamma-1) (1-\overline{CQ} \overline{CP}) \right. \\ \left. + \left[\frac{(\gamma-1)^3}{r_\alpha r_\beta} + r_\alpha r_\beta \gamma^3 \right] \overline{SQ} \overline{SP} \right\}$$

$$g \begin{vmatrix} 14 \\ 13 \end{vmatrix} = g \begin{vmatrix} 23 \\ 13 \end{vmatrix} = g \begin{vmatrix} 24 \\ 14 \end{vmatrix} = g \begin{vmatrix} 24 \\ 23 \end{vmatrix} = -i \left(\frac{\gamma-1}{r_\beta} \right) \overline{CP} \overline{SQ} + r_\alpha \gamma \overline{CQ} \overline{SP}$$

$$g \begin{vmatrix} 14 \\ 14 \end{vmatrix} = g \begin{vmatrix} 23 \\ 23 \end{vmatrix} = 1 + 2\gamma(\gamma-1) (1-\overline{CQ} \overline{CP}) + \left(\frac{(\gamma-1)^2}{r_\alpha r_\beta} + \gamma^2 r_\alpha r_\beta \right) \overline{SP} \overline{SQ}$$

$$g \begin{vmatrix} 14 \\ 23 \end{vmatrix} = g \begin{vmatrix} 23 \\ 14 \end{vmatrix} = g \begin{vmatrix} 14 \\ 14 \end{vmatrix} - 1$$

$$g \begin{vmatrix} 24 \\ 12 \end{vmatrix} = g \begin{vmatrix} 34 \\ 13 \end{vmatrix} = + (\rho \lambda^2 k) \left[\frac{(\gamma-1)^2}{r_\beta} \overline{CP} \overline{SQ} + r_\alpha \gamma^2 \overline{SP} \overline{CQ} \right]$$

$$g \begin{vmatrix} 24 \\ 13 \end{vmatrix} = + \frac{r_\alpha}{r_\beta} \overline{SP} \overline{SQ}$$

$$g \begin{vmatrix} 34 \\ 12 \end{vmatrix} = (\rho \lambda^2 k)^2 \left[2\gamma^2(\gamma-1)^2 (\overline{CP} \overline{CQ} - 1) - \left[\frac{(\gamma-1)^4}{r_\alpha r_\beta} + \gamma^4 r_\alpha r_\beta \right] \overline{SP} \overline{SQ} \right]$$

EXPLICIT FORMS OF $t \begin{vmatrix} 12 \\ ab \end{vmatrix}$

$$t \begin{vmatrix} 12 \\ 12 \end{vmatrix} = -\frac{\beta^2 \mu}{2\omega^2} (4k^4 r_\alpha r_\beta + p^2)$$

$$t \begin{vmatrix} 12 \\ 13 \end{vmatrix} = -\frac{r_\alpha}{r_\beta} \quad \checkmark t \begin{vmatrix} 12 \\ 24 \end{vmatrix} = \frac{i\beta^2}{2\omega^2} r_\alpha k(2k^2 - p)$$

$$\checkmark t \begin{vmatrix} 12 \\ 14 \end{vmatrix} = \checkmark t \begin{vmatrix} 12 \\ 23 \end{vmatrix} = \frac{i\beta^2 k}{2\omega^2} (2k^2 r_\alpha r_\beta + p)$$

$$\checkmark t \begin{vmatrix} 12 \\ 34 \end{vmatrix} = -\frac{\beta^2 k^2}{2\mu\omega^2} (r_\alpha r_\beta + 1)$$

$$P = kdr_\alpha$$

$$Q = kdr_\beta$$

$$\gamma = \frac{2\beta^2}{c^2}$$

$$p = 2k^2 - \frac{\omega^2}{\beta^2}$$

$$r_\alpha = \sqrt{\frac{c^2}{\alpha^2} - 1}$$

$$SP = \sin P$$

$$CP = \cos P$$

$$c \geq \alpha$$

$$r_\beta = \sqrt{\frac{c^2}{\beta^2} - 1}$$

$$SQ = \sin Q$$

$$CQ = \cos Q$$

$$c \geq \beta$$

$$r_\alpha = -i \sqrt{1 - \frac{c^2}{\alpha^2}}$$

$$SP = \sinh P$$

$$c < \alpha$$

$$CP = \cosh P$$

$$r_\beta = -i \sqrt{1 - \frac{c^2}{\beta^2}}$$

$$SQ = \sinh Q$$

$$c < \beta$$

$$CP = \cosh Q$$

The g_{ij} expressions are written for the hyperbolic functions ($c < \alpha$, $c < \beta$).

For $c > \alpha$, $c > \beta$, the hyperbolic functions transform according to

$$\cosh P \longrightarrow \cos P \quad c > \alpha$$

$$\cosh Q \longrightarrow \cos Q \quad c > \beta$$

$$\sinh P \longrightarrow -i \sin P \quad c > \alpha$$

$$\sinh Q \longrightarrow -i \sin Q \quad c > \beta$$

APPENDIX III

FORTRAN LISTINGS OF COMPUTER PROGRAMS

FLATRAY, STRESS, INTEGRAL, TRAVEL, VARGRAV, AND PRESID

INPUT DATA AND FORMAT FOR FLATRAY

<u>CARD</u>	<u>FORMAT</u>	<u>DATA DESCRIPTION</u>
1	I4	Model identification no.
	I4	No. of layers <41
	I4	No. of modes to be computed <11
	F10.4	Precision of root values of k
	F10.4	Cutoff k value to automatically stop computation
2	8F10.6	Layer parameters stored in sequence α , β , ρ , d ; two layers to a card
3	F10.6	Starting c value
	F10.6	Minimum c value
	F10.6	Decrement of c
	F10.6	Starting k value
	F10.6	k increment for individual modes
	F10.6	k increment to find starting points of different modes
	F10.6	c perturbation
	F10.6	k perturbation
4	?0I4	Mode no. to be found stored sequentially

```

DIMENSION ALPHA(40),BETTA(40),MHO(40),THICK(40),ROOTS(15,40),MODE
1(14),PERIOD(15,40),B(6),E(8),G(6,6),A(6),UD[SP(40),WU]SP(40)
1.4(4)
COMMON UD[SP,MODIS,F,H
MEAU 150,MODEL,NLAYER,NMODE,XMIN,XMAX
150 FOMMAT (314.2F10.4)
MEAD 200,(ALPHA(I),BETTA(I),RHO(I),THICK(I),I=1,NLAYER)
200 FOMMAT(BF10.6)
PRIN 900,MODEL
900 FOMMAT(314-LAYER PARAMETERS FOR MODEL RT: 14 // 6H LAYER,5X,4M AL
1M4,5X,6H BETTA,74,4M MHO,5X,14M THICKNESS(KM),3X, 6H M(KM) /)
ITHICK=0.
UD 902 I=1,NLAYER
ITHICK=ITHICK+THICK(I)
PRIN 902,1,ALPHA(I),BETTA(I),MHO(I),THICK(I),ITHICK
902 FOMMAT(1A.13,3X,F10.4,4X,F8.4,4X,F8.4,5A,F8.2,5X,F8.2)
I)IAL=ITHICK
MEAD 200, CMAX,CMIN,DELC,AK,DELK,DELK1,PTRBC,PTRB K
MEAD 350, (MODE(I),I=1,NMODE)
350 FOMMAT(2014)
I)UV=0
N=MODE(I)
CMAX1=CMAX
MHO=10
I)RMODE(1)
ISIN=10
IA=N-LAYER-1
IV=1
AK=UD(1)(M,IN)=AK
I)IV=1
C=CMAX
JUMP=1
500 I)ISP=1
JUMP=1
I)M=1
UD=XX
S)IV=1.
I)XAC=10
I)VUX=1
10J I=1A
OMEGA=XX=C
HALPH=SQRT(ABS((C/ALPHA(I))**2-1.))
MBET=SUMT(ABS((C/BETTA(I))**2-1.))
A_2=AK**2-OMEGA**2/(BETTA(I)**2)
HEFAC=BETTA(I)**2/(2.*OMEGA**2)
AMU=BETTA(I)**2*MHO(I)**2
M(1)=11+HEFAC*AMU*(-4.,AK**4+RALPH+MBET*AL**2)
M(2)=11+HEFAC*RALPH*AK*(2.,AK**2-A_)
M(3)=11+HEFAC*AK*(-2.,AK**2+RALPH+MBET*AL)
M(4)=11+T13
M(5)=11+MBET*T12/HALPH
M(6)=11+HEFAC*AK**2*(-HALPH*MBET*1.)/AMU
S) GAM=2.* BETTA(I) **2/C**2
U)VS=1.
M)UD=RU(I)*C**2*AK
M)LP=SUMT(ABS((C/ALPHA(I))**2-1.))
M)ET=SQRT(ABS((C/BETTA(I))**2-1.))
M)X=RALPH+THICK(I)
M)A=RBET*THICK(I)
IF(C-ALPHA(I))1,2,2
2 FACA=1.
CP=COS(P)
SP=SIN(P)
GD TU 3
1 FACA=-1.
CP=(EXP(P)+EXP(-P))/2.
SP=(EXP(P)-EXP(-P))/2.
3 IF(C-BETTA(I))5,4,4
4 FACA=1.
CP=COS(Q)
SP=SIN(Q)
GD TU 6
7 FACA=-1.
CP=(EXP(Q)+EXP(-Q))/2.
SP=(EXP(Q)-EXP(-Q))/2.
U)VS=CP*CP
6 G(1,1)=(GAM-1.)*2/(HALPH*RBET)+GAM**2*HALPH*RBET+FACA*FACB
G(1,2)=G(1,1)*SQ*SP-2.*GAM*(GAM-1.)*(2.*GAM**2-2.*GAM+1.)*CP*CU
G(1,3)=(SQ*CP/MBET+HALPH*SP*CO*FACA)/RHOC
G(1,4)=(GAM-1.)/(HALPH*RBET)+GAM*HALPH*RBET+FACA*FACB)*SP*SU*(2.*
GAM-1.)*(1.-CP*CO)
G(1,5)=G(1,3)/MHOC
G(1,6)=G(1,3)
G(1,7)=-(RBET*CP*SQ*FACB+SP*CO/RALPH)/RHOC
G(1,8)=-(2.*(1.-CP*CO)*(1./(HALPH*MBET)+RALPH*RBET+FACA*FACB)*SU*S
1M)/(M)UD**2)
G(2,1)=RHOC*(GAM**2*RBET*FACB*CP**2+(GAM-1.)*2*SP*CO/RALPH)
G(2,2)=CO*CP
G(2,3)=GAM*MBET*FACB*CP*SQ*(GAM-1.)*SP*CO/RALPH
G(2,4)=G(2,3)
G(2,5)=MBET*SQ*SP*FACB/RALPH
G(2,6)=G(1,5)
G(3,1)=(GAM-1.)*3/(HALPH*RBET)+RALPH*RBET+GAM**3*FACB*FACA)*SU
1*SP
G(3,2)=RHOC*(GAM*(GAM-1.)*(2.*GAM-1.)*(1.-CO*CP)+G(3,1))
G(3,3)=(1.4-1.)*CP*SQ*MBET+RALPH*GAM*FACA*CO*SP
G(3,4)=1.+2.*GAM*(GAM-1.)*(1.-CP*CO)*(GAM-1.)*2/(RALPH*RBET)+GAM
1*2*HALPH*MBET*FACA*FACB)*SP*SU
G(3,5)=G(3,3)-1.
G(3,6)=G(2,3)
G(3,7)=G(1,3)
G(4,1)=G(3,1)
G(4,2)=G(3,2)
G(4,3)=G(3,3)-1.
G(4,4)=G(3,3)

```

```

G(4,7)=-G(2,3)
G(4,8)=-G(1,5)
G(5,1)=(GAM-1.)**2*CP*SQ/HBEI*(HALP+4*GAM*GAM*SP*CO*FACA)*HMOC
G(5,2)=HALP*SP*SU*FACA/HBEI
G(5,3)=-G(3,2)
G(5,4)=-G(3,2)
G(5,5)=G(2,2)
G(5,6)=G(1,2)
G(6,1)=(GAM-1.)**4/(HALP*HBEI)*GA**4*RALPH*HBEI*FACA*FACH)**SP*S
10
G(6,1)=HMOC**2*(2.*GAM*GAM+GAM-1.)**2*(CP*CO-1.)-G(6,1)
G(6,2)=G(5,1)
G(6,3)=G(3,1)
G(6,4)=G(3,1)
G(6,5)=G(2,1)
G(6,6)=G(1,1)
IF(IUSF-1)62,62,6012
62 IF(I-1)402,402,101
101 D3 J3 J=1.6
SUM=0
D3 40 K=1.6
SUM=SUM+8(K)*G(K,J)
40 CONTINUE
A(J)=SUM
30 CONTINUE
D3 8 J=1.6
B(J)=A(J)/DIVS
6 CONTINUE
I=I-1
G3 T3 51
402 F=0.1)*G(1,1)+B(2)*G(2,1)+B(3)*G(3,1)+B(4)*G(4,1)+B(5)*G(5,1)+B(6)
1*3(6,1)
F=F/DIVS
IF(I>NMT-1) 603,301,603
C ** COMPUTE FIRST ROOT OF EACH MODE
603 IF(INDX2-1)605,604,605
604 INDX=10
K<1=K4
F1=F
K<L KK=DELK1
G3 T3 100
605 AF=XBS(F)
AF<1=XBS(F1)
IF(AF-AF1) 606,607,607
607 IF(XMS(F1)-AF) 608,609,609
608 IF(AOS(F1-F)-AF1) 608,609,609
609 IF(XMS(KK1-KK)-KKMIN) 308,308,610
610 G3 T3 (703,704),JUMP
702 F2=F
JJMP=2
K<2=K4
K<L XBS(1*KK+F1-KK1*F2)/(F1-F2)
I3MAC=1
G3 T3 1100,60),JUMP1
706 I3MAC=0
F1=F2
K<1=K<2
704 I3MAC=0
IF(KK-KK1) 614,613,613
614 K<=KK+KKMIN
F2=F
K<2=K<1
G3 T3 (370,60),JUMP1
313 F2=AF
K<2=K<1
K<L XBS(KK-KKMIN)
G3 T3 1100,60),JUMP1
606 IF(I3MAC-1)306,706,707
707 IF(V*00-1)617,618,617
617 IF(AF-AF1) 619,619,620
620 K<=KK-2.*DELK1
D[UN=-1.
IF(KK=0,)1014,1014,100
1014 K<=KK+DELK1
N4UD=1
G3 T3 500
619 K<1=K<1
F1=F
K<=KK+SIGN*DELK1
IF(KK=0,)1014,1014,100
303 IF(I3INT-1)3000,508,3000
3000 IF(I3RAC-10) 300,708,708
708 F2=F1
K<2=K<1
300 F1=F
K<L XBS((KK2*F1-KK*F2)/(F1-))
M3U(I3IM,IN)=KK
M<=I3U(I3M,IN)=(2.*3,1416)/IXK*0)
IF(I3INT-1) 950,901,950
950 I3M=1
IF(I3M-MODE(NMODE)) 615,615,616
616 F1=F
K<1=K<1
K<=KK+DELK1
G3 T3 100
617 K<=KK+2.*KKMIN
DELK1=MODES(I3M-1,1)
K<MIN= .01*DELK1
I3M=10
N4UD=1
G3 T3 500
618 I3M=1
JJMP=1
I4UD=1
I4 =MODE(I4UD)

```

```

)DISP=10
JUMP1=2
XK=MODTS(IM .1)
)X1
XKMIN=.01*XK
IJMP=1
)V=1
)L=IX
8000 A_2=.XK*XK-(XK*C)**2/(BETTA(I+1))**2
ALSO=AL*AL
MALPH=SQRT(ABS((C/ALPHA(I+1))**2-1.))
AMU=BETTA(I+1)**2*HMU(I+1)
B(1)=BETTA(I+1)**2/(XK*C**2)
B(2)=AL*BETTA(I+1)**2/(2.*XK**3*C*RALPH)
B(3)=-BETTA(I+1)**2/(2.*AMU*(XK*C)**2)
B(4)=BETTA(I+1)**2/(2.*AMU*MALPH*(C*XK)**2)
8001 IF(IL-1) 8010,8010,8009
8009 B(1)=BETTA(I)**2
AMU=BETTA(I)**2*HMU(I)
MALPH=SQRT(ABS((C/ALPHA(I))**2-1.))
MBET=SQRT(ABS((C/BETTA(I))**2-1.))
M=AL*MALPH*THICK(I)
U=XK*RBET*THICK(I)
)F(C-ALPHA(I)) 8002,8003,8003
8003 FACB=1.
CP=CUS(P)
SP=SN(P)
GO TO 8030
8004 FACB=-1.
CP=(EXP(P)+EXP(-P))/2.
SP=(EXP(P)-EXP(-P))/2.
8030 IF(C=BETTA(I)) 8004,8005,8005
8005 FACB=1.
CJ=CUS(Q)
SJ=SN(Q)
GO TO 8006
8006 FACB=-1.
CJ=(EXP(Q)+EXP(-Q))/2.
SJ=(EXP(Q)-EXP(-Q))/2.
8006 BIG = BETTA(I)**2/(XK*C)
A_2=.XK*XK-(XK*C)**2/BETTA(I)**2
G(1,1)=2.*B(1)*SU*CP/(C*C)-AL*BIG*CO/XK
G(1,2)=-AL*BIG*SP/(RALPH*XK)*2.*B(3)*RBET*SQ*FACB*XK
G(1,3)=-BIG*(CP-CU)/AMU
G(1,4)=B(1)*SP/(AMU*MALPH)*BIG*SU*MBET*FACB/AMU
G(2,1)=-2.*BIG*RALPH*SP*FACA*XK-AL*BIG*SO/(XK*RBET)
G(2,2)=-AL*BIG*CP/XK*2.*BIG*CO*XK
G(2,3)=MALPH*BIG*SP*FACA/AMU*d)G*SU/(RBET*AMU)
G(2,4)=-G(1,3)
G(3,1)=2.*AMU*AL*BIG*(CP-CU)
G(3,2)=-AMU*AL*AL*BIG*SP/(RALPH*XK*XK)-4.*AMU*RBET*SU*FACB*BIG*XK
)XK
G(3,3)=G(2,2)
G(3,4)=-G(1,2)
G(4,1)=-4.*AMU*XK*XK*RALPH*BIG*SP*FACA-AMU*AL*AL*BIG*SO/
)XK*XK*MBET)
G(4,2)=-G(3,1)
G(4,3)=G(2,1)
G(4,4)=G(1,1)
)D 8007 J=1,4
)JM=0,
)D 8008 K=1,4
)JM=)JM+B(K)*G(K,J)
8009 )CONTINUE
A(J)=SUM
8007 )CONTINUE
)D 8011 J=1,4
E(J)=B(J)
M(J)=B(J)*A(J)
8011 )CONTINUE
)F(IL-1)89,83,84
)S I=1-1
)D TU 8001
8010 E(5)=E(1)
E(6)=E(2)
E(7)=E(3)
E(8)=E(4)
)F(IL-1)81,81,82
81 )LOAD=THICK(I)
)FICK(I)=0.
)L=10
)L=1
)D TU 8009
84 )F(IL-1) 85,85,86
85 )FICK(I)=)LOAD
)IVS=1.
)D TU 51
8012 IF(IL-1)90,87,88
87 )DISP(2 )=-A(2)*G(1,1)-A(3)*G(2,1)-A(4)*G(3,1)
)DISP(2 )=A(1)*G(1,1)+A(3)*G(4,1)-A(4)*G(5,1)
)DISP(2)= )DISP(2)/DIVS
)DISP(2)= )DISP(2)/DIVS
)L=10
M(1)=E(1)
M(2)=E(2)
M(3)=E(3)
M(4)=E(4)
)D TU 8009
88 )FICK(I)=0.
)IVS=1.
)D TU 51
88 )DISP(1 )=-A(2)*G(1,1)-A(3)*G(2,1)-A(4)*G(3,1)
)DISP(1 )=A(1)*G(1,1)+A(3)*G(4,1)-A(4)*G(5,1)
)DISP(1)= )DISP(1)/DIVS
)DISP(1)= )DISP(1)/DIVS

```

```

IDISP=1
I4ICK(1)=HOLD
L=IX+1
PUNCM 2701,MODEL,IM,L,TOTAL,C,PERIOD(M,IN)
PUNCM 1032,(UDISP(J),NDISP(J),J=1,L)
JIV=NDISP(1)
DO 1001 J=1,IX+1
UDISP(J)=UDISP(J)/DIV
NDISP(J)=NDISP(J)/DIV
1001 CONTINUE
IPUN=IPUN+2
PUNCM 2701,MODEL,IM,L,TOTAL,C,PERIOD(M,IN)
PUNCM 1032,(UDISP(J),NDISP(J),J=1,L)
2701 FCHMAT(314,3F9.3)
1032 FCHMAT(6E13.6)
GO TO (8025,901,8026),IJMP
82 MOLA=THICK(1)
I4ICK(1)=0,
L=0
GO TO 8009
87 I4ICK(1)=HOLD
L=0
M=1
DIVS=1,
GO TO 51
90 GO TO(92,91,93,96),M
92 GO 8014 K=1,6
SJM=0,
DO 8015 J=2,4
SJM=SUM(B(J)*G(J-1,K))
8015 CONTINUE
A(K)=SUM
8014 CONTINUE
DO 8031 J=1,6
B(J)=A(J)/DIVS
8031 CONTINUE
I=1-1
M=2
GO TO 51
91 IF(I-1) 94,94,95
95 GO 8016 J=1,6
SJM=0,
DO 8017 K=1,6
SJM=SUM(B(K)*G(K,J))
8017 CONTINUE
A(J)=SUM
8016 CONTINUE
DO 8018 J=1,6
B(J)=A(J)/DIVS
8018 CONTINUE
I=1-1
GO TO 51
94 UDISP(L+1)=-A(1)*G(1,1)-A(2)*G(2,1)-A(3)*G(3,1)-A(4)*G(4,1)
I=A(5)*G(5,1)-A(6)*G(6,1)
UDISP(L+1)=UDISP(L+1)/DIVS
B(1)=M(1)
B(2)=M(2)
B(3)=M(3)
B(4)=M(4)
I=L
M=3
DIVS=1,
GO TO 51
95 A(1)=-B(1)*G(1,1)-B(3)*G(4,1)+B(4)*G(5,1)
A(2)=-B(1)*G(1,2)-B(3)*G(4,2)+B(4)*G(5,2)
A(3)=-B(1)*G(1,3)+B(3)*G(4,3)-B(4)*G(5,3)
A(4)=-B(1)*G(1,4)+B(3)*G(4,4)-B(4)*G(5,4)
A(5)=-B(1)*G(1,5)-B(3)*G(4,5)+B(4)*G(5,5)
A(6)=-B(1)*G(1,6)-B(3)*G(4,6)+B(4)*G(5,6)
DO 8019 J=1,6
B(J)=A(J)
8019 CONTINUE
M=4
I=1-1
GO TO 51
96 IF(I-1) 97,97,98
98 G(1,3)=-G(1,3)
G(1,4)=-G(1,4)
G(2,3)=-G(2,3)
G(2,4)=-G(2,4)
G(3,1)=-G(3,1)
G(3,2)=-G(3,2)
G(3,5)=-G(3,5)
G(3,6)=-G(3,6)
G(4,1)=-G(4,1)
G(4,2)=-G(4,2)
G(4,5)=-G(4,5)
G(4,6)=-G(4,6)
G(5,3)=-G(5,3)
G(5,4)=-G(5,4)
G(6,3)=-G(6,3)
G(6,4)=-G(6,4)
DO 8020 J=1,6
SJM=0,
DO 8021 K=1,6
SJM=SUM(B(K)*G(K,J))
8021 CONTINUE
A(J)=SUM
8020 CONTINUE
DO 8022 J=1,6
B(J)=A(J)/DIVS
8022 CONTINUE
I=1-1
GO TO 51
97 UDISP(L+1)=-A(1)*G(1,1)-A(2)*G(2,1)+A(3)*G(3,1)+A(4)*G(4,1)

```



```

1=A(5)*G(5,1)-A(6)*G(6,1)
MDISP(L+1)=MDISP(L+1)/DIVS
B(1)=E(5)
B(2)=E(6)
B(3)=E(7)
B(4)=E(8)
L=L-1
L=L-1
L=L-1
802> A<=MODTS(IM, 1)*DELK
      IN=2
      C<=CMAX-DELC
2000 PRINT 1030,IM,TOTAL
1030 P<=MAT(6H-MODE 13 /19H SECTION THICKNESS F8.2 //11X, 15H PHASE VEL
      UC=ITY,4X,2H K, 8X,10H PERIOD(S),4X,15H GROUP VELOCITY,8X,10H PERIO
      D(S))
      PRINT 1031,CMAX,RDTS(IM,1),PERIOD(IM,1)
1031 P<=MAT(12X,F10.4,3X,F10.5,4X,F10.4)
      GO TO 500
301 IF(INDX2-1) 502,501,502
501 INDX2 = 10
      A<1=A<
      P1=F
      A<=A< + DELK
      GO TO 100
502 AF=ABS(F)
      AF1=ABS(F1)
      IF(AF-AF1) 504,503,503
503 IF(ABS(F1-F) -AF) 507,506,506
504 IF(ABS(F1-F)-AF)1507,506,506
506 IF(ABS(XK1-XK)-XKMIN)508,508,610
507 IF(ORAC-1) 508,706,513
513 IF(AF-AF1) 510,510,511
511 IF(IUP-1) 2004,2004,510
2004 IF(IUP1-1) 2006,2006,2005
2005 A<1=A<
      P1=F
      GO TO 2006
400> D1=V-1,
      A<=XK-2,* DELK
      IJ=10
4002 A<=RDTS(IM,IN-1) 2002,2002,60
      IJ=10
      D1=V+1,
      GO TO 500
510 A<1=A<
      P1=F
      A<=XK+DELK+SIGN
      IF(XK-MDTS(IM,IN-1)) 2002,2002,60
      6) IF(XK-XKMAX) 100,100,520
508 IF(ORAC-10) 709,710,710
710 P2=F1
      A<2=A<1
707 P1=F
      A<= ABS((XK2+F1-XK+F2)/(F1-F2))
      IF(IPTMB-.1530,529,530
529 RDTS(IM,IN)=XK
      PERIOD(IM,IN)=(2.*3.1416)/(XK*C)
      DISP=10
      IJMP=2
      L=L+1
      GO TO 8000
901 IF(IPTMB -.1531,528,531
528 C=C+PTRBC
      IF(C-CMIN)520,520,546
546 IF(IN-3)532,533,533
532 A<=RDTS(IM,IN)
      IJ=10
      IJ=1
      IF(XK-XKMAX) 500,500,61
533 A<1=RDTS(IM,IN-2)
      A<2=RDTS(IM,IN)
      A<3=RDTS(IM,IN-1)
      C1=CMAX1-C
      D1=-(XK3-XK1)/(2.*DELC)
      D2=(XK3-2.*XK2+XK1)/DELC**2
      A<=A<1-D1*C1+(D2*C1*(C1-DELC))/2,
      IJ=10
      IJ=1
      IF(XK-XKMAX) 500,500,61
531 C=C-DELC
      IJ=10
      IF(C-CMIN)520,521,521
521 IF(IN-3) 522,523,523
522 A<=RDTS(IM,IN)+.5*(RDTS(IM,IN)-RDTS(IM,IN-1))
      IJ=IN+1
      IJ=1
      IF(XK-XKMAX)500,500,520
523 A<1=RDTS(IM,IN-2)
      A<2=RDTS(IM,IN-1)
      A<3=RDTS(IM,IN)
      C1=CMAX1-C
      CMAX1=CMAX1-DELC
      D1=-(XK3-XK1)/(2.*DELC)
      D2=(XK3-2.*XK2+XK1)/DELC**2
      IJ=IN+1
      A<=A<1-D1*C1+(D2*C1*(C1-DELC))/2,
      IJ=1
      IF(XK-XKMAX)500,500,520
520 IF(IN-MODE(NMODE))524,525,525
524 IJ=I+1
      NEMUD = 1

```

```

I4=NUDE (IMUD)
K<=RUO)S(IM,1)
K<MIN=.01*XK
K<MAX=10.*RODTS(IM,1)
I>IRB=1
C<X1=C<MAX
C<C<MAX
IDISP=10
IL=1
I<MP=3
IN=1
IX=N<LAYER-1
IDIAL=ITMICK
GO TO 8000
8026 C<C<MAX-DELC
I4=2
IX=N<LAYER-1
I<MP=1
GO TO 2000
530 M1=RUO)S(IM,IN)*(C<PTRBC)
M2=K<C
D<=MODTS(IM,IN)-XK
M<=(M2-M1)/DK
C<=C<PTRBC
I<MP=2+.3.1416/((M2-M1)/2.*M1)
I>IRB=1
K<MAX=MODTS(IM,IN)+10.*(MODTS(IM,IN)-RODTS(IM,IN-1))
K<MIN=.01*RODTS(IM,IN)
M<IN=1020.C.RD)S(IM,IN).PERIOD(IM,IN).R.TGRR
1020 F<MMAT(12X.F10.4.3X.F10.5.4X.F10.4.6X.F10.4.12X.F10.4)
GO TO 531
61 C<C<PTRBC
M<IN=1031.C.RD)S(IM,IN).PERIOD(IM,IN)
GO TO 520
520 P<JNCH 2701,IPUN
M<AUSE 7
M<EAD 350,IPUN
GO 556 I=1,IPUN
M<EAD 2701,MODEL,IM,L,TOTAL,C,PERIOD(1,1)
M<EAD 1042,UDISP(J),MDISP(J),J=1,L)
M<IN=557,MODEL,IM,C,PERIOD(1,1),TOTAL
557 F<MMAT(104-MODEL RTI 14 /, 5M MODE 14/ .15M PHASE VELOCITY F9.3 /,
1 7M PERIOD F9.3/ .22M SECTION )MICAVESS(KM) F9.3 /// )
M<IN=2703
2703 F<MMAT ( 52M DISPLACEMENTS AT LAYER INTERFACES NORMALIZED TO THE/
101M VERTICAL DISPLACEMENT AT THE SURFACE (INTERFACE 0) / )
M<IN=2704
2704 F<MMAT(10M INTERFACE .5X.13M HORIZ. DISP..5X.12M VERI. DISP.)
GO 556 J=0,L-1
M<IN=556 .J,UDISP(J+1),MDISP(J+1)
556 F<MMAT (5X.13.11X.E13.6.9X.E13.6)
M<IN=1024
1024 F<MMAT (19M END OF COMPUTATION )
M<AUSE
END

```

INPUT DATA AND FORMAT FOR STRESS

<u>CARD</u>	<u>FORMA.</u>	<u>DATA DESCRIPTION</u>
1	I5	No. of layers in model
	I5	No. of (c,k) pairs for which modal shape is to be computed
2	8F10.4	Layer parameters stored in sequence, α, β, ρ, d ; two layers to a card
3	E13.6	c
	E13.6	k
	E13.6	Horizontal to vertical surface displacement ratio, $\frac{u_0}{w_0}$

Repeat card 3 for each set of c,k, $\frac{u_0}{w_0}$.

```

PROGRAM STRESS.          J.M.DUMM   GU-161
DIMENSION ALPHA(50),BETA(50),D(50),MHO(50),LAMBDA(50),AN(4),K,
1 HU(50)
REAL LAMBDA,HU
DOUBLE PRECISION AN,WATIO,SIGU,TAGU,UNDO,MMO,MMSIG,MMTAU,MMH1,
1COSPH,COSQH,SINPH,SINQH,UDOT,UDOTM,MDOT,MDOTM,X,Y,PH,QH,NALPAN
DOUBLE PRECISION DEXPPH,RECIPP,DEXPQH,RECIPQ,MBETA,OH1,MHC2,ALFA
DOUBLE PRECISION MHO,MOH,PERIOD
DOUBLE PRECISION C,ALPHA,BETA,BATEA,K,D,DH,GAHNAH,TESTER,CSQARE
DOUBLE PRECISION MMHAT(4),OLDPAT(4)
1000 CONTINUE
READ(1,1) LAYERS,NCASES
NCASES IS THE NUMBER OF CASES OF C,K,RATIO FOR A GIVEN SET OF
C LAYER PARAMETERS, ALPHA, BETA, RHO, D.
561 HEAD(1,1) = (ALPHA(1),BETA(1),MHO(1),D(1)), Y = 1, LAYERS)
WRITE(3,3) (ALPHA(I),BETA(I),RHO(I),D(I)), I=1, LAYERS)
1 FORMAT(4F10.4)
1 FORMAT(2F5)
KMYTR = LAYERS - 1
DO 200 LO=1,NCASES
HEAD(1,2) = C,K,WATIO
CSQARE = C**2
PERIOD = 6.2811951072/4K**C
UDOT=HATIO
MDOT=1.0
OLDPAT(1) = UDOT
OLDPAT(2) = MDOT
2 FORMAT(4E11.6)
WRITE(1,9) C,PERIOD
3 FORMAT(1M1,5X,15#PHASE-VELOCITY#,E20.12,/,5X,7#PERIOD#,4X,E20.12,
1//,10X,4#HORIZONTAL DISP.#,1X,10X,12#HORIZONTAL DISP.#,1X,10X,11#VERT. DISP.#,/<
#0
4RTM(1,3) = 10,K,DDOT,MDOT
10 FORMAT(10X,2X,15,7X,1X,6X,E20.12,6X,E20.12)
DO 100 M=1,LAYERS
MHO(1) = BETA(1) ** 2 * RHO(1)
LAMBDA(1) = RHO(1) * ALPHA(1) ** 2 - 2.0 * BETA(1) ** 2
100 CONTINUE
1201 SIGU=0.
1202 TAU=0.
1201 OLDPAT(1) = SIGU
1204 OLDPAT(2) = TAU
1205 DO 200 N = 1, KMYTR
1206 M = N + 1
1207 ALPHA = ALPHA(N)
1208 RHO = RHO(N)
1209 BATEA = BETA(N)
1210 DH = D(N)
1211 Y=DARS((C/ALPHA)**2-1.)
1212 Y = DABS((C/BATEA)**2-1.)
1213 RALPAN = DSQRT(Y)
1214 MBETA = DSQRT(Y)
1215 GAHNAH = 2.0*BATEA/C**2
1216 PH = K * RALPAN * DH
1217 OH = K * MBETA * DH
1218 TESTER = C-ALPHA
1219 TP (C-ALPHA) 225,220,220
220 COSPH = DCOS(PH)
SINPH = DSIN(PH)
APASYN=1.0
GO TO 230
225 DEXPPH = DEXP(PH)
RECIPP = 1.0/DEXPPH
COSQH = DEXP(PH) * RECIPP/2.0
SINQH = DEXP(PH) * RECIPP/2.0
APASYN=1.0
230 CONTINUE
TESTER = C - BATEA
IP (C-BATEA) 231,237,237
231 DEXPQH=DEXP(QH)
RECIPQ = 1.0/DEXPQH
COSQH = DEXPQH * RECIPQ/2.0
SINQH = DEXPQH * RECIPQ/2.0
BTASIN=1.0
GO TO 239
237 SINQH = DSIN(QH)
COSQH = DCOS(QH)
BTASIN=1.0
239 CONTINUE
GH1 = GAHNAH-1.
PHC2 = RHO(M) * CSQARE
1111 AN(1,1) = GAHNAH * COSPH - GH1 * COSQH
1112 AN(1,2) = GH1 * SINPH / RALPAN & GAHNAH * MBETA * SINQH * BTASYN
1113 AN(1,3) = -COSPH - COSQH / MHC2
1114 AN(1,4) = SINPH / RALPAN & MBETA * SINQH * BTASYN / MHC2
1115 AN(2,1) = -GAHNAH * RALPAN * SINPH * APASYN & GH1 / MBETA * SINQH
1116 AN(2,2) = -GH1 * COSPH & GAHNAH * COSQH
1117 AN(2,3) = RALPAN * SINPH * APASYN & SINQH / MBETA / MHC2
1118 AN(2,4) = AN(1,3)
1119 AN(3,1) = PHC2 * GAHNAH * GH1 * COSPH - COSQH
1120 AN(3,2) = PHC2 * GH1 * GH1 * SINPH / RALPAN & GAHNAH ** 2 * MBETA
1121 AN(3,3) = AN(2,2)
1122 AN(3,4) = AN(1,2)
1123 AN(4,1) = PHC2 * GAHNAH ** 2 * RALPAN * SINPH * APASYN & GH1 * GH1 / MBETA *
1124 AN(4,2) = AN(3,1)
1125 AN(4,3) = AN(2,1)
1126 AN(4,4) = AN(1,1)
WRITE(1,10)
1010 FORMAT(' MATHS OF A-5. ')
DO 101 M=1,4
101 WRITE(1,11) (AN(M),L),L=1,4)
1111 FORMAT(5X,6E20.12)
DO 9999 IMP = 1,8
MODIMP = MOD(IMP,2)
MIMP10 = MOD(IMP-1)
WRITE(1,IMP) = 0.0

```

```

S.0101 DO 8888 KXY 8 1,4
S.0102 MODKXY 8 MODKXY,2<
S.0103 MPKP 8 MHP1*MODKXY
S.0104 MPAC 8 1<*MPKP
S.0105 PAC 8 PLOATMPAC<
S.0106 MPMATMHP<PAC*ANSHP,KXY<OLDNATKXY<6HEMNATMHP<
S.0107 8888 CONTINUE
S.0108 UOOTH 8 RPNAT 41<
S.0109 UDOT 8 HEHAT 42<
S.0110 WRITE 41,10<N,UOOTH,UOOTH
S.0111 DO 8888 KLJ 8 1,4
S.0112 8888 OLDNAT 4KLJ< 8 HEHAT 4KLJ<
S.0113 200 CONTINUE
S.0114 GO TO 1967
S.0115 END

```

		STORAGE MAP		VARIABLES (TAGS: C=COMMON, Z=EQUIVALENCE)							
NAME	TAG	RPL ADR	NAME	TAG	REL ADR	NAME	TAG	REL ADR	NAME	TAG	REL ADR
X		000158	X		000219	Y		000270	C		000278
AM		000300	AM		000308	PM		000388	QM		000390
MHO		000399	MHO		000340	ON1		000530	NOM		000536
BETA		000540	BETA		000600	SIGU		000860	YA00		000868
MHO		000870	MHO		000878	UOOT		000940	WDOT		000948
RATIO		000990	RATIO		000898	MHON1		000940	COSP		000948
SINQ		000980	SINQ		000888	SINQ		000800	UOOT		000808
ALPHA		000950	ALPHA		000808	BATEA		000820	NEWSIO		000828
RALPAN		000970	RALPAN		000878	OXIPPH		000900	RECIPP		000908
RECIPQ		000910	RECIPQ		000918	NDTAN		000920	PENIOD		000928
TESTPR		000930	TESTPR		000938	CQARE		000940	HEHAT		000948
I		000968	I		000988	4		000980	L		000990
10		000998	10		000A50	HI		000A60	HK		000A68
KXY		000A68	KXY		000A60	PAC		000A70	KLJ		000A78
MHP1		000A78	MHP1		000A70	MHP1		000A80	MHP1		000A88
LAYERS		000A88	LAYERS		000B50	NCASES		000B54	APASYN		000B58
MODTNP		000B50	MODTNP		000B60	MODKXY		000B64			

EXTERNAL REFERENCES

NAME	REL ADR	NAME	REL ADR	NAME	REL ADR	NAME	REL ADR
DCOS	000868	DCOS	000860	DSIN	000870	OEZP	000874

CONSTANTS

NAME	REL ADR	NAME	REL ADR	NAME	REL ADR	NAME	REL ADR
0000000	000B50	0000000	000B54	00000002	000B58	41100000	000B5C
0000000	000B50	0000000	000B54	4164672D51121B7F	000B5C		
000019	000B58						

IMPLIEO EXTERNAL REFERENCES

INPUT DATA AND FORMAT FOR INTEGRAL

<u>CARD</u>	<u>FORMAT</u>	<u>DATA DESCRIPTION</u>
1	I10	No. of layers in model
	F10.4	Factor for singular matrix criteria in curve fitting subroutine, generally = .99.
	I10	degree+1 of the polynomial fit to the displacement data
	I10	Read option; 1 if read every set of displacements; 0 if read every other set
2	8F10.6	Layer parameters stored in sequence α, β, ρ, d ; two layers to a card
3	20A4	Text identification ≤ 80 characters
4	I4	Model identification no.
	I4	Mode no.
	I4	No. of layers
	F9.3	Total section thickness
	F9.3	Phase velocity in km/s
	F9.3	Period in sec
	5	6E13.6

For computations involving more than one set of displacements corresponding to a (a,T) pair, repeat cards 4 & 5 for each set.


```

S.0001 SUBROUTINE GJ33 NA,N,EPS4
S.0002 DIMENSION A(10),Z(4),R(20),C(20),L(20),Q(20)
S.0003 DOUBLE PRECISION A,B,C,EPS,PIVOT,Z
S.0004 INTEGER I,J
S.0005 DO 10 J=1,N
      DETERMINATOR OF THE PIVOT ELEMENT
      PIVOT=0.
S.0006 DO 20 I=J,N
S.0007 DO 20 I=J,N
S.0008 IPIVOT=ABS(A(I,J))-DABS(PIVOT)<<20,20,30
S.0009 10 PIVOT=ABS(A(I,J))
S.0010 PIVOT=ABS(A(I,J))
S.0011 20 CONTINUE
S.0012 IPIVOT=PIVOT<<EPS<<40,40,50
S.0013 EXCHANGE OF THE PIVOTAL ROW WITH THE KTH ROW
S.0014 50 IPIVOT=K<<60,60,60
S.0015 60 DO 70 J=1,N
S.0016 I=IPIVOT
S.0017 Z(I,J)=A(I,J)
S.0018 Z(I,J)=A(I,J)
S.0019 A(I,J)=A(K,J)
S.0020 70 A(K,J)=Z(I,J)
S.0021 EXCHANGE OF THE PIVOTAL COLUMN WITH THE JTH COLUMN
S.0022 80 IPIVOT=K<<90,90,95
S.0023 95 DO 100 I=1,N
S.0024 L(I,K)=A(I,K)
S.0025 Z(I,K)=A(I,K)
S.0026 100 A(I,K)=L(I,K)
S.0027 90 CONTINUE
S.0028 JORDAN STEP
S.0029 DO 110 I=1,N
S.0030 IPIVOT=K<<120,120,130
S.0031 120 A(I,I)=1./PIVOT
S.0032 CRIC(I)
S.0033 DO 130 J=1,N
S.0034 A(I,J)=A(I,J)-A(I,I)*PIVOT
S.0035 CRIC(I)=A(I,I)
S.0036 130 A(I,I)=PIVOT
S.0037 DO 140 J=1,N
S.0038 DO 140 I=1,N
S.0039 140 A(I,J)=A(I,J)-A(I,I)*A(I,J)
S.0040 EXCHANGE OF THE PIVOTAL ROW WITH THE KTH ROW
S.0041 DO 150 I=1,N
S.0042 IPIVOT=K<<160,160,160
S.0043 160 DO 170 J=1,N
S.0044 I=IPIVOT
S.0045 Z(I,J)=A(I,J)
S.0046 A(I,J)=A(K,J)
S.0047 170 A(K,J)=Z(I,J)
S.0048 EXCHANGE OF THE PIVOTAL COLUMN WITH THE JTH COLUMN
S.0049 180 IPIVOT=K<<190,190,195
S.0050 195 DO 200 I=1,N
S.0051 L(I,K)=A(I,K)
S.0052 Z(I,K)=A(I,K)
S.0053 200 A(I,K)=L(I,K)
S.0054 180 CONTINUE
S.0055 JORDAN STEP
S.0056 DO 210 I=1,N
S.0057 IPIVOT=K<<220,220,230
S.0058 220 A(I,I)=1./PIVOT
S.0059 CRIC(I)
S.0060 DO 230 J=1,N
S.0061 A(I,J)=A(I,J)-A(I,I)*PIVOT
S.0062 CRIC(I)=A(I,I)
S.0063 230 A(I,I)=PIVOT
S.0064 DO 240 J=1,N
S.0065 DO 240 I=1,N
S.0066 240 A(I,J)=A(I,J)-A(I,I)*A(I,J)
S.0067 210 CONTINUE
S.0068 45 TORNAI=ABS(PIVOT)-DABS(PIVOT) I=1,3,7H J=1,3,7H PIVOT=16.9/K
S.0069 DO 250 I=1,N
S.0070 250

```

SYMBOLIC MAP VARIABLES (C=COMMON, E=EQUIVALENCE)

NAME	TAG	REL. ADDR	NAME	TAG	REL. ADDR	NAME	TAG	REL. ADDR	NAME	TAG	REL. ADDR
A		000160	P		000160	C		000200	Z		000200
B		000200	PIVOT		000200	N		000200	P		000200
C		000200	F		000200	I		000200	J		000200
Z		000200	N		000200						

EXTERNAL REFERENCES

NAME	REL. ADDR	NAME	REL. ADDR	NAME	REL. ADDR	NAME	REL. ADDR

CONSTANTS

NAME	REL. ADDR	NAME	REL. ADDR	NAME	REL. ADDR	NAME	REL. ADDR
0000000	000100	0000000	000100	41100000	000100		
0000000	000100	0000000	000100	000400	000100		

INDEXED EXTERNAL REFERENCES

NAME	REL. ADDR	NAME	REL. ADDR	NAME	REL. ADDR	NAME	REL. ADDR

STATEMENT NUMBER	REL. ADDR	STATEMENT NUMBER	REL. ADDR	STATEMENT NUMBER	REL. ADDR	STATEMENT NUMBER	REL. ADDR
00010	000100	00020	000100	00050	000200	00060	000200
00020	000100	00030	000100	00085	000200	00100	000200
00030	000100	00040	000100	00065	000200	00140	000200
00040	000100	00050	000100	00072	000200	00190	000200
00050	000100	00060	000100	00080	000200	00155	000200
00060	000100	00070	000100	00090	000200		

TYPE OF COMMON 000200 PROGRAM 000200

END OF COMPILATION GJ33

INPUT DATA AND FORMAT FOR TRAVEL

<u>Card</u>	<u>Format</u>	<u>Data Description</u>
1	I4	No. of models for which T-D curves are to be computed
2	20A4	Identification for models \leq 80 characters
3	I4	NLAYER = no. o. velocity layers in model
	I4	NR; depths of penetration for which T-D values are to be computed = (NR)*(DELR)
	F8.4	DELR = Interval in (km) for numerical integration
	F8.4	DEPTH = maximum depth (km) of penetration \leq depth of last velocity value
	F8.4	EPSLON = distance (km) from maximum depth to begin using modified trapezoidal rule of integration; usually .3km
	F8.4	DELTA = distance from maximum depth at which integration is stopped; usually .01km
4	10F8.4	Velocities in km/sec
5	10F8.4	Depths (km) from surface of given velocities

```

DIMENSION T(200),DEL(200),R(200),VEL(200),Z(900),ANGLE(200),V(900)
1.04(200),TEXT(20)
DOUBLE PRECISION T,DEL,R,VEL,Z,V,DZ,DELR,DEPTH,EPS,DELTA,H1,R2,H3,
DELTA,B,C,DEPTH1,RO,XP,P,P2,SUM,SUM1,SUM2,ETA,FACT,FACT1,FACT2,
2.1EST,VV1,DD,DL1,DEPTH2,FACT5,FACT6,FACT3,FACT4,TAO,SLOP,SKD,A1,A2
3.1,1,1,1,C1,C2
DOUBLE PRECISION ZMAT(4,4),NDUMMY,VVEC(4),AVEC(4),D
70 FOMMAT(4E25,16)
HEAD (1,100) MMUN
DO 300 IRUN = 1, NRUN
HEAD (1,400) (TEXT(I),I=1,20)
HEAD (1,100) NLAYER,NR,DELR,DEPTH,EPSLON,DELTA
HEAD (1,200) (VEL(I),I=1,NLAYER)
HEAD (1,200) (H(I),I=1,NLAYER)
100 FOMMAT (214,4F8,4)
200 FOMMAT (10F8,4)
Z(I)=D
I=1
19 I=I+1
Z(I)=Z(I-1)+DELR
IF (Z(I)-DEPTH) 19,19,20
20 J=1
R=1
I=1
IJMP=1
7 J=J+1
NR=NR+1
42 CONTINUE
DO 710 LI=1,4
NDUMMY = NR - 4 + LI
DJMNT = R(NDUMMY)
WRITE (3,5000) DUMMY
ZMAT(LI,1) = 1.
DO 705 LJ=2,4
ZMAT(LI,LJ) = DUMMY*(LJ-1)
705 CONTINUE
710 CONTINUE
NDUMMY = 4
EPS = 0.001
CALL GJR4(ZMAT,NDUMMY,EPS)
DO 715 IJ=1,4
NDUMMY = NR - 4 + LJ
VVEC(IJ) = VEL(NDUMMY)
715 CONTINUE
DO 725 LI=1,4
DJMNT = 0.
DO 720 LJ=1,4
DJMNT = DJMNT + ZMAT(LI,LJ)*VVEC(LJ)
720 CONTINUE
AVEC(LI) = DUMMY
725 CONTINUE
A = AVEC(1)
B = AVEC(2)
C = AVEC(3)
D = AVEC(4)
DO 730 TU(31,40),IJMP
V(I) = A + B*Z(I) + C*Z(I)**2 + D*Z(I)**3
I=I+1
IF (Z(I)-H(I)) 31,31,30
30 IF (Z(I)-DEPTH) 33,33,34
33 IF (I(J+3)-DEPTH) 7,7,32
32 H(J)=DEPTH
HJ TU 31
34 U=PTH1+6371.-DEPTH
I=U
37 I=I+1
Z(I)=6371.-Z(I)
IF (Z(I)-DEPTH) 36,36,35
36 I=I
H3=6371.0
X4=VM
INC= DEPTH/(XR*DELR)
INC= INC*NR
NR=1
NRP1 = NR + 1
INCPI > INC < 1
NRH = 4
DO 8 J > NRP1,INCPI,NR
DELT=DELM
IJMP=2
UZ(V) = 6371.-Z(J)
X2 = XR*DELM
IF (6371.0-Z(IJ)-H(NRR )) 42,42,45
45 NRM = NRH + 3
DO TU 42
40 P=Z(J)/V(J)
P2=P**2
IF ((RO/V(1))**2-P2) 4000,405,405
405 CONTINUE
SJM=USQRT((-RO/V(1))**2-P2)
IF (J=2) 11,11,10
11 SJM1=0.
SJM2=0.
DO 10 12
10 SJM1=1./(RO*SJM)
SJM2=SJM1*(RO/V(1))**2
K=Z
24 ETA=Z(K)/V(K)
IF (ETA-P) 4000,240,240
240 CONTINUE
FACT=DSORT((ETA-P)*(ETA+P))
FACT1=1./FACT*Z(K)
FACT2= FACT1 *(Z(K)/V (K))**2
SJM1=SJM1+2.*FACT1

```

```

SUM2=SUM2+2.*FACT2
N = N + 1
IF (Z(K)-Z(J)-EPSLON)22,23,24
22 TEST=Z(J)+EPSLON-.01
IF (Z(K)-TEST)12,23,23
23 DEPTH1=Z(J)+EPSLON
DEPTH1 = 6371.-DEPTH1
VV1=A+DEPTH1*(B+DEPTH1*(C+DEPTH1*D))
DEPTH1 = 6371.-DEPTH1
DD=EPSLON
ETA=DEPTH1/VV1
IF (ETA-P) 4000,240,230
230 CONTINUE
FACT=DSQRT((ETA-P)*(ETA+P))
FACT1=1./(FACT*DEPTH1)
FACT2=FACT1*(DEPTH1/VV1)**2
SUM1 =SUM1+DELK * FACT1*DEL1
SUM2 = SUM2+DELR * FACT2*DEL1
GO TO 21
12 DEL1=-Z(J) - EPSLON *Z(K-1)
GO TO 23
21 I=1
PDW=0.
DD = EPSLON
DEPTH2=Z(J)+DD
14 PDW=PDW+1.
IF (I-1)16,15,17
16 DEPTH1=DEPTH2
DEPTH1 = 6371.-DEPTH1
VV1=A+DEPTH1*(B+DEPTH1*(C+DEPTH1*D))
DEPTH1 = 6371.-DEPTH1
ETA=DEPTH1/VV1
IF (ETA-P) 4000,160,160
160 CONTINUE
FACT=DSQRT((ETA-P)*(ETA+P))
FACT1=1./(FACT*DEPTH1)
FACT2=FACT1*(DEPTH1/VV1)**2
I=10
GO TO 18
17 FACT3 = FACT1
FACT6 = FACT2
FACT1=FACT3
FACT2=FACT4
18 DEPTH2=Z(J)+DD/(2.**PDW)
DEPTH2 = 6371.-DEPTH2
VV2=A+DEPTH2*(B+DEPTH2*(C+DEPTH2*D))
DEPTH2 = 6371.-DEPTH2
ETA=DEPTH2/VV2
IF (ETA-P) 4000,180,180
180 CONTINUE
FACT=DSQRT((ETA-P)*(ETA+P))
FACT3=1./(FACT*DEPTH2)
FACT4=FACT3*(DEPTH2/VV2)**2
SUM1=SUM1+DD*2.*(FACT1+FACT3)/(2.**PDW)
SUM2=SUM2+DD*2.*(FACT2+FACT4)/(2.**PDW)
IF (DD/(2.**PDW)-.03 )15,15,14
15 IF (DD/2.**PDW- DELTA)60,60,61
61 TAD = DD/(2.**PDW)
S_UP = (V(J)-VV2)/TAD
62 FACT5 = FACT1
FACT6 = FACT2
FACT1 = FACT3
FACT2 = FACT4
TAD = TAD/2.
DEPTH1 = Z(J)+TAD
SKD = SLDP+TAD
VV1 = V(J)-SKD
FACT = 2.*P*(V(J)+TAD + Z(J)+SKD) / (V(J)**2-2.*V(J)+SKD)
FACT3 = 1./(DSQRT(FACT)*DEPTH1)
FACT4 = FACT3*(DEPTH1/VV1)**2
SUM1 = SUM1 +TAD*(FACT1 *FACT3)*2.
SUM2 = SUM2 + TAD*(FACT2 *FACT4)*2.
IF (TAD-DELTA)60,60,62
60 A1 = FACT3
A2 = FACT4
B1 = FACT1
B2 = FACT2
C1 = FACT5
C2 = FACT6
ERRDM = TAD*(FACT4+3*A2-5.*B2/2.*.5*C2)/SUM2
WRITE(3,1050) ERRDM
SUM1 = TAD*(FACT3+3.*A1-5.*B1/2.*.5*C1)+SUM1
SUM2 = TAD*(FACT4+3.*A2-5.*B2/2.*.5*C2)+SUM2
DEL(N)=P*SUM1+6371.
I(N)=SUM2
SINIU = P*V(1)/RD
CDSIU = SQRT(1. - SINIU**2)
ANGLE(N) = ATAN(SINIU/CDSIU)*180./3.1416
N=N+1
GO TO 8
400 CONTINUE
DEL(N) = 0.
I(N) = 0.
ANGLE(N) = 0.
N = N + 1
8 CONTINUE
N=N-1
WRITE(3,401) (TEXT(I), I=1,20)
WRITE(3,1000)
1000 FORMAT ( 5X,10M DEPTH(KM) , 10A,18M VELOCITY(KM/SEC) )
WRITE(3,1050) (Z(J),V(J),J=1,11)
1050 FORMAT (2X,E13,6,6X,E13,6)
WRITE(3,401) (TEXT(I), I=1,20)
WRITE(3,2000)
2000 FORMAT (2X,18M TRAVEL TIME (SEC) ,5X,11M DELTA (KM),5X,21M DEPTH (
1) PENETRATION ,5X ,19M ANGLE OF INCIDENCE )
WRITE(3,2050) (T(J),DEL(J),DZ(J),ANGLE(J),J=1,N)
2050 FORMAT ( 5X,FB,2,13X,FB,1,14X,F7,1,16X,F7,2)
401 FORMAT (14I //,20A4,///)
400 FORMAT (20A4)
300 CONTINUE
STOP
END

```

INPUT DATA AND FORMAT FOR VARGRAV

<u>CARD</u>	<u>FORMAT</u>	<u>DATA DESCRIPTION</u>
1	I3	No. stations
	F10.5	Station spacing in km, Staspa
	F6.1	Depth to mass sheet in km , Depth
	I3	No. of Density layers ≤ 50
	I3	No. of Density profiles ≤ 100
	F10.5	Minimum φ value
	F10.5	Delta z spacing for integration
	F10.5	Subcrustal Density

$$\phi_{\min} \geq \frac{[\exp(\pi \cdot \text{Depth}/\text{Staspa}) - 1.] * \text{Depth}/\text{Staspa}}{\left(\frac{\text{Depth}}{\text{Staspa}}\right)^2 + k^2}$$

$$k = \frac{\text{No. of } \phi \text{'s to be used}}{2}$$

2	10F8.2	Gravity values in milligals
3	40I2	No. of Density profile to be used at each station
4	16F5.2	Density values stored by profile

```

DIMENSION GRAV(100),DENSTY(50,50),XCURR(100),DEPDIF(100),PHI(50),I
1PROF(100)
READ 100,NOSTA,STASPA,DEPTH,IOENS,NPROF,PHIMIN,DELZ ,SUBCRU
100 FORMAT(13,F10.5,F6.1,2I3,3F10.5)
READ 200,(GRAV(I),I=1,NOSTA)
200 FORMAT(10F8.2)
READ 150,(IPROF(I),I=1,NOSTA)
150 FORMAT(40I2)
READ 300,((DENSTY(I,J),J=1,IOENS),I=1,NPROF)
300 FORMAT(16F5.2)
DO 1492 I=1,NPROF
DO 1492 J=1, IOENS
DENSTY (I,J)= SUBCRU-DENSTY (I,J)
1492 CONTINUE
EXP000 = (-EXP(3.1416* DEPTH/STASPA)-1.)*DEPTH/STASPA
EXPEVN = (EXP(3.1416*DEPTH/STASPA)-1.)*DEPTH/STASPA
A1=0.
IX1
PART = (DEPTH**2)/(STASPA**2)
6 IF( (1 +1)/2 - 1/2)1,1,2
1 PH1(I)=EXP000/(PART+A1**2)
PRINT 101,PH1(I)
101 FORMAT (F10.5)
DO TO 3
2 PH1(I)=EXPEVN/(PART + 1**2)
102 FORMAT(F10.5)
3 IF (ABS(PHI(I))-PHIMIN)4,4,5
> 1=1+1
A1 =A1+1.0
DO TO 6
4 IX1 = 2*I-1
IX = 1+1
IX2=:
J=IX
DO18 I=2,IX2
PH1(J)=PH1(I)
J=J+1
18 CONTINUE
PH1(IX2 )=PH1(1)
J=IX1
IX2=IX2-1
DO 7 I=1,IX2
PH1(I)=PH1(J)
J=J-1
7 CONTINUE
PRINT 400,DEPTH,STASPA
400 FORMAT(23H-COMPUTED PHI FACTORS/10H DEPTH(KM),F6.1,2X,20H STATION
15PACING(KM),F10.5)
PRINT 401,(PHI(I),I=1,IX1)
401 FORMAT(2X,E13.6)
M=IX1-1
IXK =M=IX-1
IXK=K-1
DO8 I=1,IX2
XCURR(I)=0.
DO 9 J=1,IX
XCURR(I)= GRAV(J)*PHI(K) +XCURR(I)
K=K+1
9 CONTINUE
500 FORMAT(2X,F10.2)
IX=IX+1
K= N =N-1
8 CONTINUE
IX3=NOSTA-IX+1
J=IX2+1
DO 10 I=1,IX3
XCURR(J)=0.
K=1
DO 11 L=1,IX1
XCURR(J)=GRAV(K)*PHI(L) +XCURR(J)
K=K+1
11 CONTINUE
600 FORMAT(2X,F10.2)
J=J+1
10 CONTINUE
IX3=IX3+1
N=NOSTA-IX2
DO 12 I=IX3,N
K=1
XCURR(J)=0.
DO 13 L=1,M
XCURR(J)=GRAV(K)*PHI(L) +XCURR(J)
K=K+1
13 CONTINUE
700 FORMAT(2X,F10.2)
J=J+1
M=N-1
12 CONTINUE
FACT=2.*(3.1416**2)*6.67
DO 14 I=1,NOSTA
XCURR(I)= XCURR(I)/FACT
14 CONTINUE
DO 50 J=1,NOSTA
SUM=0.
AMAX=XCURR(J)
IF (AMAX=0.)50,51,52
50 >=1.0
DO TO 53
52 >=1.0
DO TO 53
51 DEPDIF(J)=DEPTH
DO TO 50
53 I=IPROF(J)
DEPDIF(J)= 0.
K=0

```

```

40 K=K+1
   DENS = DENSTY(I,K)
   DENS1=DENSTY(I,K-1)
   IF (K-IDENS)43,43,44
4  DEPDIF(J)=DEPDIF(J)+DELZ
   SUM= SUM+DENS*DELZ
   F=ABS(SUM)-ABS(AMAX))40,41,42
42 IF(K-1)54,53-54
52 DENS1=DENS
54 F=ABS(AMAX)-SUM+DENS*DELZ
   DEPDIF(J)=DEPTH-SGN*(DEPDIF(J)+F/DENS1-DELZ)
   GO TO 30
41 DEPDIF(J)=DEPTH-SGN* DEPDIF(J)
   GO TO 30
44 DENS = DENSTY(I,K-1)
   DENS1=DENSTY(I,K-1)
   K=K-1
   GO TO 43
30 CONTINUE
   PRINT 2000
2000 FORMAT(1M-,43X,27H THICKNESS OF CRUSTAL LAYER /)
   PRINT 3000
3000 FORMAT(17H DENSITY PROFILES // 2X,10H DEPTH(KM),5X, 9H DENSITY )
   DEPTH= -DELZ
   DO 3500 I=1, NPROF
   DEPTH= DEPTH + DELZ
   PRINT 3600,(DENSTY (I,J),J=1,IDENS)
3500 CONTINUE
3600 FORMAT ( 10F9.3)
   PRINT 1966
1966 FORMAT(8M-STATION,5X,19H GRAVITY(MILLIGALS),2X,10H DEPTH(KM),
14X,21H DENSITY PROFILE USED)
   DO 17 I=1,NOSTA
   PRINT 4000,I,GMAY(I), DEPDIF(I),IPWJF(I)
4000 FORMAT(2X,13.13X,F8.2,9X,F8.2,13X,13)
17 CONTINUE
   PAUSE /
   END

```


INPUT DATA AND FORMAT FOR PRESID

<u>CARD</u>	<u>FORMAT</u>	<u>DATA DESCRIPTION</u>
1	I3	No. of stations at which residuals will be computed
2	16F5.1	Jeffreys-Bullen P-travel times in sec
3	20F4.1	Latitude corrections for converting to geocentric coordinates
4	I3	No. of epicenter locations for each station
5	F6.1	Station latitude (geocentric)
	F6.1	Station longitude
6	18F4.1	USGS origin times for earthquakes stored in sequence as HH:MM:SS.S
7	18F4.1	Record arrival times and store in sequence as HH:MM:SS.S
8	16F5.1	USGS focal depths in km
9	12F6.1	USGS latitude and longitude of epicenters stored in pair sequence Lat ₁ , Long ₁ , Lat ₂ , Long ₂ , ... Sign Convention East Long - West Long + North Lat + South Lat -

```

DIMENSION QUALOC(200),ORTIM(300), DEPTH(100),STALIM(300),RESID(100)
1,RTTEM(100), DELTA(100),AZIMUT(100), P(14,103),LOCCEL(100),GEOC(9
11),GEQUA(200)
MEAD 100, LIMSTA
100 FORMAT(13)
MEAD 150,((P(I,J),I=1,14),J=1,103)
150 FORMAT(16F5.1)
MEAD 1112,(GEOC(J),J=1,91)
.112 FORMAT(20F4.1)
3 DEL STATION INDLX
UD 1 I=1,LIMSTA
MEAD 200, LIMQUA
200 FORMAT(13)
IX=2*LIMQUA
MEAD 700,STALAT, STALNG
700 FORMAT(F6.1,F6.1)
IX2 = 3* LIMQUA
MEAD 600, (OPTIM(J),J=1,IX2)
90 FORMAT (18F4.1)
MEAD 400, (STALIM(J),J=1,IX2)
100 FORMAT(18F4.1)
MEAD 500,(DEPTH(J), J=1,LIMQUA)
500 FORMAT(16F5.1)
MEAD 300,(QUALOC(J),J=1,IX)
300 FORMAT(12F6.1)
UD 1111 J=1,IX,2
K=2
ALAT =1.0
502 IF(QUALOC(J)-ALAT)565,501,501
501 ALAT =A .T +1.0
K=K+1
UD TU 502
565 UJMA=GEOC(K) -(GEOC(K)-GEOC(K-1))*(ALAT-QUALOC(J))
1111 GEUCA(J) =QUALOC(J) - CORR
UD 2 J=1,IX,2
INDX=J/2+1
STAANG = STALAT*3.1416/180.
QUANG =GEQUA(J)*3.1416/180.
POLANG = STALNG - QUALOC(J+1)
IF (POLANG-180.)3,3,4
4 POLANG = POLANG -360.
3 POLANG =POLANG*3.1416/180.
COSDEL = SIN(STAANG)*SIN(QUANG)+COS( STAANG)*COS(QUANG)+COS(POLANG)
SINDEL=SOMT(1.-COSDEL**2)
UJTA(INDX)=ATAN(SINDEL/COSDEL) +180./3.1416
DELTA(INDX)= DELTA(INDX)+90. -SIGN(UJTA,DELTA(INDX))
SINBET=COS(QUANG)*SIN(POLANG)+SINQU
COSBET=(SIN(QUANG)*COS(STAANG)-COS(QUANG)*SIN(STAANG)*COS(POLANG)
1/SINVEL
ASIN=ABS(SINBET)
BETA=ATAN(SIN/COSBET)+180./3.1416
BETA= BETA + 90.-SIGN(90.,BETA)
IF(SINBET -0.)82,84,83
84 IF(COSBET -0.)85,83,83
85 BETA =180.
83 AZIMUT(INDX)=360.-BETA
UD TU 81
82 AZIMUT(INDX)=BETA
91 UJ=FINVE
CONTINUE
M=1
UD 12 J=1,LIMQUA
K=2
DEP = 33.0
IF(DEPTH(J)-102.) 13,13,14
13 IF(DEPTH(J)-DEP)15,15,16
16 DEP = DEP + 63.0
K=K+1
UD TU 13
L=2
DIST = 1.0
17 IF(DELTA(J)-DIST)17,17,18
18 DIST=DIST + 1.0
L=L+1
UD TU 19
17 UJF 1 = P(K,L) - (P(K,L) - P(K,L-1))*(DIST-DELTA(J))
UJF 2 =P(K-1,L) - (P(K-1,L) - P(K-1,L-1))*(DIST -DELTA(J))
IF(DEPTH(J)- 1.0) 90,90,91
90 TIMEJ = OIF2 - (OIF1-LIF2) * (DEP-DEPTH(J))/63.0
UD TU 92
91 TIMEJ = UJF1 - (OIF1 -OIF2)*(DEP-DEPTH(J))/63.0
92 TIME=ORTIM(M)+3600.*UMTIME(M+1)+60.*ORTIM(M+2)
TIME = STATIM(M)*3600. + STATIM(M+1)*60.+SIATIM(M+2)
M=M+3
IF(OJIME - 8552.6)20,4000,4000
400. IF(SJIME - 8552.6) 21,20,20
21 SJIME = SJIME + 86400.
20 RESID(J)= SJIME -OJIME - TIMEJ
UD TU 12
C M=M BRANCH OF RESIDUAL TIME
14 RESID(J)=0.
M=M+3
12 CONTINUE
C ORDER EPICENTERS BY DISTANCE
RTTEM(1)=DELTA(J)
RTTEM(2)=DELTA(J)
LOCCEL(1)=1
LOCCEL(2)=2
UD 80 K=3, LIMQUA
M=1
L=1
90 IF(DELTA(K)-RTTEM(L))22,22,23

```

```

23 L=L+1
   IF (L-K)24,25,25
24 M=M+1
   GO TO 33
25 XITEM(L)=DELTA(K)
   LDCDEL(M+1)=K
   GO TO 80
26 IX1=K
27 XITEM(IX1)=XITEM(IX1-1)
   LDCDEL(IX1)=LDCDEL(IX1-1)
   IX1=IX1-1
   IF (IX1-M)27,27,51
27 XITEM(IX1)=DELTA(K)
   LDCDEL(IX1)=K
80 CONTINUE
   PRINT 800
800 FORMAT(25H-RECORDING STATION COORD /26X,9H LATITUDE,4X,10H LONGI
   TITUDE)
   PRINT 900, STALAT, STALNG
900 FORMAT(27X,F6.1,9X,F6.1)
   PRINT 1000
1000 FORMAT(/80H EPICENTER PARAMETERS ORDERED BY DISTANCE -AZIMUTH MEAS
   URED COUNTER-CLOCKWISE FROM NORTH //)
   PRINT 2000
2000 FORMAT(3X,9H DISTANCE,3X,9H LATITUDE,3X,10H LONGITUDE,3X,6H DEPTH,
   13X,8H AZIMUTH,3X,33H P-RESIDUAL(OBSERVED-THEORETICAL))
   DO 60 K=1,IX,2
   IX1=K/2+1
   L=LDCDEL(IX1)
   M=2*L-1
   PRINT 3000,XITEM(IX1),QUALOC(M),QUALUC(M+1),DEPTH(L),AZIMUT(L),RES
   ID(L)
3000 FORMAT(5X,F7.2,5X,F6.1,7X,F6.1,7X,F6.1,7X,F6.1,12X,F7.1)
60 CONTINUE
C ORDER EPICENTERS BY AZIMUTH
XITEM(1)=AZIMUT(1)
XITEM(2)=AZIMUT(2)
LDCDEL(1)=1
LDCDEL(2)=2
DO 93 K=3,LIMQUA
M=1
L=1
105 IF (AZIMUT(K)-XITEM(L)) 101,101,102
102 L=L+1
   IF (L-K) 103,104,104
103 M=M+1
   GO TO 105
104 XITEM(L)=AZIMUT(K)
   LDCDEL(M+1)=K
   GO TO 93
101 IX1=K
107 XITEM(IX1)=XITEM(IX1-1)
   LDCDEL(IX1)=LDCDEL(IX1-1)
   IX1=IX1-1
   IF (IX1-M)108,107,107
108 XITEM(IX1)=AZIMUT(K)
   LDCDEL(IX1)=K
93 CONTINUE
   PRINT 5000
5000 FORMAT ( 25H-RECORDING STATION COORD, /32X,9H LATITUDE,9X,10H LONG
   ITUDE)
   PRINT 5001,STALAT,STALNG
5001 FORMAT(36X,F6.1,23X,F6.1)
   PRINT 5002
5002 FORMAT(/87H EPICENTER PARAMETERS ORDERED BY AZIMUTH-AZIMUTH MEASUR
   ED COUNTER-CLOCKWISE FROM NORTH )
   PRINT 5003
5003 FORMAT(/3X,8H AZIMUTH,37,9H LATITUDE,3X,10H LONGITUDE,7X,6H DEPTH
   1,7X,18H DISTANCE(DEGREES) ,12X,33H P-RESIDUAL(OBSERVED-THEORETICAL
   ))
   DO 199 K=1,IX,2
   IX1=K/2+1
   L=LDCDEL(IX1)
   M=2*L-1
   PRINT 5004,XITEM(IX1),QUALOC(M),QUALUC(M+1),DEPTH(L),DELTA(L),
   RESID(L)
5004 FORMAT(5X,F6.1,5X,F6.1,7X,F6.1,7X,F6.1,11X,F6.1,27X,F7.1)
109 CONTINUE
XITEM(1)=DEPTH(1)
XITEM(2)=DEPTH(2)
LDCDEL(1)=1
LDCDEL(2)=2
DO 207 K=3,LIMQUA
M=1
L=1
202 IF (DEPTH(K)-XITEM(L)) 203,203,204
204 L=L+1
   IF (L-K)205,206,206
205 M=M+1
   GO TO 202
206 XITEM(L)=DEPTH(K)
   LDCDEL(M+1)=K
   GO TO 207
203 IX1=K
209 XITEM(IX1)=XITEM(IX1-1)
   LDCDEL(IX1)=LDCDEL(IX1-1)
   IX1=IX1-1
   IF (IX1-M) 209,209,208
209 XITEM(IX1)=DEPTH(K)
   LDCDEL(IX1)=K
207 CONTINUE
   PRINT 801
801 FORMAT (25 H-RECORDING STATION COORD, /26X,9H LATITUDE,4X,10H LONG
   ITUDE)
   PRINT 802,STALAT,STALNG

```

```

802 FORMAT (27X,F6.1,9X,F6.1)
PRINT 803
803 FORMAT (/85M EPICENTER PARAMETERS ORDERED BY DEPTH-AZIMUTH MEASUR
ED COUNTER-CLOCKWISE FROM NORTH //)
PRINT 804
804 FORMAT(3X,6M DEPTH,3X,9M DISTANCE,5X,9M LATITUDE,3X,10M LONGITUDE,
13X,3M AZIMUTH,3X,33M P-RESIDUAL (OBSERVED-THEORETICAL)
D3 B55 K=1,1X,2
IX1=N/2+1
L=LOCDEL(IX1)
M=2*L-1
PRINT 806, XITEM(IX1), DL(V,L), QUALOC(M), QUALOC(M+1), AZIMUT(L),
RESID(L)
806 FORMAT (5X,F6.1,5X,F6.1,7X,F6.1,7X,F6.1,7X,F6.1,27X,F7.1)
807 CONTINUE
1 CONTINUE
PAUSE 7
END

```

APPENDIX IV

CURVES OF PARTICLE DISPLACEMENT

CURVES OF PARTIAL DERIVATIVES OF PHASE VELOCITY WITH RESPECT
TO LAYER PARAMETERS

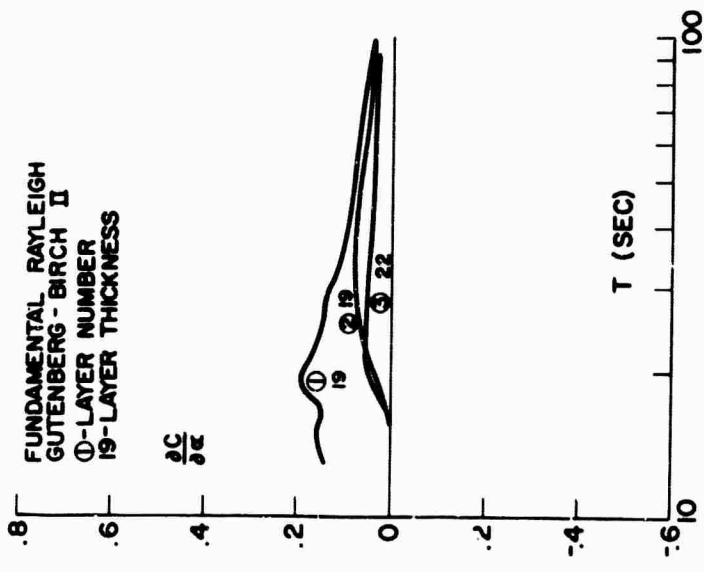


Fig. IV-1
VARIATION OF PHASE VELOCITY WITH COMPRESSIONAL WAVE VELOCITY.

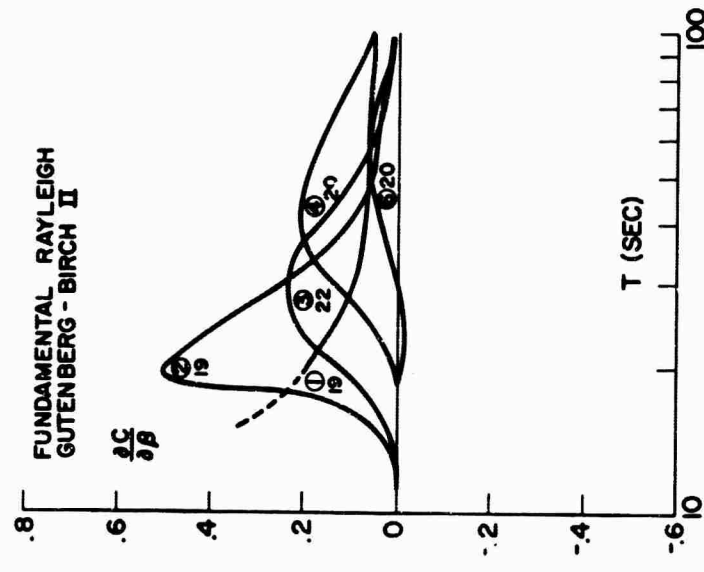


Fig. IV-2
VARIATION OF PHASE VELOCITY WITH SHEAR WAVE VELOCITY.

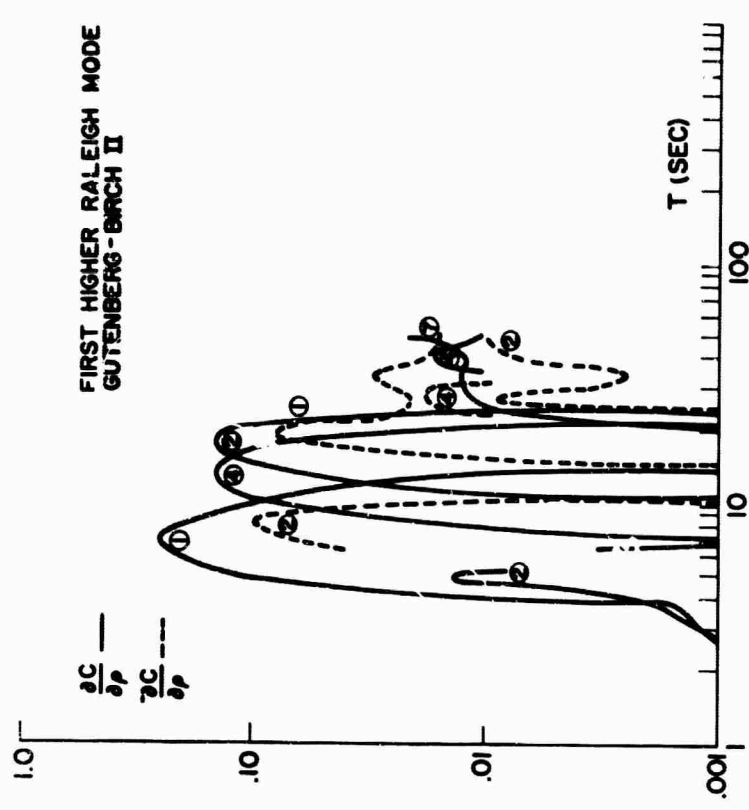


Fig. IV-3
VARIATION OF PHASE VELOCITY WITH DENSITY.

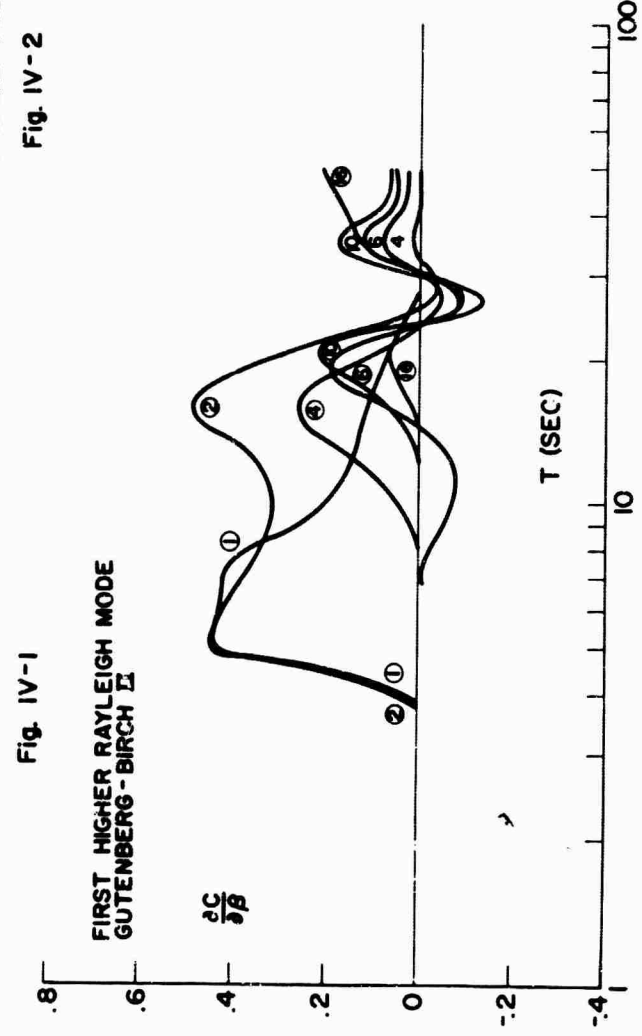


Fig. IV-4
VARIATION OF PHASE VELOCITY WITH SHEAR WAVE VELOCITY.

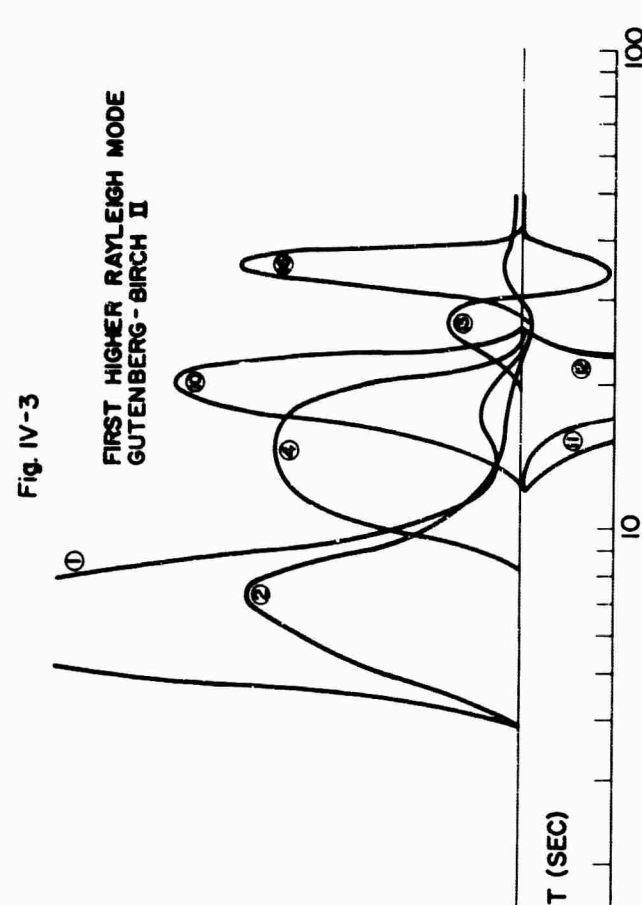
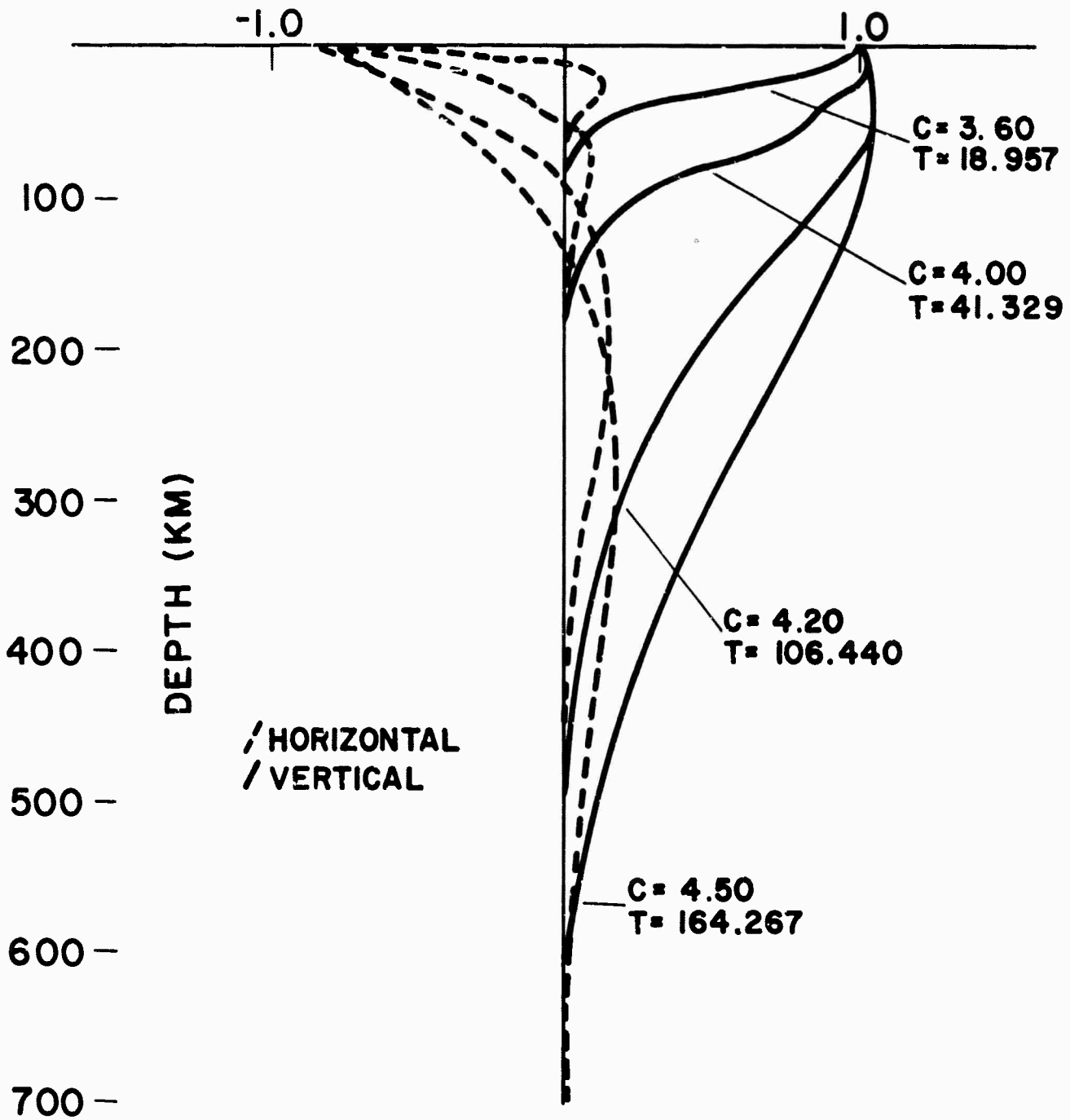
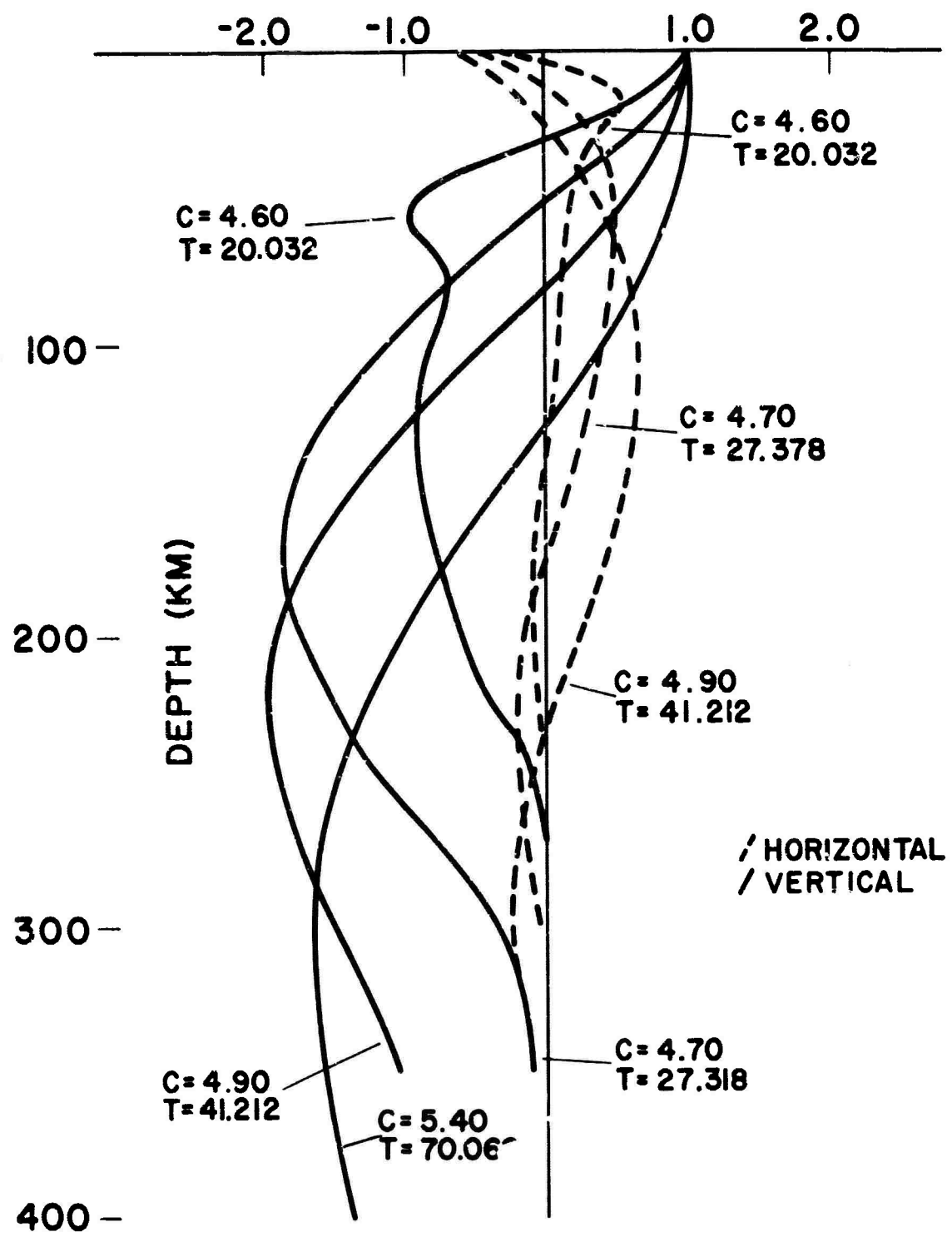


Fig. IV-5
VARIATION OF PHASE VELOCITY WITH COMPRESSIONAL WAVE VELOCITY.



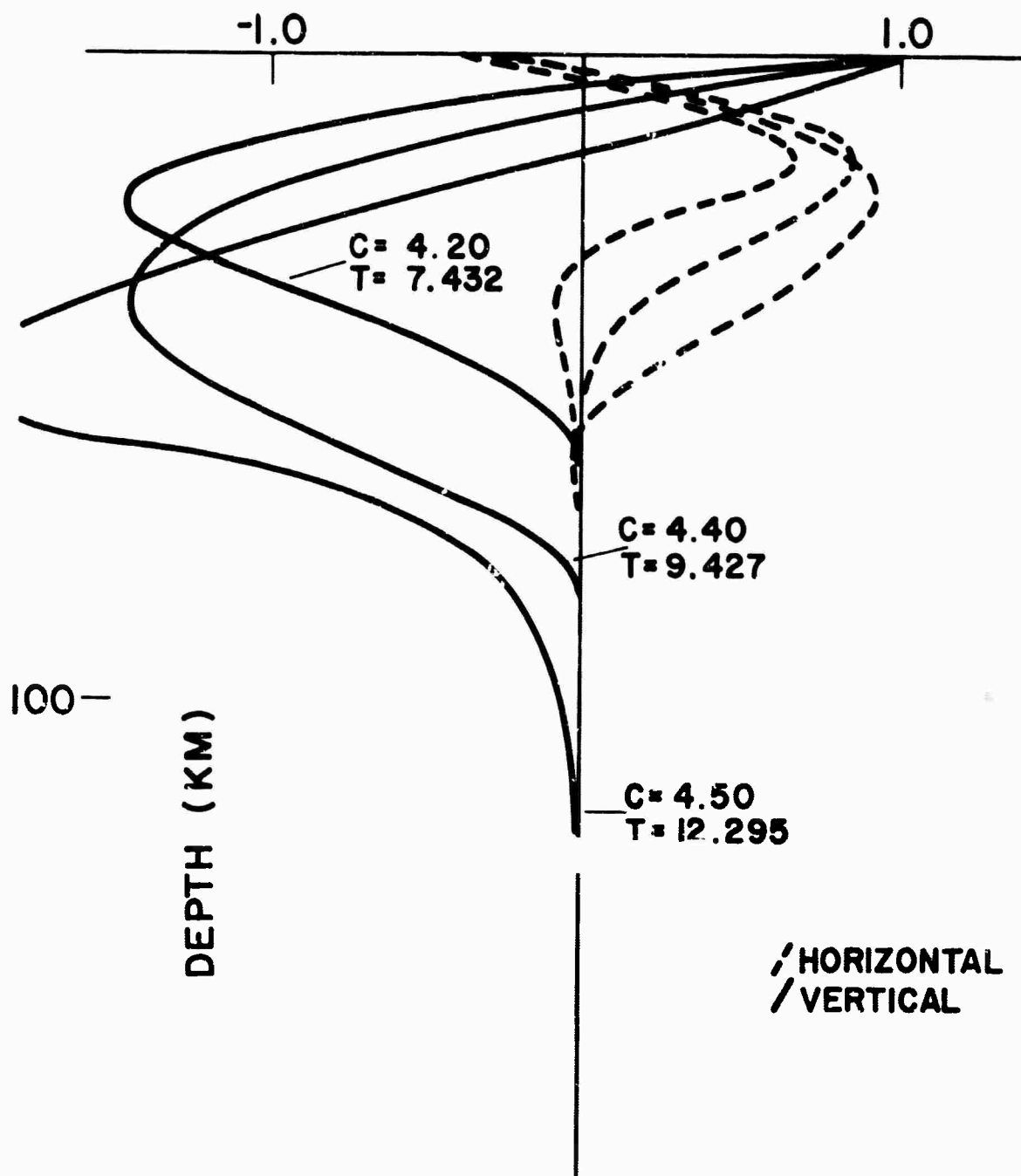
HORIZONTAL AND VERTICAL PARTICLE AMPLITUDES
 NORMALIZED TO THE VERTICAL AMPLITUDE AT THE
 SURFACE FOR FUNDAMENTAL RAYLEIGH MODE,
 GUTENBERG - BIRCH II MODEL.

Fig. IV - 6



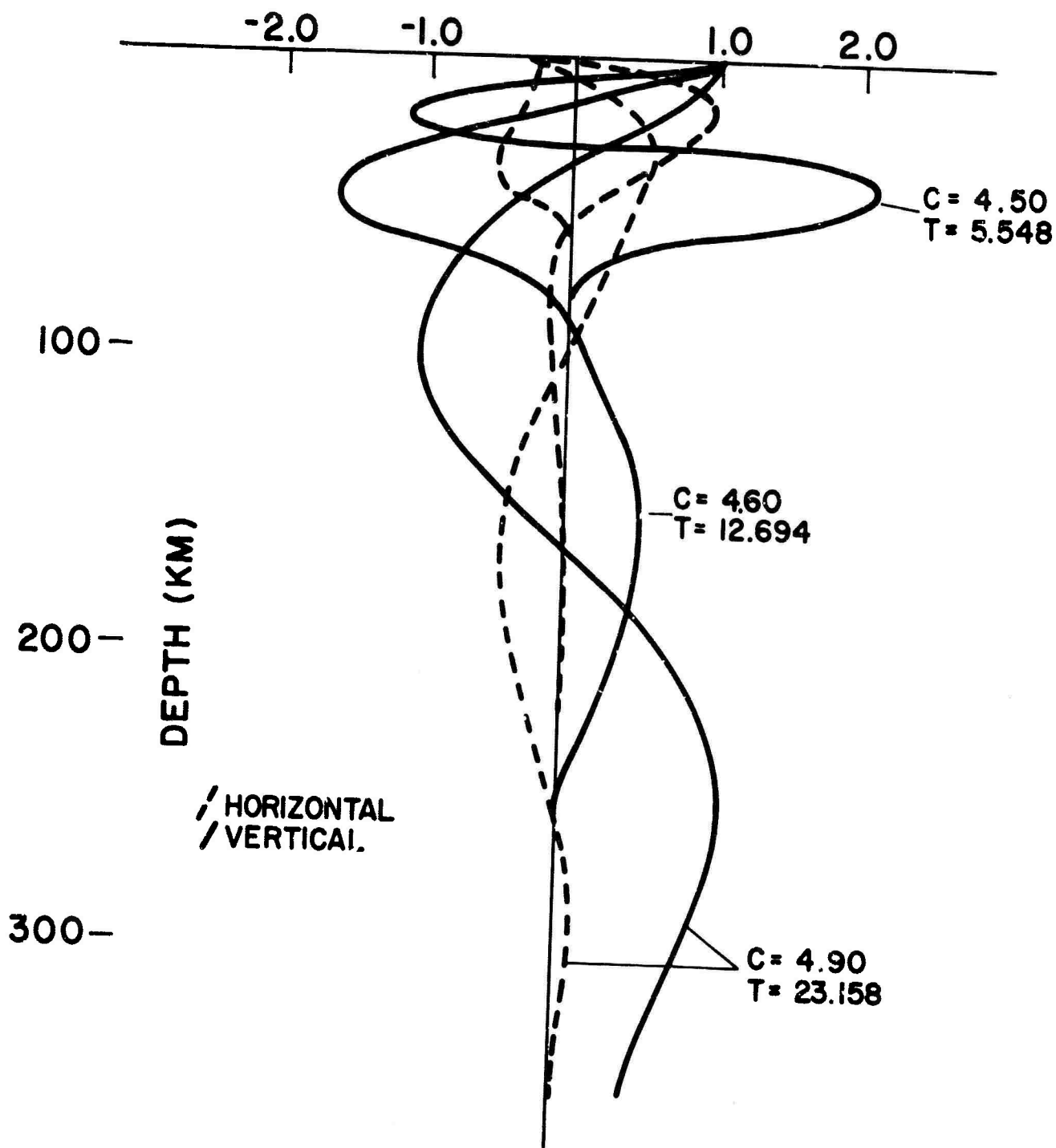
FIRST HIGHER RAYLEIGH MODE PARTICLE AMPLITUDES NORMALIZED TO THE VERTICAL AMPLITUDE AT THE SURFACE FOR THE GUTENBERG-BIRCH II MODEL.

Fig. IV-7



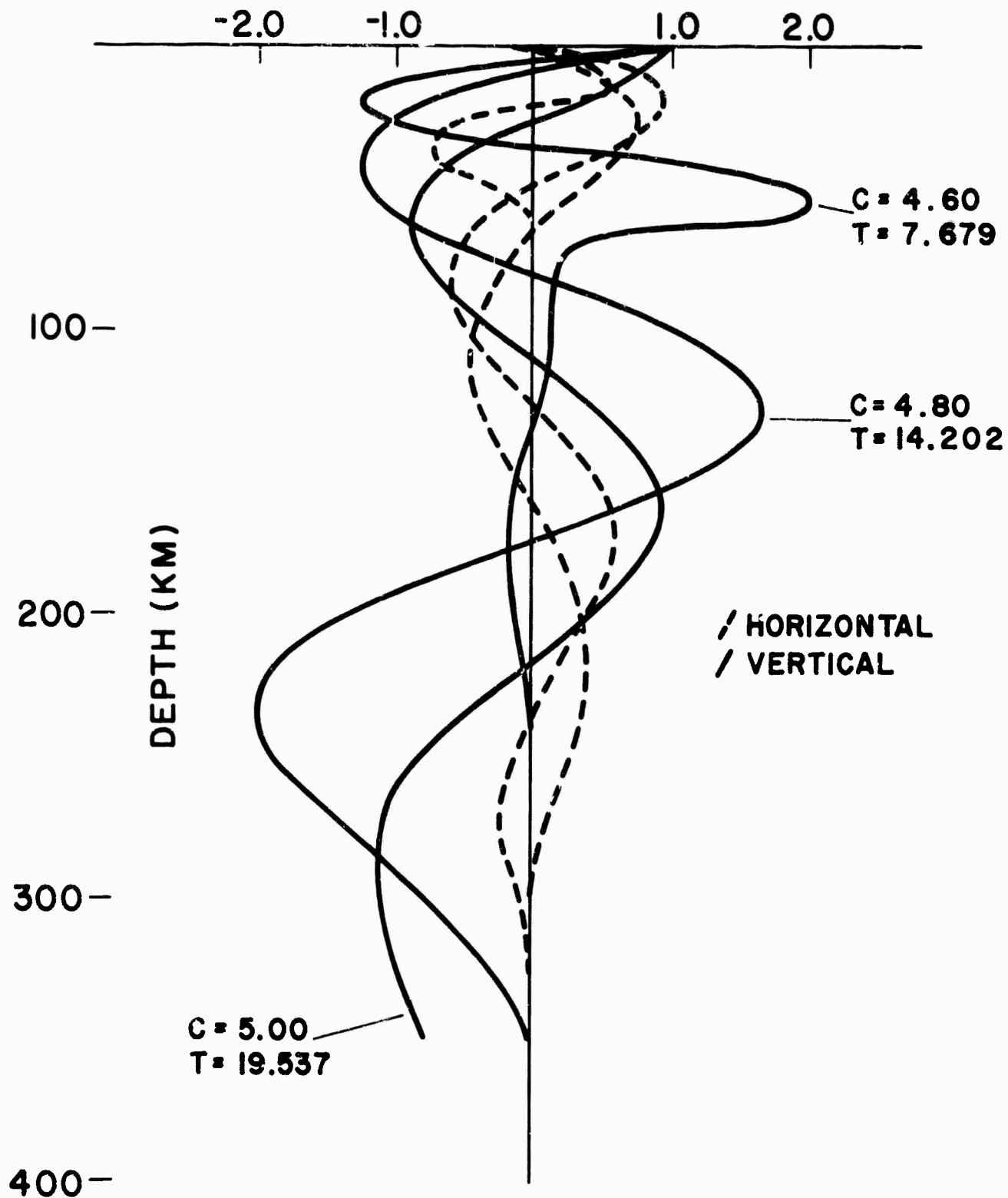
FIRST HIGHER RAYLEIGH MODE PARTICLE AMPLITUDES
 NORMALIZED TO THE VERTICAL AMPLITUDE AT THE
 SURFACE FOR THE GUTENBERG - BIRCH II MODEL.

Fig. IV-8



SECOND HIGHER RAYLEIGH MODE PARTICLE AMPLITUDES
 NORMALIZED TO THE VERTICAL DISPLACEMENT AT THE
 SURFACE FOR THE GUTENBERG - BIRCH II MODEL.

Fig. IV-9



THIRD HIGHER RAYLEIGH MODE NORMALIZED TO THE
 VERTICAL AMPLITUDE AT THE SURFACE FOR
 THE GUTENBERG-BIRCH II MODEL.

Fig. IV-10